24506

UNLIMITED
UNCLASSIFIED

ILLIMITÉ
NON CLASSIFIÉ

Technical Report

Rapport technique

1985/05

TR-RW-003
NRC NO. 24506

AN ANALOG ANALYSIS OF DELAY-LOCK TRACKING OF STOCHASTIC SIGNALS

C.M.G. Zwarts

Division of
Mechanical Engineering

Division de
génie mécanique

National Research Council Canada
Conseil national de recherches Canada

Canada

88-04474/

DIVISION OF MECHANICAL ENGINEERING PUBLICATIONS

DM **(Division of Mechanical Engineering Report)**
Scientific and technical information considered important, complete and a lasting contribution to existing knowledge.

TR **(Technical Report)**
Information less broad in scope but a substantial contribution to existing knowledge.

CTR **(Controlled/Classified Technical Report)**
A Technical Report with controlled distribution for national security, proprietary or other reasons.

LM **(Laboratory Memorandum)**
Preliminary or exploratory information with controlled distribution.

CAT **(Calibration Analysis and Test Report)**
Information on minor laboratory projects or services.

PUBLICATIONS DE LA DIVISION DE GÉNIE MÉCANIQUE

DM **(Rapport de la Division de génie mécanique)**
Informations scientifiques et techniques jugées importantes, complètes et susceptibles de contribuer de façon durable à l'avancement des connaissances courantes.

TR **(Rapport technique)**
Informations de moindre importance, mais pouvant contribuer substantiellement à l'avancement des connaissances actuelles.

CTR **(Rapport technique à diffusion contrôlée/classifiée)**
Rapport technique à diffusion contrôlée pour des raisons de sécurité nationale, de propriété intellectuelle et autres.

LM **(Mémoire de laboratoire)**
Informations préliminaires ou de nature exploratoire à diffusion contrôlée.

CAT **(Rapport d'étalonnage d'analyse et d'essai)**
Informations sur de petits projets ou des services de laboratoire.

UNLIMITED
UNCLASSIFIED

ILLIMITÉ
NON CLASSIFIÉ

AN ANALOG ANALYSIS OF DELAY-LOCK TRACKING OF STOCHASTIC SIGNALS

ANALYSE ANALOGIQUE DE LA POURSUITE DE SIGNAUX ALÉATOIRES À L'AIDE D'UNE BOUCLE DE VERROUILLAGE À RETARD

C.M.G. Zwarts

Division of Mechanical Engineering Report

1985/05

Rapport de la Division de génie mécanique

TR-RW-003
NRC No. 24506

C.A.M. Smith, Head/Chef
Railway Laboratory/
Laboratoire de génie ferroviaire

E.H. Dudgeon
Director/Directeur

ABSTRACT

The non-contacting measurement of velocity, length and distance with a delay-locked loop, using a novel theoretical approach, is discussed in this report.

A theory is developed, analyzing the non-linear behaviour of the loop for both inherent system noise and externally generated noise.

It is shown how non-linear functions, inserted in the loop can be used to optimize performance.

Analytical methods are developed to analyze the non-linear behaviour for both small and large amplitude time-delay perturbations.

RÉSUMÉ

Le rapport discute des mesures sans contact de vitesse, de longueur et de distance, effectuées à l'aide d'une boucle de verrouillage à retard, utilisant une technique d'analyse nouvelle.

Il établit une théorie en analysant le comportement non linéaire de la boucle, tant pour le bruit inhérent au système que pour le bruit externe.

Il montre comment on peut optimiser la performance en insérant dans la boucle des fonctions non linéaires.

Il détaille des méthodes permettant d'analyser le comportement non linéaire de perturbations de retard de faible amplitude, comme de grande amplitude.

CONTENTS

		Page
	ABSTRACT/RÉSUMÉ	(iii)
1.0	INTRODUCTION	1
2.0	DELAY-LOCKED LOOP — AN EXTENSION OF THE PHASE-LOCKED LOOP	3
3.0	BACKGROUND FOR THEORY	3
	3.1 Analog versus Stochastic Approach	3
	3.2 Variant and Invariant Noise Power Spectra	4
	3.3 Sampled Data System	4
	3.4 Non-Linear Analysis	4
	3.5 Interpretation of Graphs	5
4.0	GENERAL DESCRIPTION OF DELAY-LOCKED LOOP	5
5.0	DERIVATION OF TRANSFER FUNCTION	8
	5.1 Partial Transfer Functions	8
	5.1.1 Cross-Correlator	8
	5.1.2 Difference Integrator	12
	5.1.3 Voltage Controlled Oscillator	12
	5.1.4 Delay Line	13
	5.2 Closed Loop Transfer Function	15
6.0	OPTIMIZING LOOP PERFORMANCE WITH NON-LINEAR FUNCTIONS	17
	6.1 Inverse Non-Linear System Function	18
	6.2 Exponential Non-Linear System Function	21
7.0	TRANSDUCER TRANSFER FUNCTIONS	23
8.0	OPERATION OF DELAY-LOCKED LOOP AT CONSTANT VELOCITY	25
9.0	ANALYSIS OF PARTIAL COHERENCE AND SIGNAL-TO-NOISE RATIO	26
	9.1 Input/Output Noise Signals of Comparators	26
	9.2 Noise in Shift Registers	27
	9.3 Processing of Noise Signals by Cross-Correlator	29
	9.4 Intrinsic Noise and Additive Noise	31
	9.5 Equivalent Models for Intrinsic and Additive Noise	31
	9.6 Signal-to-Noise Ratio	33
10.0	MEASUREMENT OF DISTANCE AND "DISTANCE TRAVELLED"	35
11.0	NON-LINEAR ANALYSIS FOR LARGE AMPLITUDE SIGNALS	36
	11.1 Derivation of Non-Linear Differential Equation	38
	11.2 General Solution, over Interval Δt, for Arbitrary Input	39

CONTENTS (Cont'd)

		Page
11.3	Solution, over Interval Δt, for Velocity Ramp Input	40
11.4	Error in Velocity and "Distance Travelled" for Velocity Ramp Input	44
11.4.1	Exponential Non-Linear System Function	45
11.4.2	Inverse Non-Linear System Function	52
12.0	ANALYSIS OF FOURTH-ORDER DELAY-LOCKED LOOP SYSTEM	59
12.1	Small Signal Transfer Function	60
12.2	Derivation of Non-Linear Differential Equation	63
12.3	Solution, over Interval Δt, for Velocity Ramp Input	64
12.4	Error in Velocity and "Distance Travelled" for Velocity Ramp Input (Inverse Non-Linear System Function)	67
13.0	ANALYSIS OF LOOP BEHAVIOUR FOR INVARIANT NOISE	74
13.1	Measurement of Distance	74
13.2	Small Signal Transfer Function	75
13.3	First Order System	78
13.3.1	Constant Bandwidth	80
13.3.2	Bandwidth Proportional to L^{-1}	83
13.3.3	Bandwidth Proportional to $L^{-\frac{1}{2}}$	84
13.4	Second Order System	88
13.4.1	Bandwidth Approximately Constant	89
13.4.2	Bandwidth Proportional to L^{-1}	92
13.4.3	Bandwidth Approximately Proportional to $L^{-\frac{1}{2}}$	95
13.5	Converting Variant to Invariant Noise	95
14.0	SELF-ADAPTIVE BEHAVIOUR OF DELAY-LOCKED LOOP	97
15.0	IMPLEMENTATION OF NON-LINEAR FUNCTIONS	99
16.0	LOOP MONITOR AND AUTOMATIC LOCK-IN CIRCUIT	100
17.0	OPTIMIZING LOOP PERFORMANCE WITH PSEUDO-RANDOM NOISE GENERATOR	100
18.0	CONCLUSIONS	101
19.0	REFERENCES	101

SYMBOLS

Symbol	Definition
A	second order coefficient
B	first order coefficient
C	zero order coefficient
BW	3 dB bandwidth
E	reference voltage for cross-correlator
E_1, E_2	output voltages of cross-correlator
E_i	input voltage of non-linear function
E_o	output voltage of non-linear function
K	gain factor of V.C.O.
L	distance between sensors and distance from sensors to target
N	integer
T	time delay
T_{VCO}	period of V.C.O.
$\hat{T}$	electronic delay
V	velocity
V.C.O.	voltage controlled oscillator
b	amplitude of step in V.C.O. period T_{VCO}
c	propagation speed of carrier
d	damping factor
$h_1(p)$	complex partial transfer functions of cross-correlator
$h_2(p)$	— difference integrator
$h_3(p)$	— V.C.O.
$h_4(p)$	— electronic delay
$h_5(p)$	— non-linear function
$h_6(p)$	— physical delay

SYMBOLS (Cont'd)

Symbol	Definition
f_{VCO}	frequency of V.C.O.
$n(t)$, $n(t-T)$	coherent noise signals
$m_1(t)$, $m_2(t)$	non-coherent noise signals
n, n_1, n_2, n_3	number of stages of shift registers
p	complex frequency
v_i	input velocity
v_o	normalized velocity output
x	alternate symbol for v_i
x_0	velocity x at $t = 0$ second
$x_{0,n}$	velocity x at $t = n\Delta t$ seconds
y	normalized velocity output (alternate symbol for v_o)
y_0	normalized velocity output at t = 0 second
y_1	$\frac{dy}{dt}$ at t = 0 second
y_2	$\frac{d^2y}{dt^2}$ at t = 0 second
y_3	$\frac{d^3y}{dt^3}$ at t = 0 second
$y_{0,n}$	normalized velocity output at $t = n\Delta t$ seconds
$y_{1,n}$	$\frac{dy}{dt}$ at $t = n\Delta t$ seconds
$y_{2,n}$	$\frac{d^2y}{dt^2}$ at $t = n\Delta t$ seconds
$y_{3,n}$	$\frac{d^3y}{dt^3}$ at $t = n\Delta t$ seconds

SYMBOLS (Cont'd)

Symbol	Definition
Δt	time increment
$\Delta T, \Delta \hat{T}, \Delta \hat{T}^*$	increment in time delay
$\psi(p), \psi^*(p)$	complex transfer functions
α	input acceleration
β, γ	non-linear function constants
$\xi(E_i)$	non-linear voltage function
η	L/V
$\lambda(p)$	complex transfer function
$\mu(p)$	complex transfer function
τ, τ_0	time constants
$\tau_{1/2}$	half-width correlation time constant
ω, ω_0	angular frequency
$\mathcal{L}$	Laplace Operator
$\mathcal{L}^{-1}$	Inverse Laplace Operator

AN ANALOG ANALYSIS OF DELAY-LOCK TRACKING OF STOCHASTIC SIGNALS

1.0 INTRODUCTION

The theory presented was developed to obtain a better understanding of a delay-locked loop instrument designed to measure accurately velocities of rail vehicles.

The delay-locked loop appeared as a promising measuring concept. Whilst developing a delay-locked loop instrument it became clear that the concept is relatively unknown and that it could be used advantageously in many other areas of measurements.

The basic operation is illustrated in Figure 1. The input consists of two random signals at least partially coherent, having a certain relative time delay. The transducer converts the relative time delay with a delay-locked loop, employing a real-time correlation process, into an output frequency inversely proportional to the delay. This frequency, via the time delay, is a measure of the velocity of a "noise carrying medium" or the distance to a target.

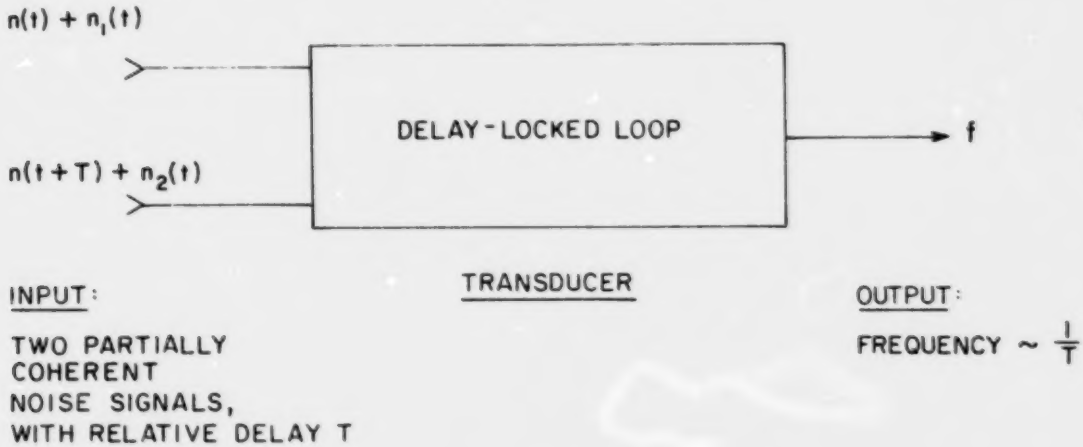

FIG. 1

The versatility of the delay-locked loop can be understood from the following considerations:

1. basic parameters are measured: length and velocity
2. any type of random input signal can be used for which one can conceive a sensor for conversion to an electrical signal
3. the flexibility in the choice of random input signals allows measurement to be made in non-contacting fashion.

Measurements related to length and velocity are omnipresent: speed and position of trains, flow of solids, fluids and gases, surface speed of rotating objects, altitude and velocity of aircraft, length measurement in paper, textile and metallurgic industries, average windspeed, etc.

All physical things or processes exhibit randomness. In any given situation there is a choice which is narrowed down by economic and/or engineering considerations. Suitable random processes for instance are: surface roughness, variations in dielectric constant of sheets of paper, inhomogeneities in gases, variations in transmission, reflection or refraction of electromagnetic waves, etc.

Noise can be sensed directly: thermometer sensing temperature fluctuations.

Noise can be excited: magnet close to surface of ferromagnetic material increases considerably the size of the random oriented magnetic clusters.

Randomness can be introduced externally: inserting particles in fluids for example.

Conversion of one system noise parameter into another more suitable for measurement: a light beam directed onto a surface converts surface roughness into intensity variations of light.

Noise, as discussed above, can be considered as a spatial random grid moving along with the medium. Relative movement between medium and sensors causes the spatial randomness to be converted, by the sensors, into random time sequences of electrical signals. The frequency spectrum of the electrical random signals compresses or expands as a function of the relative velocity.

Noise can also be generated by electronic means and transmitted on a carrier. The transmitted and reflected noise from some target are used as the input signals. In this particular case the noise is independent of the medium and its frequency spectrum therefore independent of the relative velocity between sensors and target (i.e., when relative velocity is much smaller than propagation speed of carrier). Subsequently we will refer to this type of noise as invariant noise.

The non-contact type of measurement, possible with delay-locked loop type instrumentation, is definitely an advantage and is obviously required when measuring the depth of an ocean or the altitude of an aircraft. In many industrial processes there remains a choice. However, when measuring the length of hot slabs in a steel mill, non-contacting measurement is certainly advantageous. Using the wheels of a road vehicle or a rail vehicle to measure velocity and "distance travelled" suffers from changes in diameter of the wheel due to wear and slip. Materials such as paper or textiles might be too delicate to allow reliable contact type measurement.

Non-contacting type measurement requires the use of a field interacting with the object of measurement. The electric field of a capacitor is a very versatile field and can be linked in a variety of ways to a medium to sense surface roughness, thickness variations, fluctuations in dielectric factor, etc. Magnetic fields are not as versatile as the electric field but can be used for instance to measure magnetic field fluctuations, using flux sensors, along ferromagnetic substances. Electromagnetic and acoustic waves can be made to interact with the object of measurement in a great many ways. One major category of application consists of using random variations in either transit time, reflection, transmission or refraction of the waves as they interact with the medium.

The time delay between two coherent signals are and have been measured with cross-correlation. The method however to extract the delay information consisted of measuring the full correlation curve and determining its peak value. This, however, takes considerable time and usually cannot be completed quickly enough to allow operating in real time.

The new element introduced by the delay-locked loop is that it is a real-time processor. The correlation is reduced to a minimum. Only two points are measured,simultaneously equidistant from optimum correlation. It is done in such a way that an S-type control curve typical for servo operation is obtained. This feature, essentially, allows the accurate real-time tracking of delays with delay-locked loop instruments.

The delay-locked loop has been analyzed by several authors [1-4], using a statistical approach. These theories are not transparent for the average system designer. This report presents a new approach. It is simple, general in nature and allows an instrument designer to readily understand and design delay-locked loop instrumentation.

2.0 DELAY-LOCKED LOOP — AN EXTENSION OF THE PHASE-LOCKED LOOP

In a phase-locked loop the frequency of a voltage controlled oscillator is made to track the frequency of an input signal. Once in-lock,the loop tracks the phase variations of the input signal. Essentially therefore one has an input signal with a certain phase and frequency, acting as a reference for a voltage controlled oscillator, which the phase-locked loop slaves to the input reference signal.

Noise signals don't have a well defined parameter which can be tracked. However, if one takes two coherent noise signals one can use one noise signal as a reference for the other, with regard to their relative time delay. The "early" noise signal is put through a variable digital delay line. The essential operation of the delay-locked loop is to slave the digital delay to the input delay by keeping the delayed "early" noise signal "in phase" with the "late" noise signal.

The phase-locked loop tracks a phase delay, which actually is a time delay between two well defined harnomic signals. The delay-locked loop tracks the time delay between two noise signals. Hence the delay-locked loop is an extension of the phase-locked loop for random input signals.

3.0 BACKGROUND FOR THEORY

3.1 Analog Versus Stochastic Approach

During the design and construction of a prototype delay-locked loop instrument (for which a patent was obtained in 1982) to measure, non-contacting, velocity and "distance travelled" of rail vehicles, the author had difficulty in understanding the behaviour of the loop. The output noise increased sharply for large values of delay. It was difficult to perceive how this could happen with a first order system. It was this fact which triggered off the development of the present theory. The literature published was not much help, treating the loop as a first order system and remaining somewhat academic.

The delay-locked loop has been analyzed in various papers [1-4]. They all analyze the loop with statictical theories using a first order approximation for the loop.

The approach taken in this report is quite different. The noise signals are defined by an averaged quantity, i.e., the correlation amplitude curve. A triangular correlation curve is assumed and a half-width correlation time constant is used to define the noise signals. Hence, the noise signals are characterized by an averaged analog quantity. Whereas a first order model is used in the references above it will be shown that a second order model is more accurate and even necessary to describe adequately the behaviour of the loop for large input delays.

The problem to be analyzed with this approach is therefore completely analog, i.e., a non-linear second order feedback system. Special techniques will be developed to analyze the loop behaviour analytically for both small and large amplitude signals.

The advantage of an analog theory is that it ties in with conventional system design control theory using complex transfer functions, Laplace Transforms, etc.

With the approach taken one cannot predict the acquisition behaviour, the mean variation in the output signal, the probability that the loop remains locked, etc. In a practical measuring environment it is usually possible to select a random noise process giving a signal amplitude sufficiently above all other irrelevant non-coherent noise. The restrictions above become then somewhat academic in nature. Even if one is operating the delay-locked loop in a very "noisy" environment the theory developed remains very useful as a conceptual tool and can still be used to optimize the loop. The essential element to remember is that the theory analyzes the behaviour of an averaged quantity. If the coherent part of the input noise signal decreases then the theory still predicts correctly the average, being somewhat more corrupted with additional random fluctuations.

In the remainder of the report we will assume 100% coherence for the input noise signals. The influence of non-coherent noise will be discussed in Sections 9.0 and 17.0.

An advantage of the theory developed is that it readily described the dynamic behaviour of the loop. This knowledge is required to be able to control the closed loop transfer function and for the analysis of the response to large amplitude dynamic variations in the input delay.

3.2 Variant and Invariant Noise Frequency Spectra

There are two distinct ways to operate a delay-locked loop.

1. A relative motion exists between the "noise carrying" medium and the two noise sensors (positioned in-line with the movement, a fixed distance apart). The noise frequency spectrum is variant and expands or compresses as a function of the velocity (similar to a magnetic tape recorder). The output signal of the delay-locked loop — the clock frequency driving the electronic delay — is proportional to the relative velocity whereas the accumulated number of clock pulses gives a measure of the "distance travelled".

2. Noise is generated externally to the medium, and is transmitted on a suitable carrier. The delay-locked loop operates on the delay between the transmitted noise and the reflected noise on some target or transponder. Alternatively the noise is transmitted by a remote located transmitter and received by two separate receivers. The noise frequency spectrum is invariant if the relative velocity is much smaller than the propagation speed of the carrier. In this mode of operation one measures the distance to a target (depth, altitude, distance to target) or one resolves the angle in relation to a remote located transmitter.

The distinction made with regard to the noise frequency spectrum being variant or invariant, is important. It affects the gain of the cross-correlator and hence the dynamic behaviour of the delay-locked loop.

3.3 Sampled Data System

The input noise signals are sampled at a rate determined by the clock frequency. The sampling process and the digital delay line form the sampled data portion of the delay-locked loop. Reconstruction of an analog signal takes place inside the loop by the low-pass filtering action of the difference integrator. If the sampling frequency is significantly higher than the highest signal frequency of interest one is justified to take an analog continuous model for the sampled data portion of the loop. One can then use an analog model for the digital delay line and consider the delay-locked loop as an analog continuous system.

3.4 Non-Linear Analysis

The delay-locked loop is a non-linear system. It will be analyzed for small and large amplitude perturbations.

The analysis for small signal perturbations is based on linearization around quasi-static operating points of the various loop components. The derivatives at these points are taken to obtain the incremental gain factors. The functional relations between incremental gains and operating points are expressed as a function of the quasi-static magnitude of the input delay. The analysis is directly stated in terms of complex transfer functions which is a convenient short cut to the solution of the differential-equation.

An analytical method was developed to handle large amplitude signals. The general non-linear differential-equation for arbitrary input conditions is established. It is linearized by restricting the differential-equation to small time increments. The non-linear partial gain factors of the various loop components are considered to be constant for these small time increments. The general solution is derived for the time increment starting at t = o and is used to derive the boundary conditions for

the next time interval. The solution at the end of this interval forms the boundary conditions for the next interval. This process of iteration is continued in order to find the solution at any particular time. An accurate solution is obtained if the time increment is chosen very small with regard to the rate of change of the input signal. Moreover the partial gain factors of the loop components are smooth continuous functions of the amplitude of the input signal (= delay) and hence virtually constant during one time increment.

3.5 Interpretation of Graphs

The disadvantage, inherent in non-linear systems, is that generalized graphs cannot be given, the system behaviour being dependent on the amplitude of the input signal. Both frequency (or time) and amplitude are variables and hence several graphs are necessary to demonstrate the behaviour of the system.

The first part of the analysis deals with delay-locked loops operating with time variant input noise frequency spectra. The graphs given are specifically based on the measurement of velocity and position of rail vehicles.

The second part analyzes the response of delay-locked loops for time invariant noise frequency spectra. Some arbitrarily chosen numerical examples are used to illustrate the behaviour of the delay-locked loop in graphical form.

4.0 GENERAL DESCRIPTION OF DELAY-LOCKED LOOP

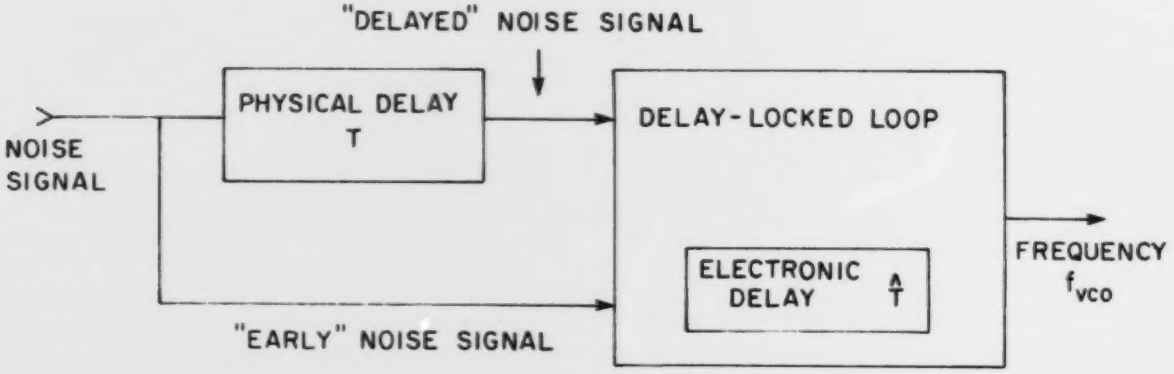

FIG. 2

The delay-locked loop tracks in some way the physical delay with its internal electronic delay.

The electronic delay is determined by the number of stages n of a shift register and the clock frequency f_{VCO}.

$$\hat{T} = \frac{n}{f_{VCO}}$$

The physical delay is equal to T and since $T = \hat{T}$, $f_{VCO} = (n) \cdot \frac{1}{T}$

The frequency f_{VCO} is therefore a measure for physical delay T.

This delay is made up of two elements, length and velocity. Keeping length constant, one measures velocity and vice versa, for constant velocity one measures length.

If the delay is produced by placing two sensors, a small fixed distance L apart, in a noise carrying medium, then the delay is determined by the relative velocity, V, between sensors and medium, see Figure 3. Hence,

$T = \frac{L}{V}$ and therefore,

$$f_{VCO} = \left(\frac{n}{L}\right) \cdot V \quad (L = \text{constant}, V = \text{variable})$$

The frequency f_{VCO} is proportional to the relative velocity V.

Other important information can be immediately derived from the frequency f_{VCO}. Counting the clock pulses gives a direct measure for the "distance travelled" of the medium relative to the sensors (Fig. 3).

$$\sum_{0}^{n} f_{VCO} = \left(\frac{n}{L}\right) \int_{0}^{t} V \, dt \sim \text{"distance travelled"}$$

The instrument is used in a different manner to measure distance (Fig. 4). Noise from a noise generator is used as one input to the delay-locked loop. Furthermore, it is used to modulate a carrier, having a propagation speed c. The reflected wave of a target is used as the second input to the delay-locked loop. The effective distance between the noise sensors, with regard to delay, is equal to twice the distance between sensors and target. The velocity is equal to the propagation speed of the carrier, hence:

$\hat{T} = \frac{2L}{c}$ and therefore,

$$f_{VCO} = \left(\frac{nc}{2}\right) \cdot \frac{1}{L} \quad (c = \text{constant}, L = \text{variable})$$

The frequency f_{VCO} is inversely proportional to the distance between sensors and target.

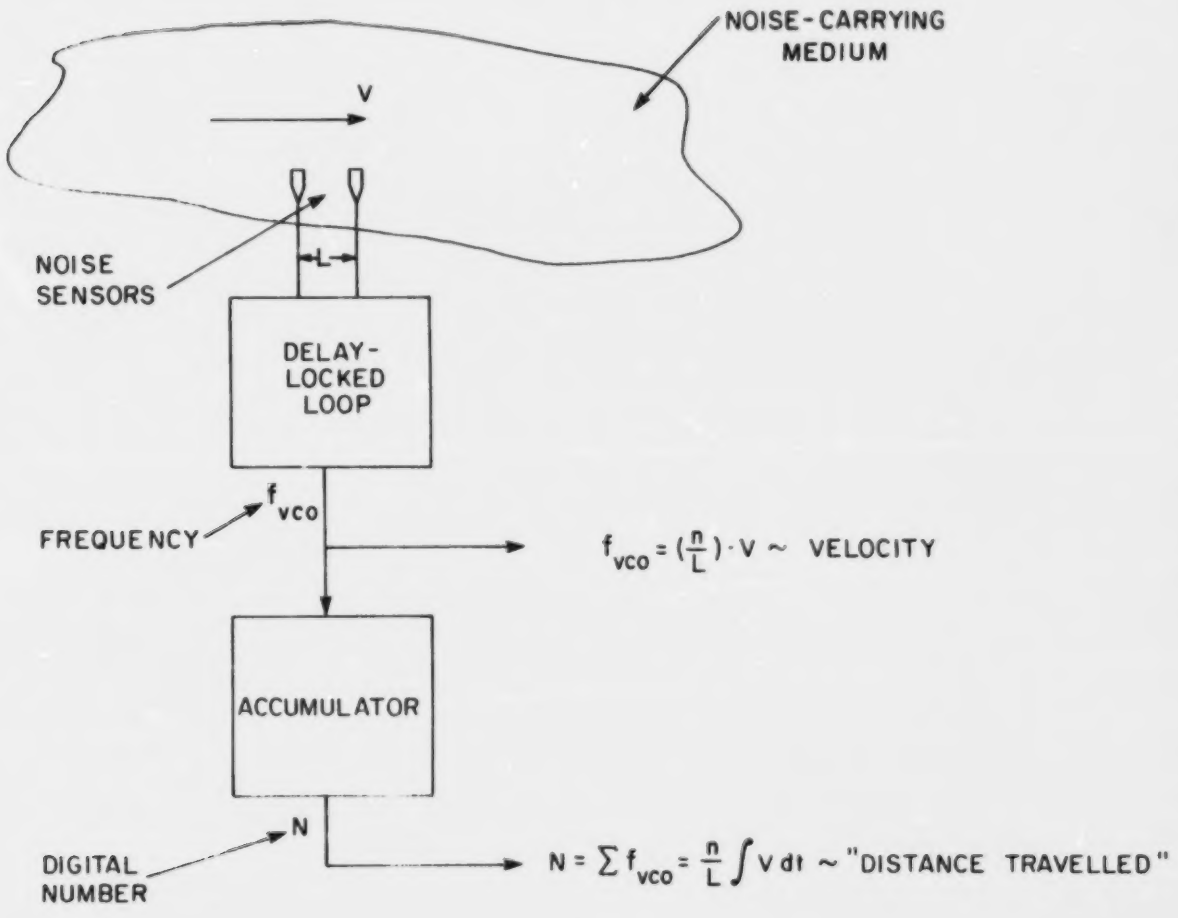
NOISE-CARRYING MEDIUM
V
NOISE SENSORS
L
DELAY-LOCKED LOOP
FREQUENCY
f_{vco}
$f_{vco} = (\frac{n}{L}) \cdot V \sim$ VELOCITY
ACCUMULATOR
DIGITAL NUMBER
N
$N = \sum f_{vco} = \frac{n}{L} \int V\,dt \sim$ "DISTANCE TRAVELLED"

FIG. 3

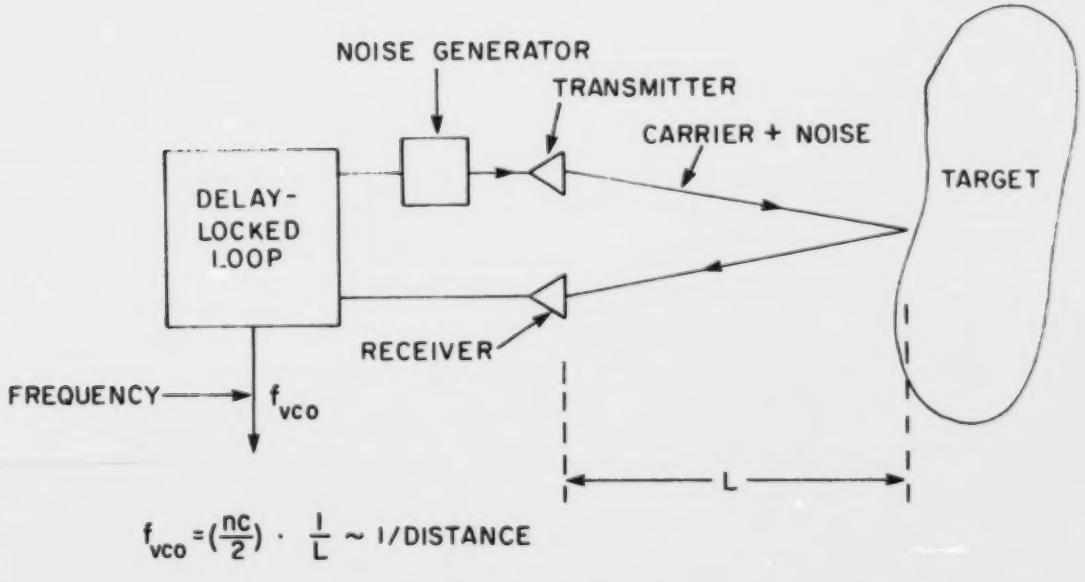
NOISE GENERATOR
TRANSMITTER
CARRIER + NOISE
TARGET
DELAY-LOCKED LOOP
RECEIVER
FREQUENCY
f_{vco}
L
$f_{vco} = (\frac{nc}{2}) \cdot \frac{1}{L} \sim 1/\text{DISTANCE}$

FIG. 4

5.0 DERIVATION OF TRANSFER FUNCTION

5.1 Partial Transfer Functions

The loop components are shown schematically in the block diagram (Fig. 5). The delay, the cross-correlator, and the VCO, have non-linear transfer functions.

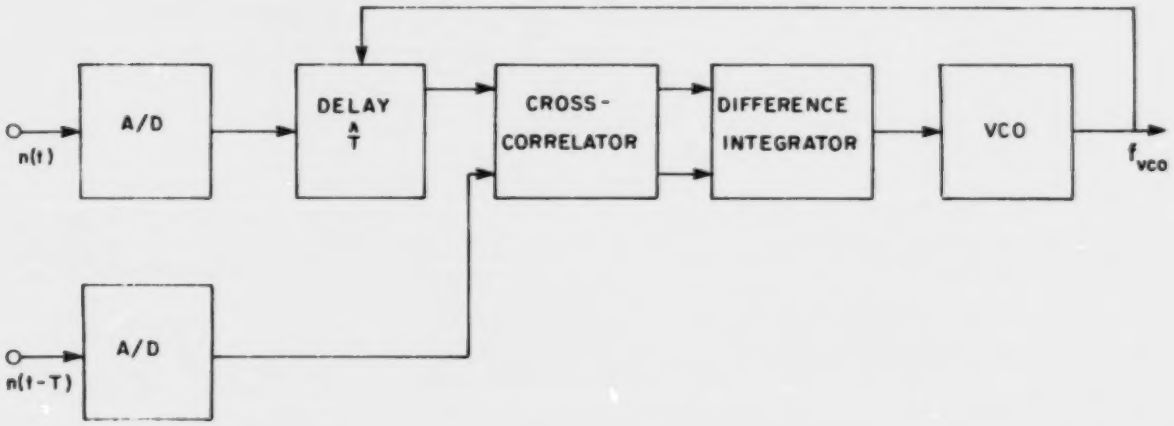

FIG. 5: BLOCK DIAGRAM OF DELAY-LOCKED LOOP

The signal flow diagram (Fig. 6) shows clearly the essential operation of the delay-locked loop, i.e., an electronic variable delay $\hat{T}$ is tracking the input delay T.

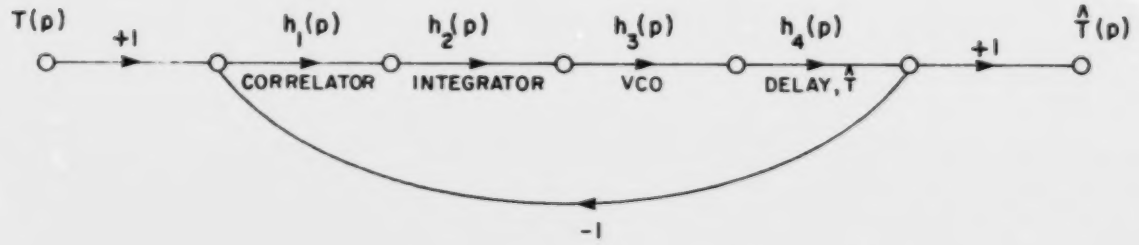

FIG. 6: SIGNAL FLOW DIAGRAM OF DELAY-LOCKED LOOP

Notice the difference between Figure 5 and Figure 6. In Figure 5 the actual in and output signals are shown, whereas Figure 6 represents the mathematically equivalent model.

5.1.1 Cross-Correlator

The cross-correlator operates on two input noise signals, at least partially coherent. We assume for the present discussion that they are completely coherent and analyze later on the effect of adding non-coherent noise. The block diagram of the correlator is shown in Figure 7.

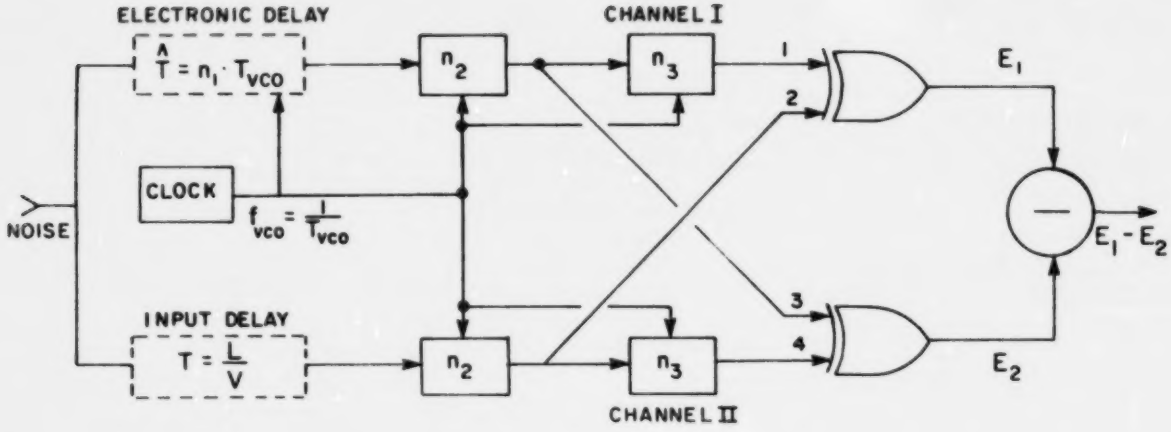

FIG. 7: BLOCK DIAGRAM OF TWO-POINT CORRELATOR

The circuitry is relatively simple for two reasons:

1. Only two points of the cross-correlation function are computed.
2. The information contained in the random zero-crossings of the noise signals is sufficient to operate the delay-locked loop.

The cross-correlation function (Fig. 8) is assumed triangular and symmetrical. The "half-correlation-width" is indicated by $\tau_{1/2}$.

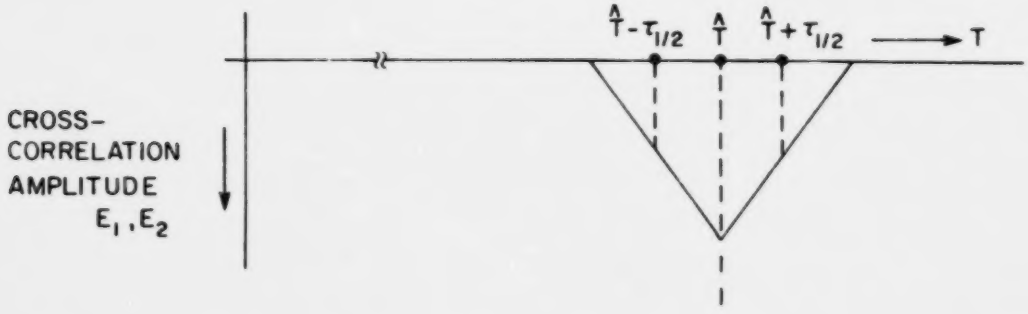

FIG. 8: CROSS-CORRELATION FUNCTION

The delays seen by the inputs of the XOR-GATES in channel I and II are respectively:

$$\text{delay}_{1,2} = (n_1 + n_2 + n_3)T_{VCO} - (n_2 T_{VCO} + T) = \hat{T} - T + n_3 T_{VCO}$$

$$\text{delay}_{3,4} = (n_1 + n_2)T_{VCO} - \left\{(n_2 + n_3)T_{VCO} + T\right\} = \hat{T} - T - n_3 T_{VCO}$$

Figure 9 illustrates the correlation amplitude of both channels and the overall transfer curve as a function of n_3. Notice that the optimum linear transfer curve is obtained for $n_3 T_{VCO} = \tau_{1/2}$.

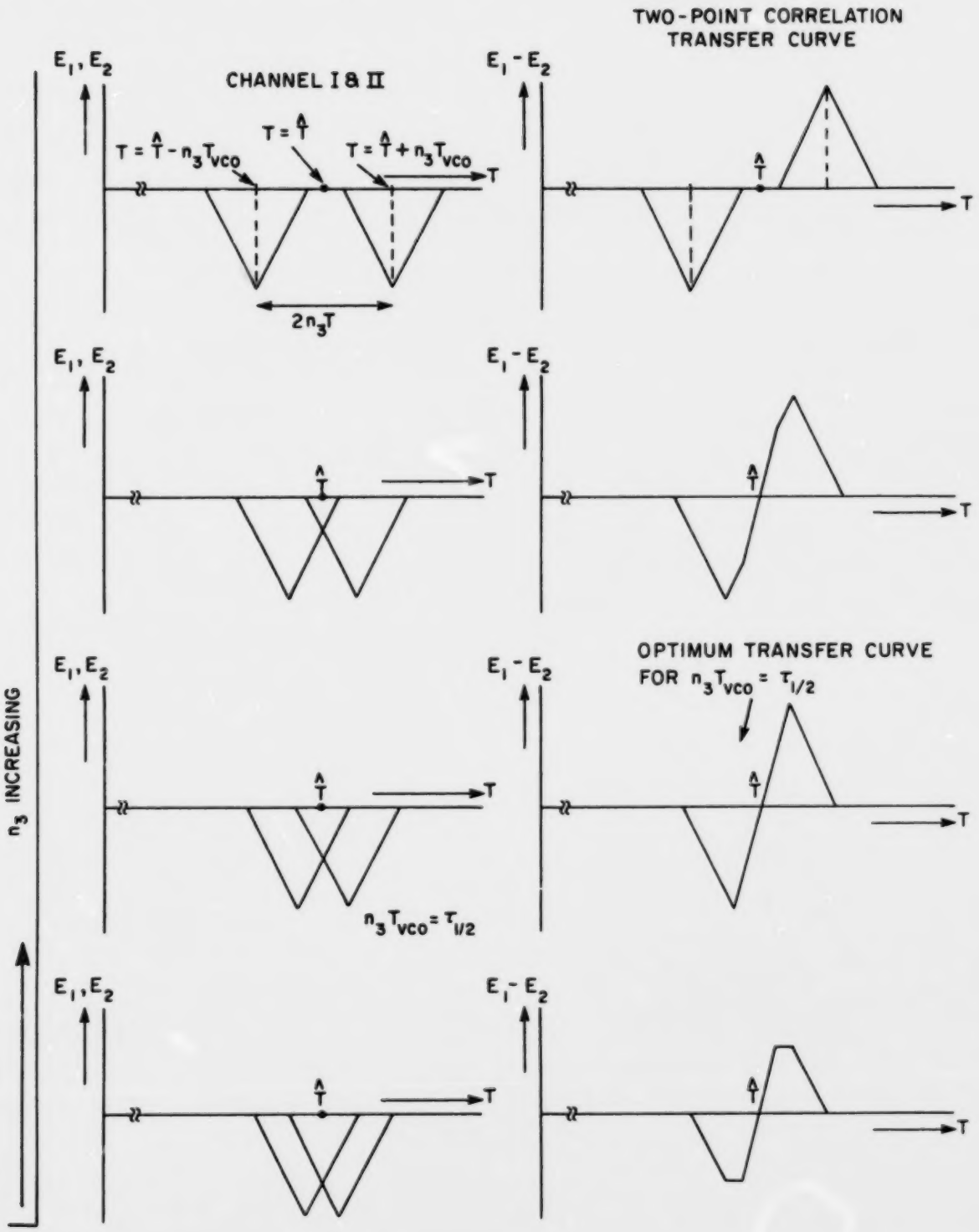

FIG. 9: INFLUENCE OF n_3 ON CROSS-CORRELATION TRANSFER CURVE

The noise input signals have a certain spatial frequency distribution. The relative motion between noise carrying medium and sensors results in a frequency spectrum proportional to velocity. The coherence time constant $\tau_{1/2}$ is therefore inversely proportional to the velocity. Hence, when the input delay decreases due to an increase in velocity, then the correlation transfer curve shifts left and compresses by the same amount that the velocity has increased, see Figure 10. The gain of the correlator is therefore proportional to the velocity.

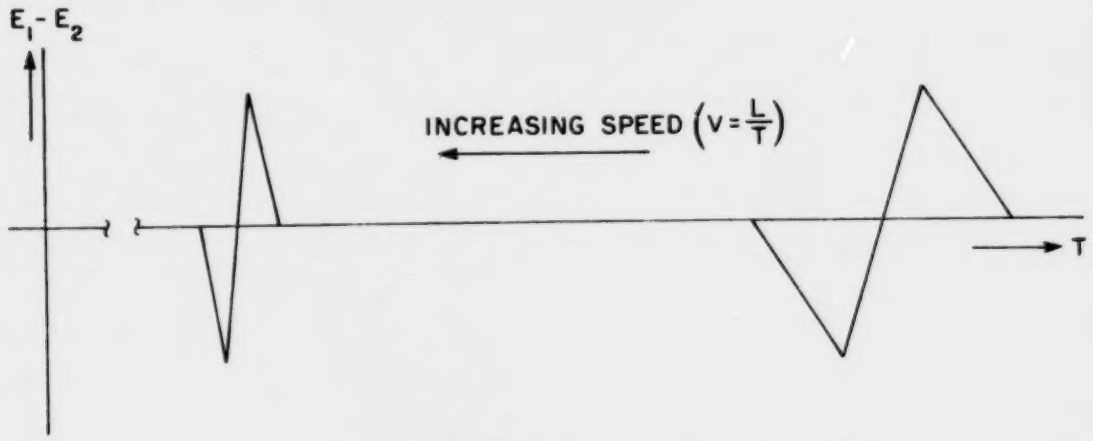

FIG. 10: INFLUENCE OF VELOCITY ON TRANSFER CURVE

Transfer function of correlator

$$(E_1 - E_2) = \left(\frac{2E}{2n_3 T_{VCO}}\right) (\hat{T} - T)$$

which holds for $n_3 T_{VCO} = \tau_{1/2}$, optimum correlator condition.

The loop is in-lock hence:

$T = \hat{T}$

with $T = \frac{L}{V}$ and $\hat{T} = n_1 T_{VCO}$

it follows that:

$$T_{VCO} = \frac{L}{n_1 V}$$

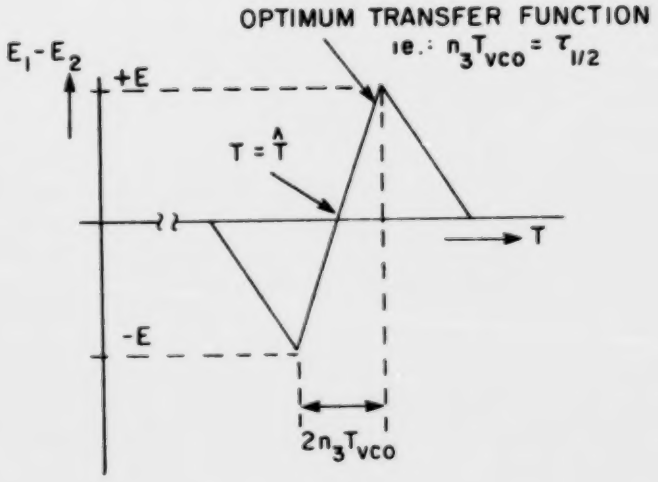

FIG. 11

For the transfer function one can write therefore:

$$h_1(p) = \left(\frac{E_1 - E_2}{\hat{T} - T}\right) = \left(\frac{n_1 E}{n_3 L}\right) \cdot V$$

We have assumed a triangular correlation curve for the input noise signals. This assumption allowed us to characterize the noise signals by the half-correlation time constant $\tau_{1/2}$. The small digital delay $n_3 T_{VCO}$ in the correlator is adjusted to be equal to $\tau_{1/2}$: $n_3 T_{VCO} = \tau_{1/2}$.

The clock period, T_{VCO}, is determined by $T = \hat{T}$, hence $n_1 T_{VCO} = \frac{L}{V}$. Therefore, it is n_3 which reflects the noise properties into the delay-locked loop. Wide band noise gives a small $\tau_{1/2}$ and hence a small n_3 and vice versa for narrow band noise.

5.1.2 Difference Integrator

The transfer function of the difference integrator is:

$$h_2(p) = \left(\frac{E_o}{E_1 - E_2}\right) = -\frac{1}{p\tau}$$

where $\tau = RC$.

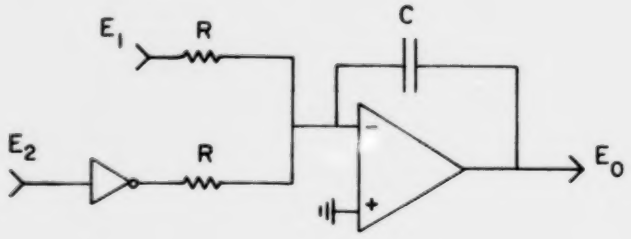

FIG. 12

5.1.3 Voltage Controlled Oscillator

There is a linear relation between the frequency and the input voltage, hence,

$$f_{VCO} = K E_{in}$$

where K is the VCO gain factor.

The period of the oscillation is therefore related to the input voltage as:

$$T_{VCO} = \frac{1}{KE_{in}}$$

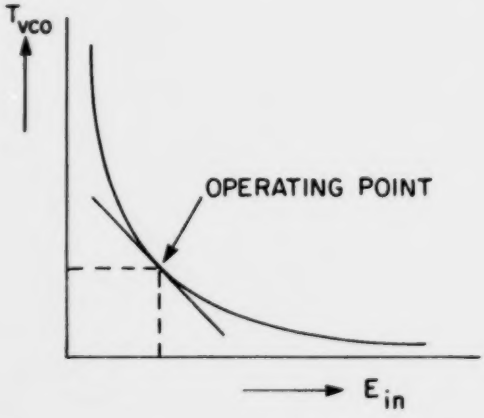

FIG. 13

The small signal transfer gain at the operating point is:

$$h_3(p) = \frac{dT_{VCO}}{dE_{in}} = \frac{-1}{KE_{in}^2}$$

Using the lock-in condition one can express E_{in} as a function of the input variables:

$$T = \hat{T} \Rightarrow \frac{L}{V} = n_1 T_{VCO} \Rightarrow E_{in} = \left(\frac{1}{KT_{VCO}}\right) = \left(\frac{n_1 V}{KL}\right)$$

Substitution given for the small signal **transfer function:**

$$h_3(p) = \left(\frac{dT_{VCO}}{dE_{in}}\right) = -\left(\frac{K L^2}{n_1^2}\right) \cdot \frac{1}{V^2}$$

5.1.4 Delay Line

One can approximate a digital delay line by an analog model if the clock frequency is much larger than the highest significant signal frequency.

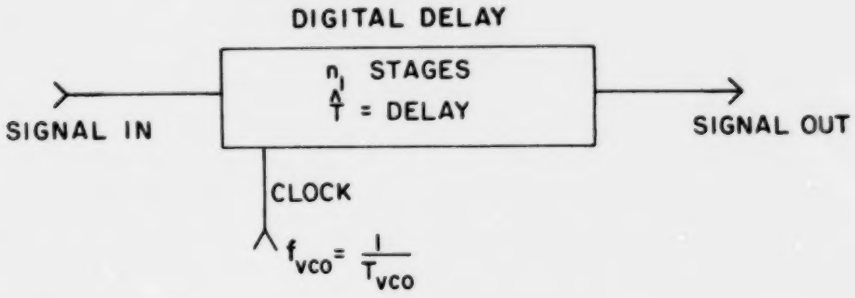

FIG. 14

The static transfer function is:

$$h_1(o) = \frac{\hat{T}}{T_{VCO}} = n_1$$

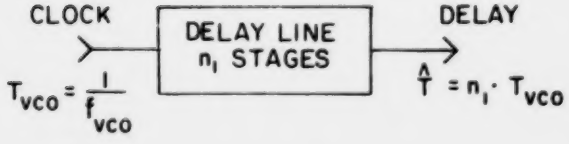

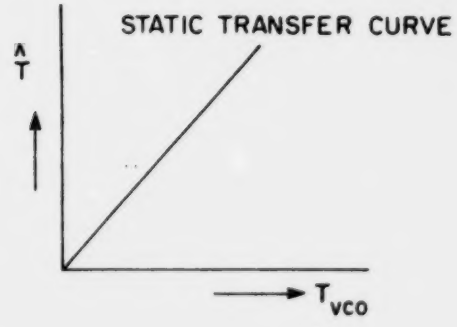

FIG. 15

What is the small-signal dynamic transfer function, as shown in Figure 16?

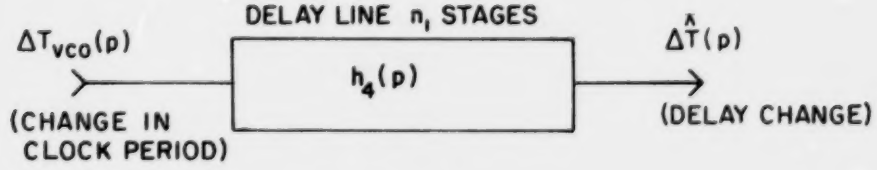

$$h_4(p) = \frac{\Delta\hat{T}(p)}{\Delta T_{VCO}(p)} = ?$$

FIG. 16

If we assume a small step input for the clock period T_{VCO} then the delay response $\Delta\hat{T}$ will be as indicated in Figure 17.

FIG. 17

Taking the Laplace Transform of these signals gives respectively:

$$\Delta T_{VCO}(p) = \frac{b}{p} \text{ and}$$

$$\Delta T(p) = \frac{b}{T_{VCO} p^2} \left(1 - e^{-n_1 T_{VCO} p}\right)$$

The transfer function can be found by dividing the output by the input response, hence:

$$h_4(p) = \frac{\Delta\hat{T}(p)}{\Delta T_{VCO}(p)} = \frac{1}{T_{VCO} p} \left(1 - e^{-n_1 T_{VCO} p}\right)$$

Using the condition $n_1 T_{VCO} \omega << 1$, it follows that,

$$h_4(j\omega) \simeq n_1 \left(1 - j \frac{n_1 T_{VCO} \omega}{2}\right)$$

The transfer function written for a physical realizable system is then:

$$h_4(p) \simeq \frac{n_1}{1 + p\left(\frac{n_1 T_{VCO}}{2}\right)}$$

From the in-lock condition $T = \hat{T}$ it follows that $T_{VCO} = \frac{L}{n_1 V}$; substitution given for the approximate transfer function of the delay line:

$$h_4(p) \simeq \left\{\frac{n_1}{1 + p\left(\frac{L}{2V}\right)}\right\}$$

Notice that the effective time constant, $\frac{L}{2V}$, is a function of the speed V for a given L.

5.2 Closed Loop Transfer Function

The closed-loop transfer function $\psi(p)$ is:

$$\psi(p) = \left[\frac{h_1(p)h_2(p)h_3(p)h_4(p)}{1 + h_1(p)h_2(p)h_3(p)h_4(p)} \right]$$

Substituting the partial transfer functions gives:

$$\psi(p) = \left[\frac{1}{1 + p\left(\frac{n_3 V\tau}{EKL}\right) + p^2\left(\frac{n_3\tau}{2EK}\right)} \right]$$

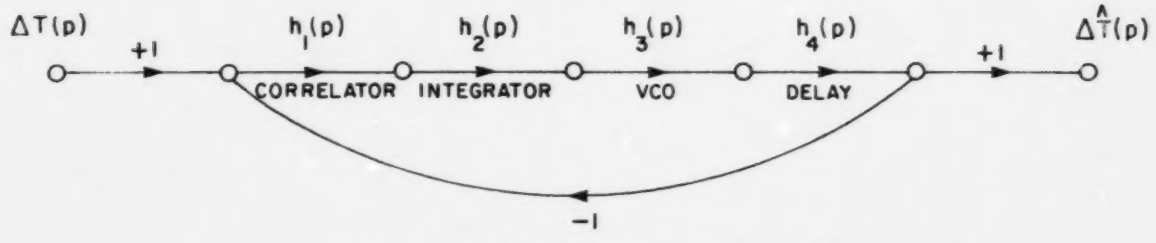

FIG. 18: SIGNAL FLOW GRAPH OF BASIC DELAY-LOCKED LOOP

$\psi(p)$ is the transfer function for the loop, when in-lock, and for optimum correlator operation, i.e., $n_3 T_{VCO} = \tau_{1/2}$.

The transfer function $\psi(p)$ is a second-order low-pass filter of the general form:

$$\psi(p) = \left[\frac{1}{1 + p\left(\frac{d}{\omega_o}\right) + p^2\left(\frac{1}{\omega_o^2}\right)} \right], \text{ where}$$

the natural frequency ω_o is

$$\omega_o = \left(\frac{2KE}{n_3\tau}\right)^{1/2}$$

and the damping factor d is

$$d = \frac{V}{L}\left(\frac{2n_3\tau}{EK}\right)^{1/2}$$

The damping factor d is proportional to the velocity V, whereas the natural frequency ω_o remains constant. Some typical graphs are shown in Figure 19. At high velocities the system is greatly overdamped whereas towards lower speeds the loop becomes very much underdamped. The loop therefore behaves like a first order system at high speed (small delays) and converts gradually to a underdamped second order system for low speeds (large delays).

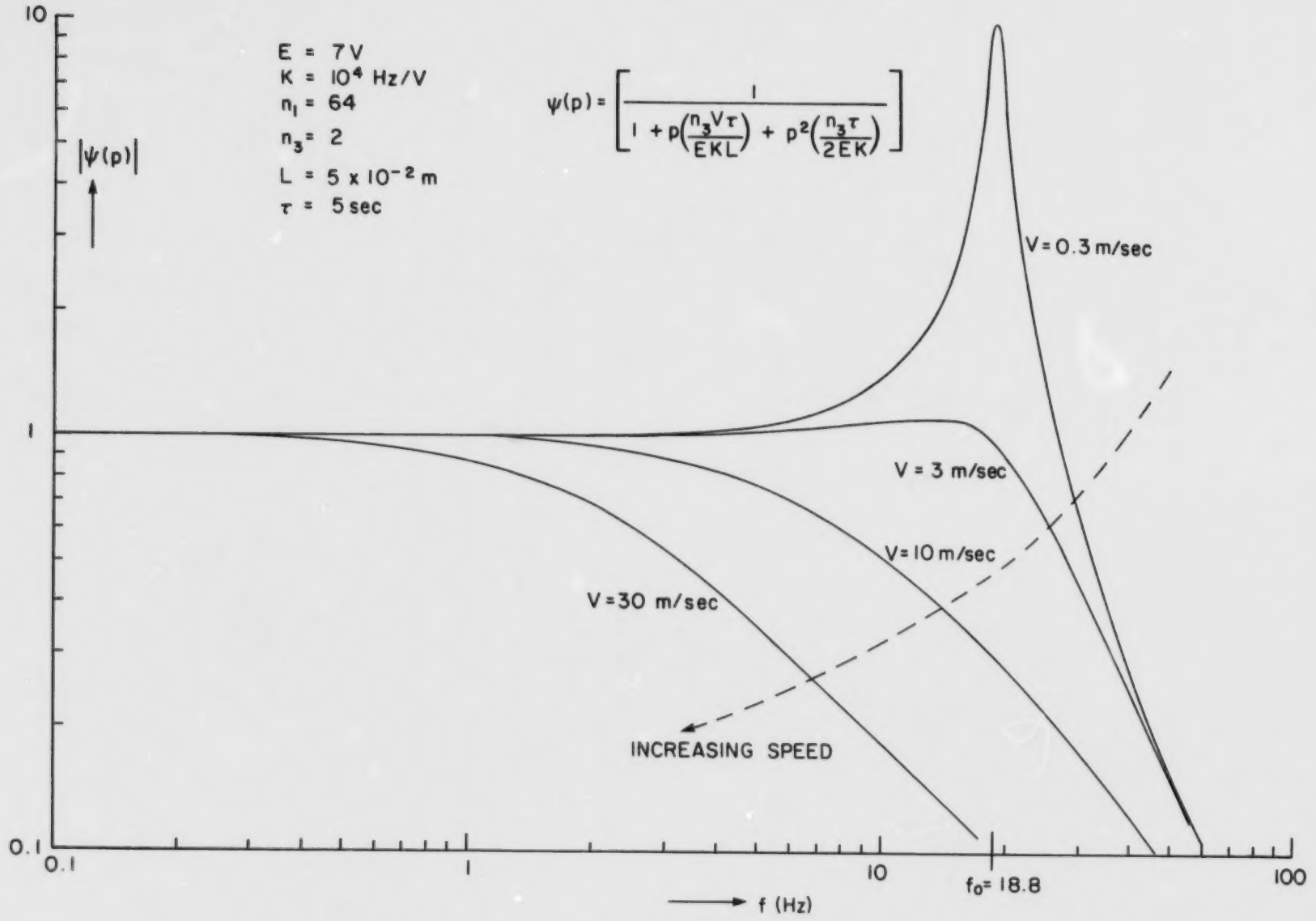
10
1
0.1
0.1
1
10
100
E = 7V
K = 10⁴ Hz/V
n₁ = 64
n₃ = 2
L = 5 x 10⁻² m
τ = 5 sec
|ψ(p)|
ψ(p) = [1 / (1 + p(n₃Vτ/EKL) + p²(n₃τ/2EK))]
V = 0.3 m/sec
V = 3 m/sec
V = 10 m/sec
V = 30 m/sec
INCREASING SPEED
f (Hz)
f₀ = 18.8

FIG. 19

The input noise frequency spectrum shifts proportionally with the magnitude of the velocity. The noise frequency spectrum compresses therefore towards lower velocities. At the same time however the effective bandwidth of the loop increases and becomes undamped.

This is highly undesirable since, at these lower speeds, an increasing portion of the noise frequencies is getting inside the closed-loop bandwidth. The noise level therefore increases substantially, even more so for frequencies close to the resonance frequency. The accuracy of the measurement therefore decreases substantially for the lower velocities. There is also a greatly increased probability for the loop to simply jump out-of-lock.

What can be done to improve the performance of the loop? For instance, is it possible to obtain a maximum flat transfer curve (Butterworth) having a natural frequency which will shift proportionally with the velocity? This certainly could be considered an optimum arrangement for the loop becoming self-adaptive. The bandwidth is automatically "slaved" to the expansion or compression of the noise frequency spectrum as a function of the velocity.

Another useful arrangement would be one where the bandwidth is independent of the velocity, i.e. constant.

The means to obtain these kind of loop performances will be discussed next. It will be shown to consist essentially of introducing appropriate non-linear functions in the loop.

6.0 OPTIMIZING LOOP PERFORMANCE WITH NON-LINEAR FUNCTIONS

The signal flow graph of the delay-locked loop, with a non-linear function included, is shown in Figure 20. The function is inserted between the loop filter and the VCO; it operates therefore on an analog signal.

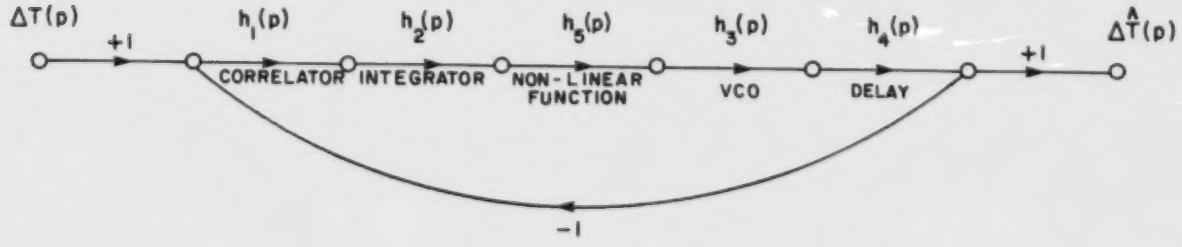

FIG. 20: SIGNAL FLOW GRAPH

The small signal transfer gain of an arbitrary non-linear function at an operating point P is:

$$h_5 = \frac{dE_o}{dE_i} = \frac{d\xi(E_i)}{dE_i} \qquad (1)$$

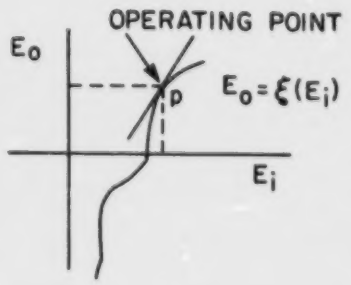

FIG. 21

Substituting the partial transfer functions into the overall transfer function:

$$\psi(p) = \left[\frac{1}{1 + p\left(\frac{n_3 V \tau}{E K L h_5}\right) + p^2 \left(\frac{n_3 \tau}{2E K h_5}\right)} \right] \quad (2)$$

The natural frequency ω_o and the damping factor d are therefore respectively:

$$\omega_o = \left(\frac{2EKh_5}{n_3 \tau}\right)^{1/2} \quad (3)$$

$$d = \left(\frac{2n_3 \tau}{EKh_5}\right)^{1/2} \frac{V}{L} \quad (4)$$

6.1 Inverse Non-Linear System Function

As defined in the previous section a very useful transfer function would be one which has constant damping and a natural frequency proportional to velocity, hence:

$$\omega_o = \gamma V, \text{ and} \quad (5)$$

$$d = \beta = \text{constant} \quad (6)$$

The problem therefore is to find a non-linear function $E_o = \xi(E_i)$ having a derivative h_5 such, that when substituted in (3) and (4) will result in relations (5) and (6).

Solving (3), (4), (5), and (6) gives for h_5 and γ:

$$h_5 = \left(\frac{2n_3 \tau V^2}{\beta^2 EKL^2}\right) \quad (7)$$

$$\gamma = \left(\frac{2}{\beta L}\right) \quad (8)$$

The non-linear function is:

$$E_o = \xi(E_i) \quad (9)$$

The "output" signal of the non-linear function is the input signal to the VCO. For E_o one can write therefore:

$$f_{VCO} = \frac{1}{T_{VCO}} = KE_o \quad (10)$$

hence:

$$E_o = \frac{1}{KT_{VCO}} \quad (11)$$

The loop is in-lock hence $T = \hat{T}$ and therefore,

$$n_1 T_{VCO} = \frac{L}{V} \tag{12}$$

Substituting (12) into (11) gives for E_o:

$$E_o = \frac{n_1 V}{KL} \tag{13}$$

Rewriting (7) gives:

$$h_S = \left(\frac{2n_3 \tau K}{\beta n_1^2 E}\right) \cdot \left(\frac{n_1^2 V^2}{K^2 L^2}\right) \tag{14}$$

From (13) and (14) it follows that,

$$h_S = \left(\frac{2n_3 \tau K}{\beta n_1^2 E}\right) \cdot E_o^2 \tag{15}$$

Substituting $h_S = \frac{dE_o}{dE_i}$ in (15),

$$\frac{dE_o}{dE_{in}} = \left(\frac{2n_3 \tau K}{\beta^2 n_1^2 E}\right) E_o^2 \tag{16}$$

and separating variables gives:

$$\frac{dE_o}{E_o^2} = \left(\frac{2n_3 \tau K}{\beta^2 n_1^2 E}\right) \cdot dE_i \tag{17}$$

Therefore,

$$E_o = - \left(\frac{\beta^2 n_1^2 E}{2n_3 \tau K}\right) \cdot \frac{1}{E_i} \tag{18}$$

The desired function is therefore an inverse function, which is readily implemented with a log-antilog amplifier module.

NOTE: The actual function is implemented in the first quadrant. To maintain correct phasing in the loop, the sign of the difference integrator's transfer gain is reversed by interchanging the input leads.

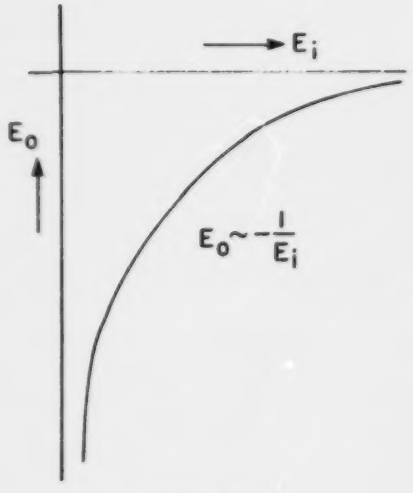

FIG. 22

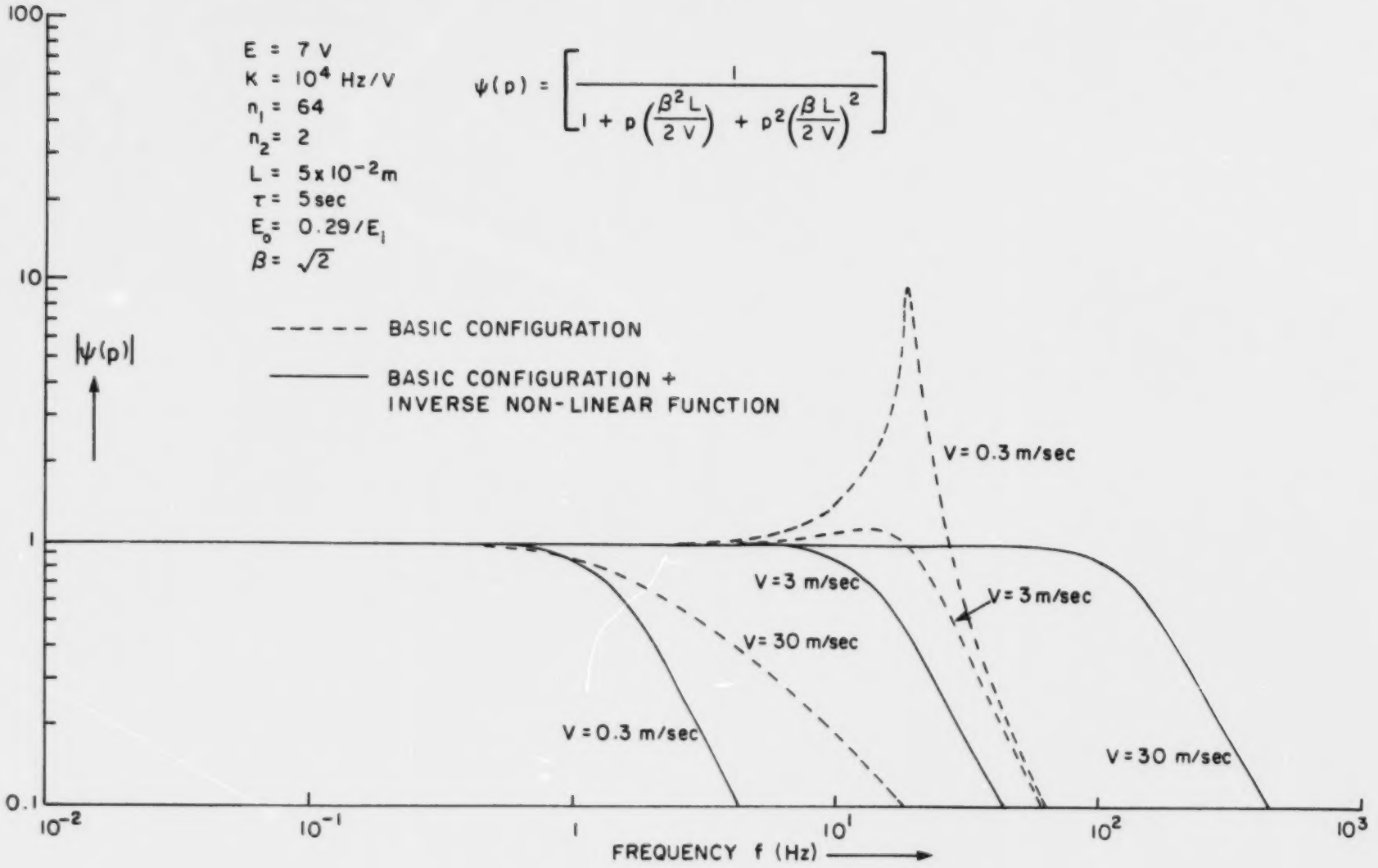
E = 7 V
K = 10^4 Hz/V
n1 = 64
n2 = 2
L = 5x10^-2 m
τ = 5 sec
E0 = 0.29/Ei
β = √2
ψ(p) = [1 / (1 + p(β²L/2V) + p²(βL/2V)²)]
BASIC CONFIGURATION
BASIC CONFIGURATION + INVERSE NON-LINEAR FUNCTION
|ψ(p)|
100
10
1
0.1
V = 0.3 m/sec
V = 3 m/sec
V = 30 m/sec
V = 3 m/sec
V = 0.3 m/sec
V = 30 m/sec
10^-2
10^-1
1
10^1
10^2
10^3
FREQUENCY f (Hz)

FIG. 23

With (5), (6) and (8) substituted in (2) yields for the transfer function $\psi(p)$:

$$\psi(p) = \left[\frac{1}{1 + p\left(\frac{\beta^2 L}{2V}\right) + p^2\left(\frac{\beta L}{2V}\right)^2}\right] \qquad (19)$$

where,

$\omega_o = \left(\frac{2V}{\beta L}\right)$, d = β, V = velocity and L = distance between sensors.

The transfer gain is plotted as a function of velocity V for $\beta = \sqrt{2}$, i.e., optimum flat transfer gain. The improvement in the loop performance is quite evident when comparing the two sets of curves in Figure 23. (The dashed curves represent the same loop configuration without the non-linear inverse function.)

With the non-linear function (18) inserted, the delay-locked loop has become self-adaptive. It automatically adjusts its natural frequency to be proportional to the velocity and it keeps the damping constant, independent of changes in velocity. Moreover, the bandwidth follows the velocity in a linear fashion. As a consequence, the lock-in range at lower speeds is substantially increased relative to the basic loop configuration.

6.2 Exponential Non-Linear System Function

The non-linear inverse function has been derived above by imposing certain conditions on the transfer function. The opposite approach consists of substituting certain simple non-linear functions and to analyze their effect on the transfer function.

This particular technique will be used to analyze the effect on the transfer function of an exponential function

$$E_o = \gamma e^{-\beta E_i} \qquad (20)$$

Hence,

$$h_5 = \frac{dE_o}{dE_i} = -\gamma\beta\ e^{-\beta E_i} \qquad (21)$$

From (20) and (21) it follows that,

$$h_5 = -\beta E_o \qquad (22)$$

The transfer gain is negative. To maintain the appropriate phasing in the loop it will be assumed again that the transfer gain of the difference integrator is invented by interchanging the input leads.

We derived earlier,

$$E_o = \frac{n_1 V}{KL} \qquad (13)$$

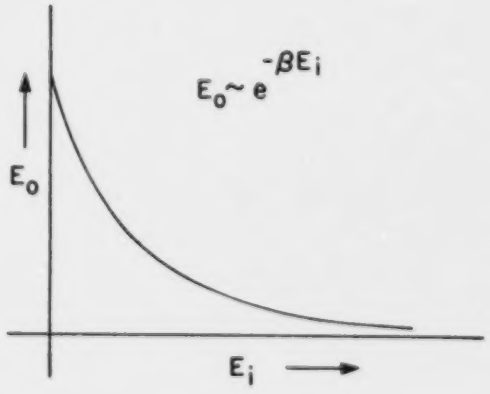

FIG. 24

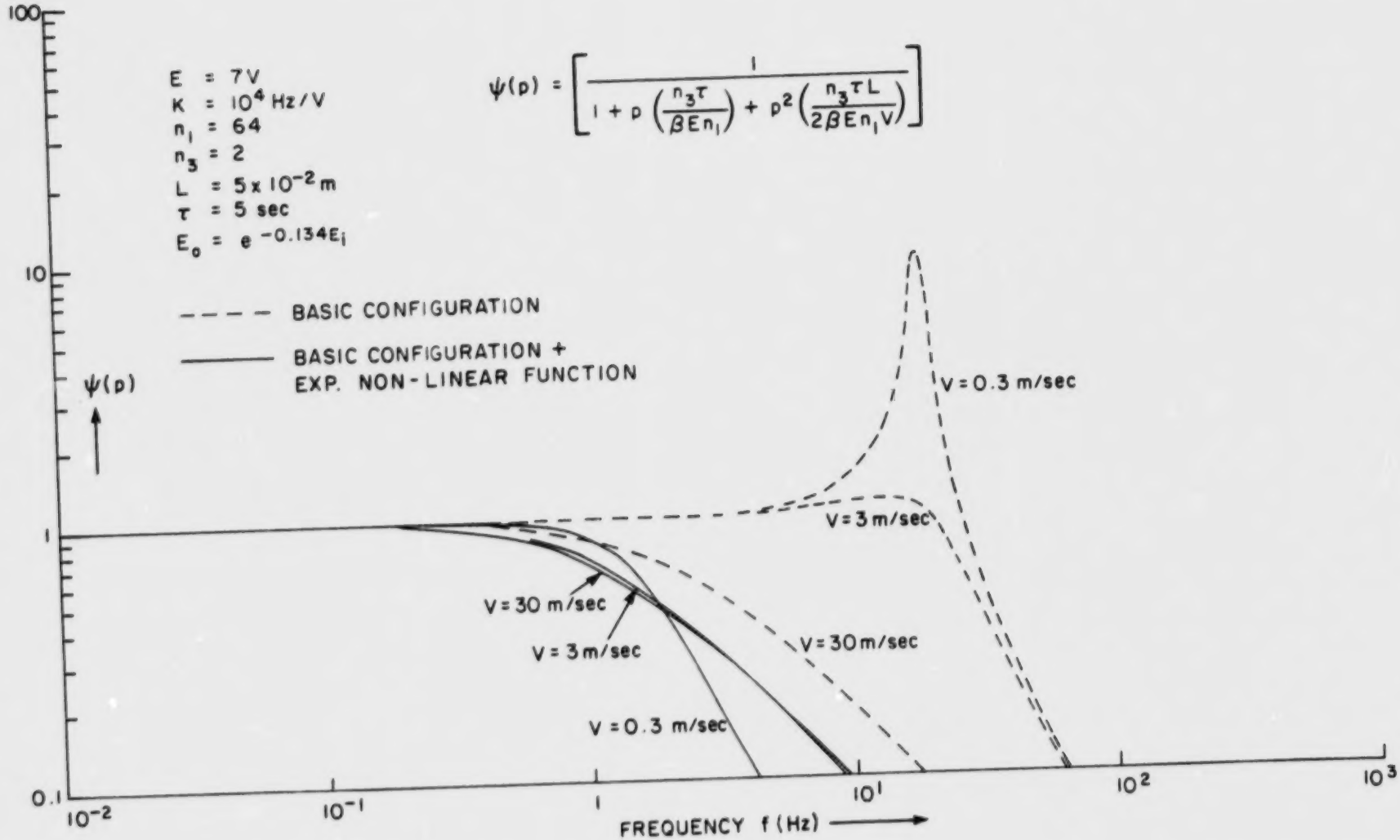
E = 7V
K = 10^4 Hz/V
n_1 = 64
n_3 = 2
L = 5×10^{-2} m
τ = 5 sec
$E_o = e^{-0.134E_i}$
$\psi(p) = \left[\frac{1}{1 + p\left(\frac{n_3\tau}{\beta E n_1}\right) + p^2\left(\frac{n_3\tau L}{2\beta E n_1 V}\right)}\right]$
BASIC CONFIGURATION
BASIC CONFIGURATION + EXP. NON-LINEAR FUNCTION
ψ(p)
100
10
1
0.1
V = 0.3 m/sec
V = 3 m/sec
V = 30 m/sec
V = 30 m/sec
V = 3 m/sec
V = 0.3 m/sec
10^{-2}
10^{-1}
1
10^1
10^2
10^3
FREQUENCY f (Hz)

FIG. 25

and substituting in (22) yields for h_5 :

$$h_5 = -\beta \frac{n_1 V}{KL} \tag{23}$$

With relationship (23) the transfer function $\psi(p)$ becomes:

$$\psi(p) = \left[\frac{1}{1 + p\left(\frac{n_3 \tau}{\beta E n_1}\right) + p^2 \left(\frac{n_3 \tau L}{2\beta E n_1 V}\right)} \right] \tag{24}$$

$$\text{where } \omega_n = \left(\frac{2\beta n_1 EV}{n_3 \tau L}\right)^{1/2} \tag{25}$$

$$\text{and } d = \left(\frac{2n_3 \tau V}{n_1 \beta EL}\right)^{1/2} \tag{26}$$

The transfer gain is plotted as a function of velocity V in Figure 25. The transfer gain curves of the basic loop configuration are shown (dashed lines) for comparison. The coefficient β was chosen such that the transfer gain for $V = 0.3$ m/sec is identical to that of the loop using the inverse non-linear function which is shown in Figure 23.

Whereas the inverse non-linear function gave a bandwidth proportional to velocity, the exponential function results in a virtual constant bandwidth. Only for very low velocities is there a small variation in the transfer gain.

7.0 TRANSDUCER TRANSFER FUNCTION

The transver function $\psi(p)$ has been derived in terms of input and output delays. In an actual delay-locked loop transducer one relates the input velocity V to either the frequency of the VCO or the voltage input of the VCO (if an analog output is required). Figure 26 shows the changes required in the signal flow graph to include these parameters:

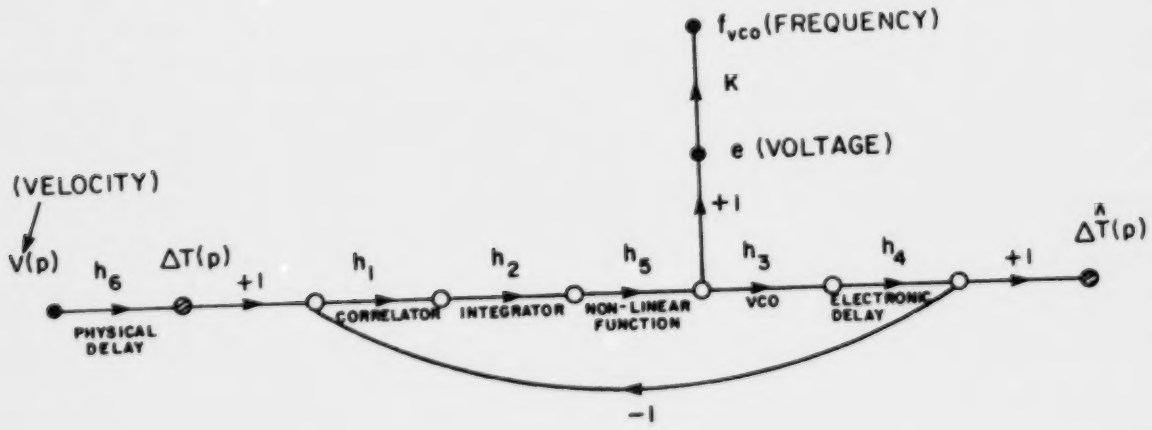

FIG. 26

Using Mason's rules to shift the branch with e and f_{VCO} to the output results in the signal flow graph of Figure 27.

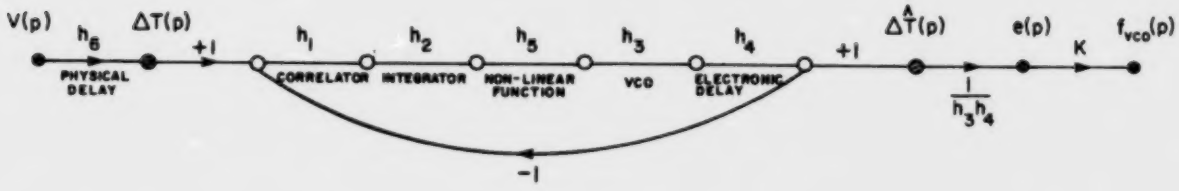

FIG. 27

which can be further simplified to give Figure 28,

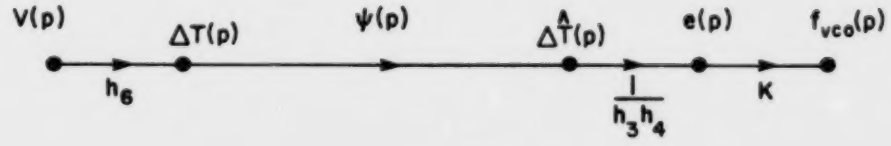

FIG. 28

The transducer transfer functions are therefore:

$$\lambda(p) = \frac{f_{VCO}(p)}{V(p)} = \left(K \frac{h_6}{h_3 h_4}\right) \psi(p), \text{ and} \tag{27}$$

$$\mu(p) = \frac{e(p)}{V(p)} = \left(\frac{h_6}{h_3 h_4}\right) \psi(p) \tag{28}$$

The partial transfer functions h_3 and h_4 have been derived in Sections 5.1.3 and 5.1.4,

$$h_3 = \left(\frac{KL^2}{n_1^2 V^2}\right) \tag{29}$$

$$h_4 = \left(\frac{n_1}{1 + p\left(\frac{L}{2V}\right)}\right) \tag{30}$$

The derivation of h_6, the transfer function of the physical delay, is similar to that of the electronic delay h_4. At an arbitrary operating point P of Figure 29 the transfer function h_6 is:

$$h_6(p) = \left(\frac{\Delta T(p)}{V(p)}\right) = \frac{-L}{V^2}\left(\frac{1}{1 + p\,\frac{L}{2V}}\right) \tag{31}$$

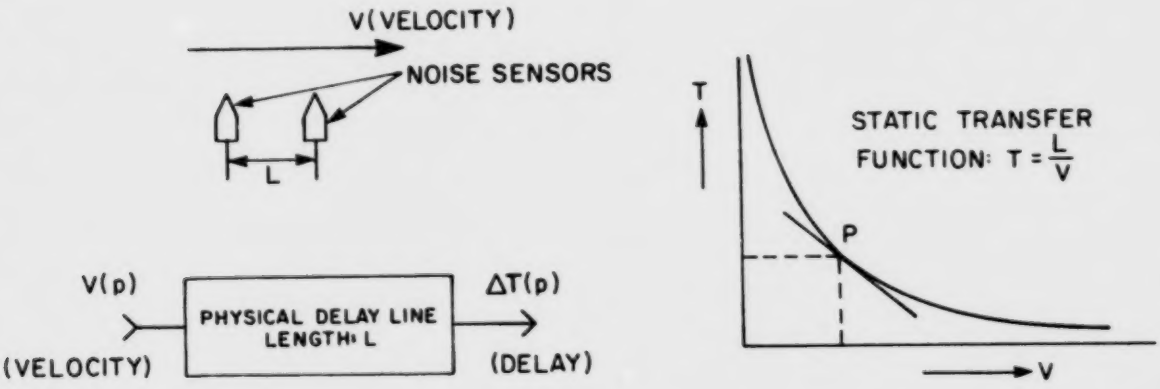

FIG. 29

With (29), (30), and (31) one can write for (27) and (28):

$$\lambda(p) = \frac{f_{VCO}(p)}{V(p)} = \left[\frac{n_1}{L}\,\psi(p)\right] \tag{32}$$

$$\mu(p) = \frac{e(p)}{V(p)} = \left[\frac{n_1}{KL}\,\psi(p)\right] \tag{33}$$

The transducer transfer functions $\lambda(p)$ and $\mu(p)$ differ only from $\psi(p)$ by a scaling factor.

It is therefore very easy to convert the transfer function expressed in terms of delays to the actual input and output parameters.

8.0 OPERATION OF DELAY-LOCKED LOOP FOR CONSTANT VELOCITY

There is a range of applications for the delay-locked loop for which the input delay remains virtually constant. Only small variations around a fixed value are of interest. In these applications we do not need the transfer function to behave reasonably well over a large range of velocities (delays). A typical illustrative example of this mode of operation is shown in Figure 30.

Paper is rolled with constant velocity on a drum. This requires accurate control of the angular speed of the drum to accommodate the increase in diameter as paper accumulates on it. The output frequency of the delay-lock loop is compared with a reference frequency. Any deviation is sensed and used as a control signal for the motor drive. The paper speed is held constant by a progressive decrease in the rotational speed of the drum.

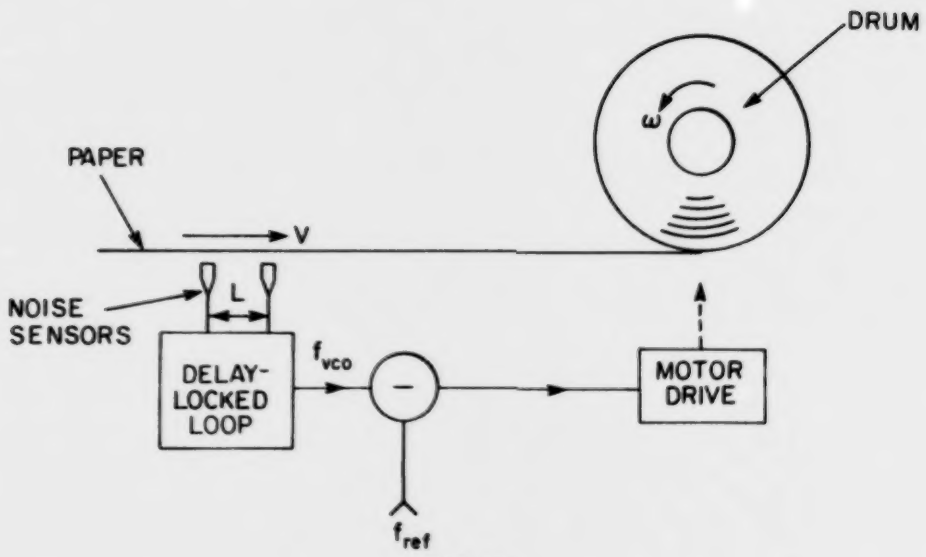

FIG. 30

9.0 ANALYSIS OF PARTIAL COHERENCE AND SIGNAL-TO-NOISE RATIO

The analysis throughout the report is concerned with a loop operating on two noise signals which are 100% coherent. In this chapter some additive non-coherent noise is assumed. A graphical presentation of the noise is given as it proceeds through the comparators, shift registers and the cross-correlator. A simple model is developed for the coherent and the non-coherent loop noise, which is used to analyze the "signal-to-noise" ratio of the loop as a function of the velocity.

9.1 Input/Output Noise Signals of Comparators

The input to the delay-locked loop consists of two random signals. Ideally, they are identical, i.e., coherent, except for a certain time delay T. In a real situation, one has to consider some additive non-coherent noise. This non-coherent noise consists of all other irrelevant noise, internal or external to the loop. The loop therefore operates on two coherent noise signals n(t) and n(t-T), having a certain relative time delay T, and two additive non-coherent noise signals $m_1(t)$ and $m_2(t)$, which are assumed to be independent from each other and the coherent signals.

$$s_1(t) = n(t) + m_1(t) \tag{34}$$

$$s_2(t) = n(t-T) + m_2(t) \tag{35}$$

The comparators operate as 2-bit analog-to-digital converters. A positive input signal is converted into +1 and a negative signal into -1. The non-coherent noise is introduced into the loop in the form of jitter between the corresponding zero-crossings of the two coherent random sequences, as illustrated in Figure 31. If the amplitude of the coherent noise is well above the amplitude of the non-coherent noise, this will be the major source of noise in the loop. However, if the non-coherent noise signals increase in amplitude, then an additional form of noise will be introduced, i.e.; additional random transitions will be present (Fig. 32). A reasonable "signal-to-noise" ratio is assumed, so that the latter form of noise will be only marginal.

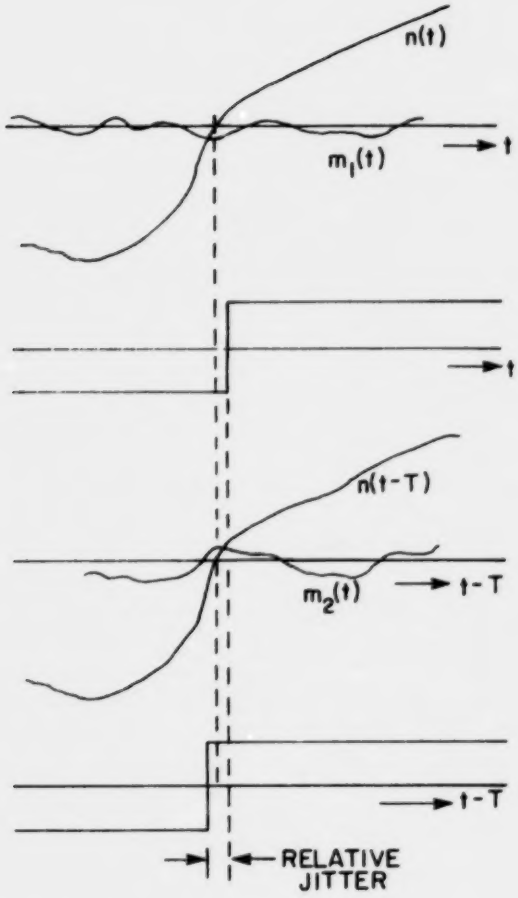

FIG. 31: RELATIVE JITTER

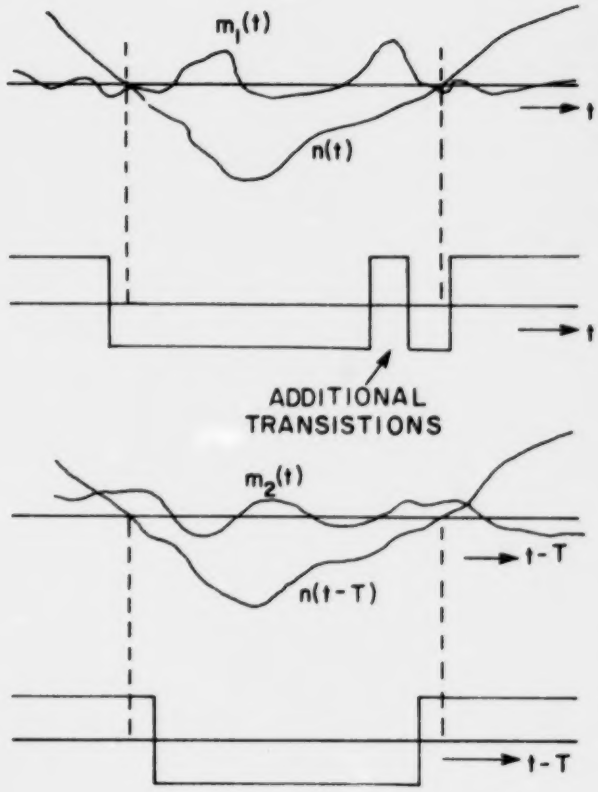

FIG. 32: ADDITIONAL TRANSITIONS

9.2 Noise in Shift Registers

The output random sequences of the comparators are sampled at a rate determined by the frequency, f_{VCO}, of the voltage controlled oscillator, and shifted into the registers at each positive clock transition. Errors in sampling the correct polarity occur, due to jitter, primarily at the zero-crossings of the coherent signals. Sampling in between will be correct most of the time, except when the coherent noise amplitude happens to be very small and comparable to the non-coherent noise.

The sampling process and the resulting signals in the shift registers are illustrated in Figure 33.

Figure 33(a) shows the ideal case: there is no additive non-coherent noise; the two random sequences line up perfectly.

Figure 33(b) illustrates the "dead-zone" inherent in the sampling process due to quantization in the time-domain. Therefore, small random jitter does not necessarily produce a relative timing error of the signals in the shift register. Also, jitter in the zero-crossings cancels out in the shift registers if they are comparable and of the same polarity, as illustrated in Figure 33(c).

Figures 33(d), (e) illustrate relative time errors developing in the two sequences in the shift registers. The probability of errors equalling two, three, or more clock periods, progressively lessens.

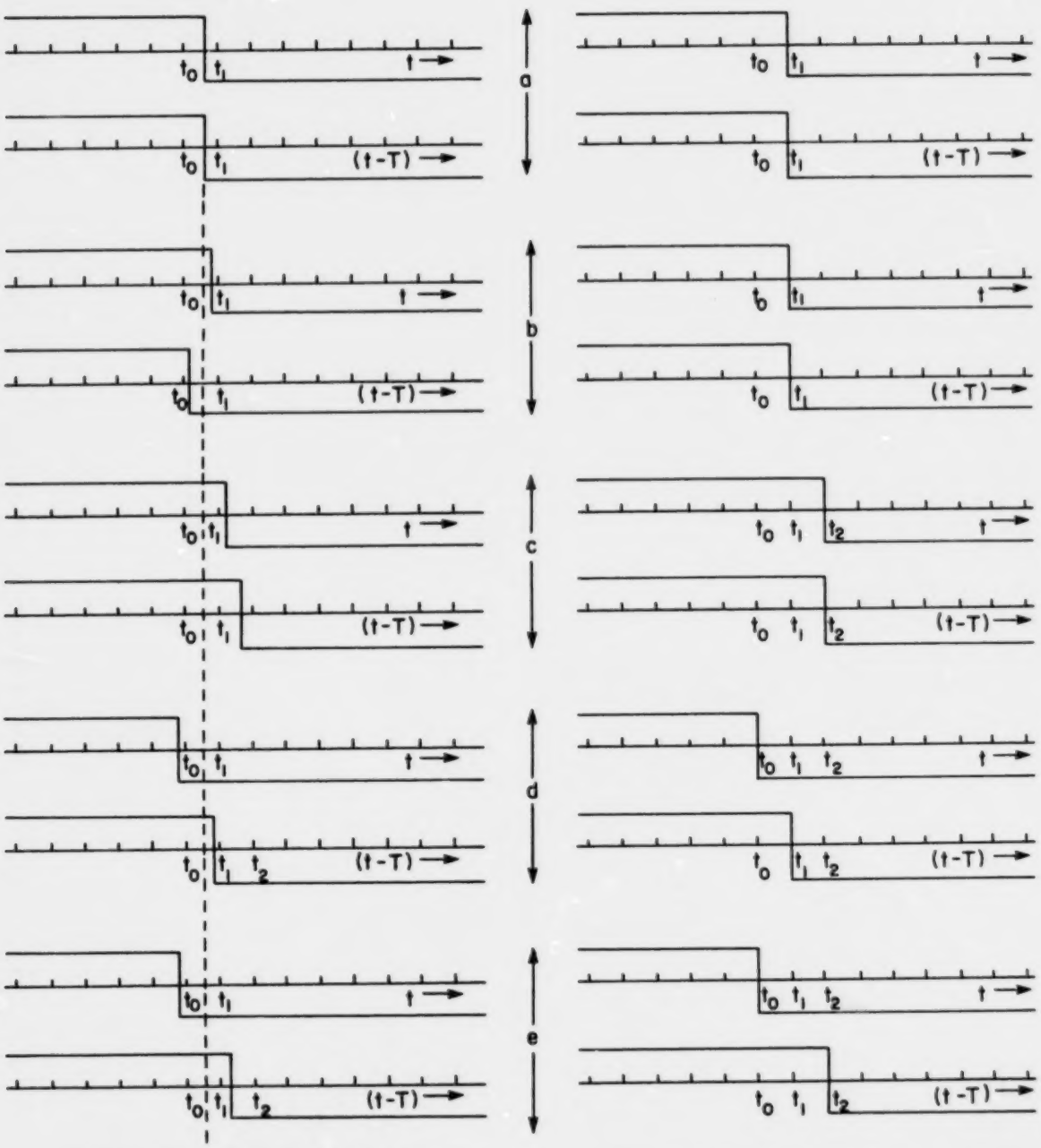

RANDOM SEQUENCES AT OUTPUTS OF ZERO-CROSSINGS DETECTORS

RANDOM SEQUENCES IN SHIFT REGISTERS

FIG. 33

9.3 Processing of Noise Signals by Cross-Correlator

The processing of two coherent random sequences, with some additive non-coherent noise, by the cross-correlator is illustrated in Figure 34. $s_1(t)$ and $s_2(t)$ are the two coherent random sequences in the shift registers for $T = \hat{T}$.

$s_1(t + \tau) \times s_2(t - \tau)$ and $s_1(t - \tau) \times s_2(t + \tau)$ are the "late-early" and "early-late" multiplications.

$s_1(t + \tau) \times s_2(t - \tau) - s_1(t - \tau) \times s_2(t + \tau)$ is the difference output signal.

As shown, each relative time error produces two pulses in the output having the same polarity and width.

For non-coherent noise, these pairs of pulses are random with regard to their polarity. The average DC-value is therefore zero. The width of these pulses will be a multiple of the VCO period. For well-behaved input signals, i. e. those with a high degree of coherence, the width of these pulses is nominally zero, one, or two clock periods. Widths of three and more clock periods will have a progressively reduced probability to occur.

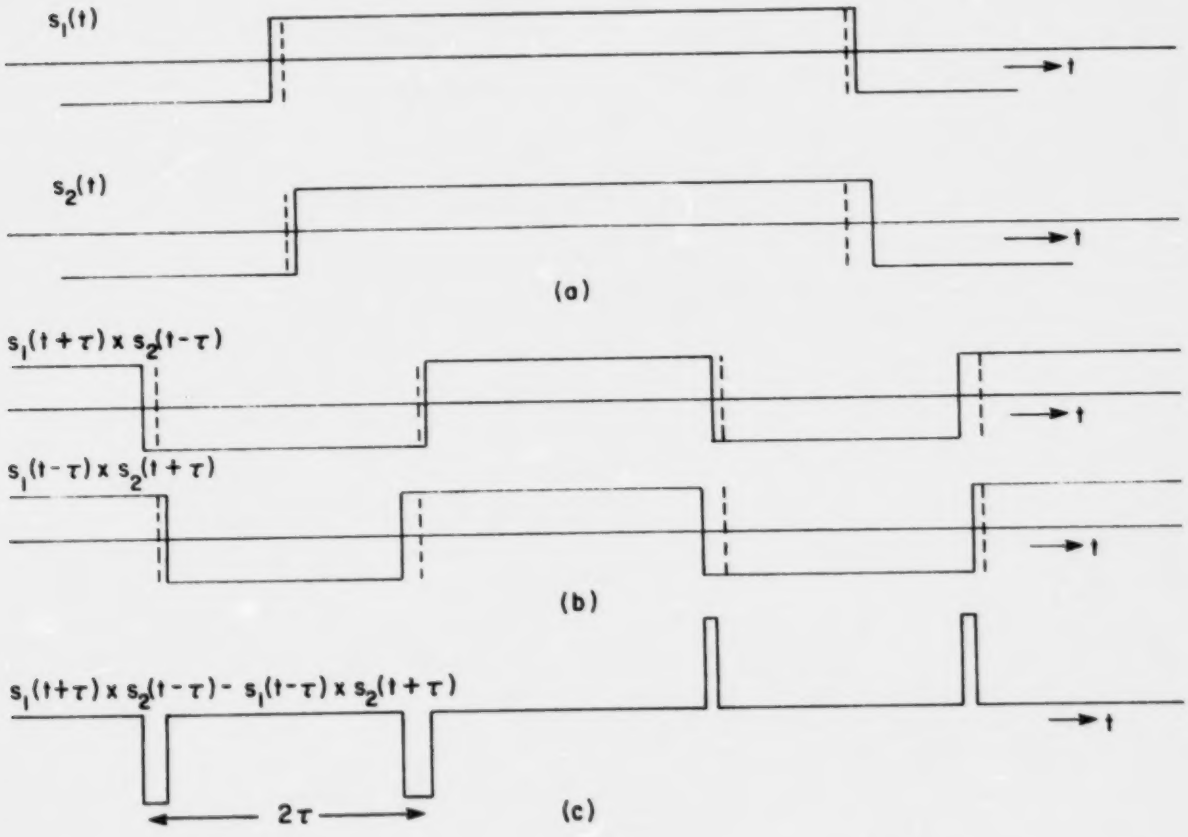

FIG. 34

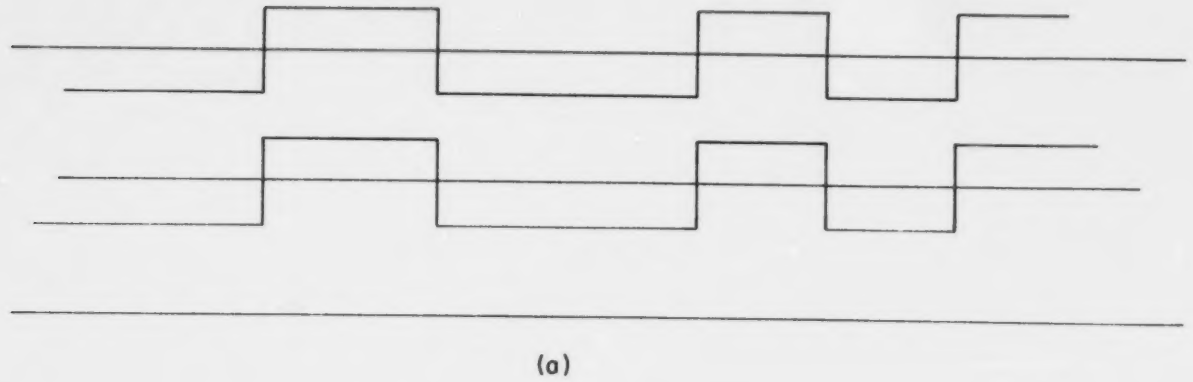

(a)

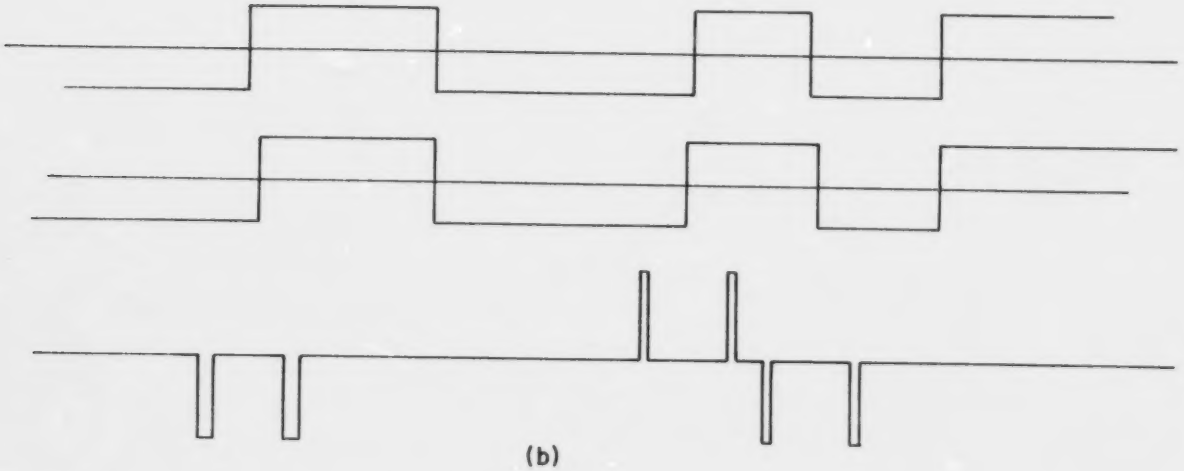

(b)

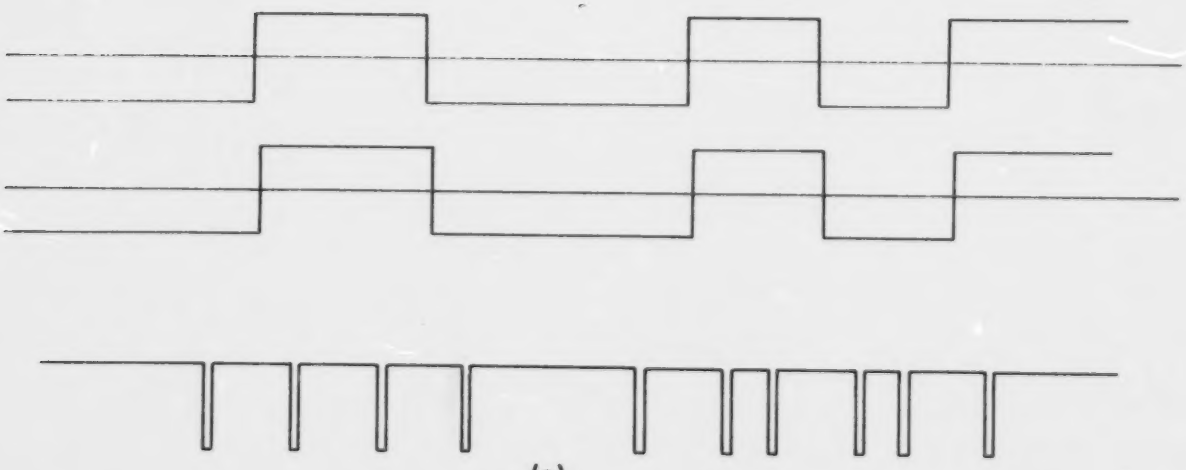

(c)

FIG. 35: OUTPUT WAVEFORMS OF CROSS-CORRELATOR

9.4 Intrinsic Noise and Additive Noise

The output noise of the cross-correlator is made up of two parts: "intrinsic noise" and "additive noise". Intrinsic noise is caused by the coherent input noise signals, whereas, additive noise is related to the non-coherent input noise signals.

It can be shown [4] that the power spectrum of intrinsic noise vanishes for a loop which is in-lock, $T = \hat{T}$, and in steady-state conditions, $\frac{dT}{dt} = 0$. However, when the loop operates for dynamic conditions, $\frac{dT}{dt} \neq 0$, there will be small deviations from the ideal lock-in condition and the coherent noise will generate some intrinsic noise at the output of the cross-correlator.

These different contributions of the coherent and non-coherent noise can be readily visualized as illustrated in Figure 35.

Figure 35(a) shows the ideal case: 100% coherence and stationary conditions. The random output sequences are identical and the difference signal is zero. Therefore, the power spectrum of the intrinsic noise vanishes.

Figure 35(b) illustrates the case of partial coherence for steady state conditions. The difference noise signal represents additive noise.

Figure 35(c) shows the case of 100% coherence, but with a small deviation from the ideal lock-in condition, as happens for dynamic operation of the loop. The resulting difference signal consists of a random sequence of uni-polar pulses. Hence, there is an average DC signal on which the loop operates, as well as intrinsic noise.

9.5 Equivalent Models for Intrinsic and Additive Noise

Using the graphical illustration of the cross-correlator noise signals as reference (Fig. 34), simple models for the intrinsic and additive noise are developed.

A reasonable degree of coherence is assumed, i.e. the amplitude of the coherent noise signals is substantially above those of the non-coherent noise.

From the additive noise time sequences shown, Figures 34, 35(c), it can be concluded:

1. pulses have constant amplitude
2. the width of the pulses is determined by the clock period
3. time between pulses of one pair is dependent upon the cross-correlation delay time
4. time between subsequent pulse pairs is determined by the zero-crossings of the coherent noise signals
5. the polarity of the pulse pairs is determined by the relative amplitude of the two non-coherent noise signals at the input of the comparators.

Notice that only the polarity is determined by the non-coherent noise signals. The operation can be viewed as a random sampling of a random signal. The random polarity of the pulses is determined at a random time, i.e. at the zero-crossings of the coherent noise signal.

When the coherent noise signals are compressed due to an increase in velocity, there is an equivalent compression in the pulse width as well as in the time interval between pulses. The correlator output signal is therefore compressing linearly with increasing speed.

The random polarity of the pulses is determined by the non-coherent noise. If the non-coherent noise is variant, it will also compress linearly with velocity. The random distribution of the polarity therefore remains unchanged, since both the "sampling signal" and the "sampled signal" compress equally with increasing velocity. Hence, the additive noise is variant.

Should the non-coherent noise input signals be invariant, the pulse width and the time interval between pulses will still compress linearly with velocity because non-coherent noise only affects the random distribution of the polarity of the pulses. The invariant non-coherent noise is therefore, at least partially, converted into variant additive noise.

The coherent noise is "sampling" the non-coherent noise. Moreover, the coherent noise time sequence is compressing as the velocity increases. Intuitively, it seems therefore reasonable to assume complete conversion of the invariant non-coherent noise into variant self-noise at low velocities and a partial conversion at very high velocities.

The invariant non-coherent noise is usually smaller in amplitude than the variant non-coherent noise. Moreover, it is largely converted into variant additive noise. Therefore it may be assumed that the additive noise is variant.

The non-coherent noise can either be variant or invariant with regard to its frequency spectrum. The non-coherent noise generated along side the coherent noise will likely be variant, whereas, the noise in the sensors and the associated amplifiers is typically invariant. It has been shown above that the additive noise of the cross-correlator can be considered to be variant, even if some of the input non-coherent noise is invariant.

Compressing a random signal in the time domain is equivalent to expanding its amplitude spectrum in the frequency domain. Therefore, the additive noise can be modelled as a series of independent sinusoidal oscillators with constant amplitudes but having frequencies linearly related to the velocity.

It was shown in Figure 35(a) that the coherent noise does not produce intrinsic noise for steady state conditions, i.e. $T = \hat{T}$ and $\frac{dT}{dt} = 0$. For dynamic conditions there will be a small tracking error and, as shown in Figure 35(b), intrinsic noise is generated.

The width of the intrinsic noise pulses is a linear function of the delay tracking error, $T - \hat{T}$. This error depends on the input signal parameter T. Therefore, the input signal must be specified to be able to generate an equivalent model for the intrinsic noise. A simple but realistic behaviour for $T - \hat{T}$ as a function of the velocity is assumed, i.e., a constant relative delay tracking error, independent of the velocity: $(T - \hat{T})/T$ = constant. Hence, the width of the intrinsic noise pulses is a linear function of the velocity. Therefore, as for the additive noise, the intrinsic noise sequence compresses linearly with velocity resulting in an equivalent expansion in the frequency domain of its amplitude spectrum.

Therefore, the intrinsic noise can be modelled as a series of independent sinusoidal generators having frequencies linearly related to velocity. This, as stated above, is for the condition that a constant percentage error is assumed, for all velocities, in the tracking error.

9.6 Signal-to-Noise Ratio

The behaviour of the signal-to-noise ratio is analyzed, for intrinsic as well as additive noise as a function of velocity, for two types of loop transfer functions: bandwidth proportional to velocity (inverse non-linear function) and constant bandwidth (exponential non-linear function).

The signal-flow-graph of the delay-locked loop, including the output noise signal of the cross-correlator, is shown in Figure 36.

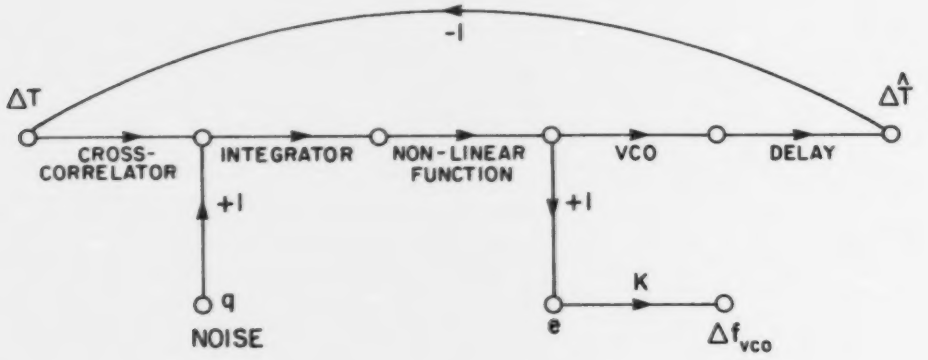

FIG. 36: SIGNAL FLOW GRAPH OF DELAY-LOCKED LOOP WITH NOISE

The signal parameter measured will be either the input voltage or the frequency output of the voltage controlled oscillator. Therefore the small-signal noise transfer functions of interest are: e/q and $\Delta f_{VCO}/q$. They are equivalent except for a scaling factor K.

Signal Bandwidth Proportional to Velocity

The noise transfer function, using the inverse non-linear function, can be derived as

$$\frac{\Delta f_{VCO}(p)}{q(p)} = \frac{n_1 n_3 V}{EKL} \cdot \left[\frac{1 + \frac{L}{2}\left(\frac{p}{V}\right)}{1 + \left(\frac{n_3 KL\beta\tau}{n_1^2 E}\right)\left(\frac{p}{V}\right) + \left(\frac{n_3 KL^2\beta\tau}{2 n_1^2 E}\right)\left(\frac{p}{V}\right)^2} \right] \tag{36}$$

The additive noise is modelled above as a series of sinusoidal oscillators having a constant amplitude but with frequencies linearly related to velocity. Hence, for each oscillator: $p = j\omega \sim V$ or $|j\omega/V| = \text{constant}$. Therefore, from (36) it can be seen that:

$$\left| \frac{\Delta f_{VCO}(j\omega)}{q(j\omega)} \right| \sim V \quad \text{or} \tag{37}$$

$$\left|\Delta f_{VCO}(j\omega)\right| \sim \left|q(j\omega)\right| \cdot V \tag{38}$$

$|q(j\omega)|$ = constant. Therefore, each noise component has an amplitude which increases linearly with velocity.

The frequency, f_{VCO}, also increases linearly with velocity.

As a result, a constant signal-to-noise ratio is maintained in the loop. This conclusion has been confirmed by experiments.

The model developed for the intrinsic noise, for constant relative delay-error, is equivalent to that of the additive noise. Hence, at any given velocity the same percentage of error in the delay results in a constant signal-to-noise ratio with regard to the intrinsic noise.

Signal Bandwidth Constant, Independent of Velocity

The noise transfer function, using the exponential non-linear function, is

$$\frac{\Delta f_{VCO}(p)}{q(p)} = \frac{n_3 V}{EKL}\left[\frac{1 + p\left(\frac{L}{2V}\right)}{1 + \left(\frac{n_3 \tau}{n_1 \beta E}\right)p + \left(\frac{n_3 \tau L}{2n_1 \beta E}\right)\frac{p^2}{V}}\right] \tag{39}$$

Except for very low velocities, one can approximate this transfer function by

$$\frac{\Delta f_{VCO}(p)}{q(p)} = \frac{n_3 V}{EKL}\left[\frac{1}{1 + \frac{n_3 \tau}{n_1 \beta E}\, p}\right] \tag{40}$$

The loop bandwidth is constant and independent of velocity.

The additive noise is modelled as a series of sinusoidal components with constant amplitude and with a frequency linearly related to velocity. It has also been assumed, for the small loop bandwidth, that the noise power spectrum is uniform.

As the velocity increases, so too does the amplitude of each noise component as it passes through the loop to the output, as can be seen from (40). While the noise spectrum is expanding linearly with velocity, the power spectral density increases in proportion. With constant loop bandwidth it follows that the rms output noise amplitude will increase as the square root of the velocity. The output frequency, f_{VCO}, increases linearly with velocity.V. Therefore, the signal-to-noise ratio will improve as the square root of the velocity V.

The signal to noise ratio for intrinsic noise, since it behaves similarly to the additive noise, has the same relation to the velocity. Again it must be remembered that the percentage error in the delay is assumed constant when the velocity is varied.

10.0 MEASUREMENT OF DISTANCE AND "DISTANCE TRAVELLED"

The delay-locked loop measures length in two different ways: dynamically and statically.

Dynamically: The delay-locked loop measures the relative velocity between sensors and medium. The frequency output is proportional to the velocity. Each period represents a small displacement interval. Hence, simply counting the periods gives a number proportional to the "distance travelled".

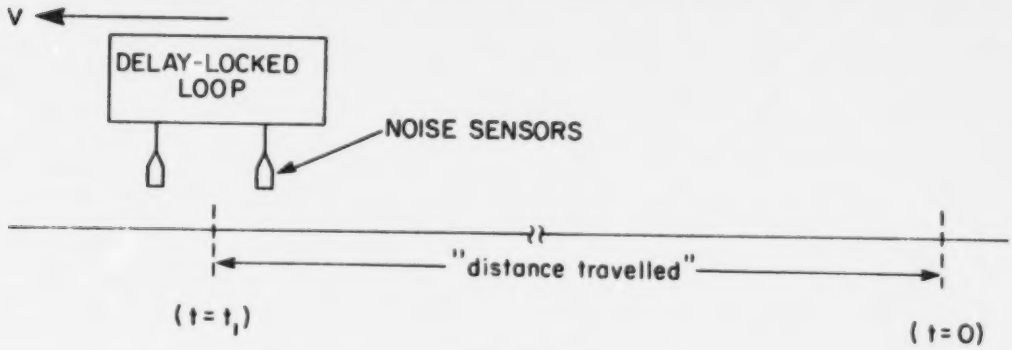

FIG. 37

Statically: The delay-locked loop measures the turn-around delay time of a noise modulated carrier between transmitter and receiver. The output frequency is proportional to the inverse of the distance to the target.

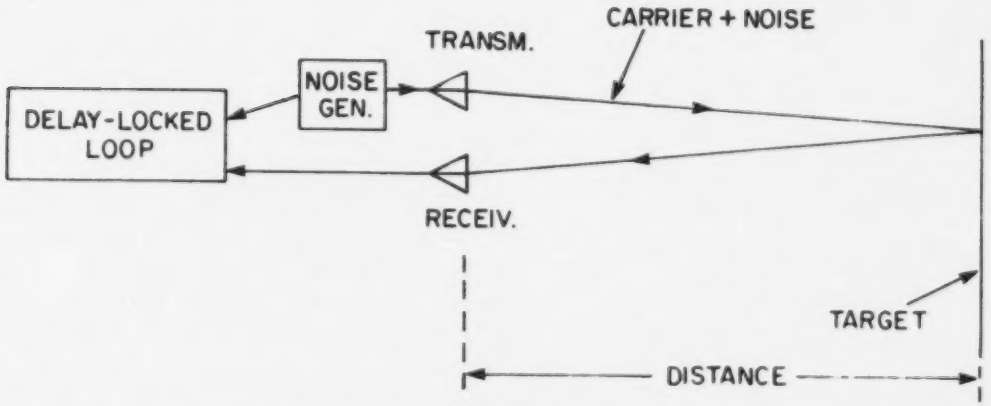

FIG. 38

We will first be concerned with the measurement of "distance travelled". The measurement of distance will be analyzed in Section 13.0.

The analysis is general. However, the prototype delay-locked transducer, designed by the author, will be used on rail vehicles. Therefore, the numerical examples given in graphical form are related to values of velocity and acceleration typical of rail vehicles.

The accuracy of the delay-locked loop for quasi-static conditions is very high. Typically it is limited by the accuracy with which one can define the separation between the sensors. The loop takes a finite time to acquire lock. This introduces a small error at start-up. Moreover the loop cannot maintain lock at very low values of velocities. We will, however, not be concerned with these aspects of accuracy, being specific to the type of transducer used and methods of calibration.

The analysis will be concerned with the measuring error for dynamic signal conditions. In effect close tracking cannot be maintained if there are dynamic variations in the velocity. This introduces errors in the velocity and hence "distance travelled". The acceleration and deceleration of rail vehicles are fairly constant. The loop behaviour will therefore be analyzed for positive and negative ramp inputs of velocity.

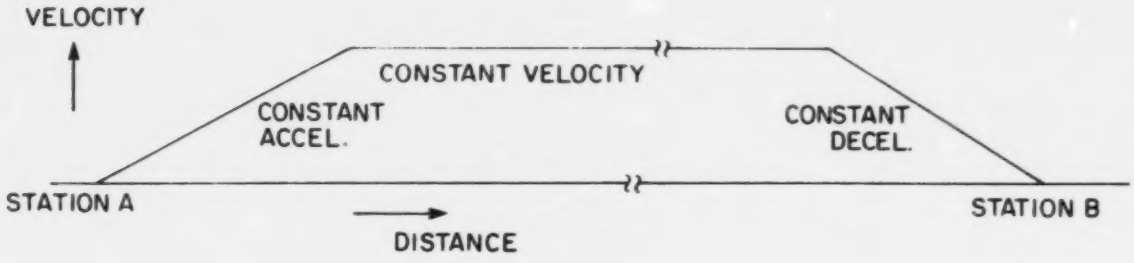

FIG. 39

This implies that we have to find a method to be able to analyze the non-linear delay-locked loop for large amplitude delay variations. The analysis starts with a general outline of the proposed method (Section 11.0). Next the non-linear differential equation will be derived (Section 11.1) and the general solution obtained for a ramp input in velocity (Section 11.2). A specific solution will be given for the loop using either the exponential or the inverse non-linear system function (Section 11.4). The accompanying graphs show the transient behaviour of the velocity, the error in velocity and "distance travelled". Furthermore the same procedure will be followed for a fourth order system where very high accuracies are obtained through phase compensation with two linked second order systems (Section 12.0).

11.0 NON-LINEAR ANALYSIS FOR LARGE AMPLITUDE SIGNALS

The response of the loop has been analyzed for small signal variations around static operating points. The resulting linearization conveniently allowed us to readily obtain the transfer function of the loop in terms of complex poles and zeros, which actually is a short-cut to the solution of the linearized differential equation.

When considering large amplitude signals such as ramp input signals, where one is steadily moving away from the initial operating point, the non-linear behaviour of the loop has to be taken into account in the analysis of the differential equation.

In general, non-linear differential equations cannot be solved analytically. However, with the method developed below, one retains the elegance of analytical solutions and Laplace Transform techniques for the non-linear differential equation of the delay-locked loop.

Consider the non-linear differential equation

$$A(x)\ \frac{d^2y(t)}{dt^2} + B(x)\ \frac{dy(t)}{dt} + C(x) = x(t) \qquad (41)$$

where A, B and C are smooth continuous non-linear functions of the input driving signal x.

Select a time interval Δt small in comparison to the dynamic variations in $A\{x(t)\}$, $B\{x(t)\}$, and $C\{x(t)\}$. The functions $A\{x(t)\}$, $B\{x(t)\}$, and $C\{x(t)\}$ are now considered to be constant over these time-intervals Δt, hence piece-wise linear approximation of the differential equation.

Solve the differential equation

$$A(x_0)\frac{d^2y(t)}{dt^2} + B(x_0)\frac{dy(t)}{dt} + C(x_0) = x(t) \qquad (42)$$

for arbitrary conditions $A(x_0)$, $B(x_0)$, $C(x_0)$, $x(0)$, $\left.\frac{dx(t)}{dt}\right|_{t=0}$ $y(0)$ and $\left.\frac{dy(t)}{dt}\right|_{t=0}$,

where x_0 is $\left.x(t)\right|_{t=0}$.

Let the general solution of Equation (42) be $y(t)$. It is restricted to a time interval Δt, from $t = 0$ to $t = \Delta t$.

To obtain the solution for the next time interval, $t = \Delta t$ to $t = 2\Delta t$, we have to derive the initial conditions at $t = \Delta t$.

The first step is to substitute the actual values for $A(x_0)$, $B(x_0)$, $C(x_0)$, $x(0)$ and $\left.\frac{dx(t)}{dt}\right|_{t=0}$ into the general solution.

One can now determine the values $y(\Delta t)$ and $\left.\frac{dy(t)}{dt}\right|_{t=\Delta t}$ which are also the initial conditions for the next time interval.

Substituting $A(x_1)$, $B(x_1)$, $C(x_1)$, $x(\Delta t)$, $\left.\frac{dx(t)}{dt}\right|_{t=\Delta t}$ $y(\Delta t)$ and $\left.\frac{dy(t)}{dt}\right|_{t=\Delta t}$, where $x_1 = \left.x(t)\right|_{t=\Delta t}$, into the general solution one obtains the differential Equation (43).

$$A(x_1)\frac{d^2y(t)}{dt^2} + B(x_1)\frac{dy(t)}{dt} + C(x_1) = x(t) \qquad (43)$$

The same procedure is repeated for each new time interval. The solution $y(n\Delta t)$ is therefore obtained through n iterations, using the general solution always with the same value for the time t, $t = \Delta t$.

The time interval Δt is very small, the values $y(n\Delta t)$ are hence closely spaced and used to plot the solutions in graphical form.

To obtain the "distance travelled", $\int y dt$, we have to integrate the solutions $y(t)$ over each small interval Δt and accumulate these partial values to obtain a value for the "distance travelled".

The peculiarity of the method developed is that the general solution, where t is restricted to $0 \leqslant t \leqslant \Delta t$, can be used to determine the solution for an arbitrary time interval. The reason for this behaviour is that the general solution, where $0 \leqslant t \leqslant \Delta t$, can be transposed to any arbitrary time

interval $n\Delta t \leq t \leq (n+1)t$ if we know the initial conditions at $t = n\Delta t$. The time variable t in the expression for y(t) however remains restricted to values $0 \leq t \leq \Delta t$. The progression in time of the solution is actually "taken away" from the time variable t and transferred to the changing boundary conditions for each particular time interval. Inside each time interval however the variable t takes on its role.

In the next two sections we will use the technique outlined above to analyze the behaviour of the non-linear delay-locked loop for ramp input signals of velocity, i.e. constant acceleration input.

11.1 Derivation of Non-Linear Differential Equation

The small signal transfer function is valid for small excursions around an equilibrium point. The differential equation to be derived has to be valid only for a small time interval Δt, hence it is also limited to small excursions around an operating point. Therefore we can use the previous analysis to readily derive the differential equation.

The general form for the small signal transfer function $\psi(p)$ of the loop is:

$$\psi(p) = \frac{\Delta\hat{T}(p)}{\Delta T(p)} = \left[\frac{1}{p^2 A(V) + pB(V) + 1}\right] \tag{44}$$

The coefficients A and B are dependent of the velocity V and are further determined by the particular system configuration.

The small signal velocity variations, $v_i(p)$ and $v_o(p)$ are related to the time delay variations in a similar fashion, hence,

$$\psi(p) = \frac{\Delta\hat{T}(p)}{\Delta T(p)} = \frac{v_o(p)}{v_i(p)} \tag{45}$$

where $v_i(p)$ is the actual velocity input and $v_o(p)$ is a normalized velocity output parameter.

To clarify the notation we will use $x = v_i$ and $y = v_o$ to avoid confusion between v_i, v_o and V.

The differential equation corresponding to the transfer function given by (44) is:

$$A(V)\frac{d^2y(t)}{dt^2} + B(V)\frac{dy(t)}{dt} + y(t) = x(t) \tag{46}$$

The various small-signal gain factors of the partial transfer functions are condensed in the coefficients A(V) and B(V). The non-linear differential equation is linearized by restricting the equation to small time intervals Δt. This allows us to consider the partial derivatives of the non-linear gain factors to be constant at the operating points.

With regard to the non-linearities in the loop, we are thus using a piece-wise linear approximation. Also it implies a staircase approximation for A(V) and B(V) which reflects the combined effect of the partial non-linear gains. This is illustrated in Figure 40.

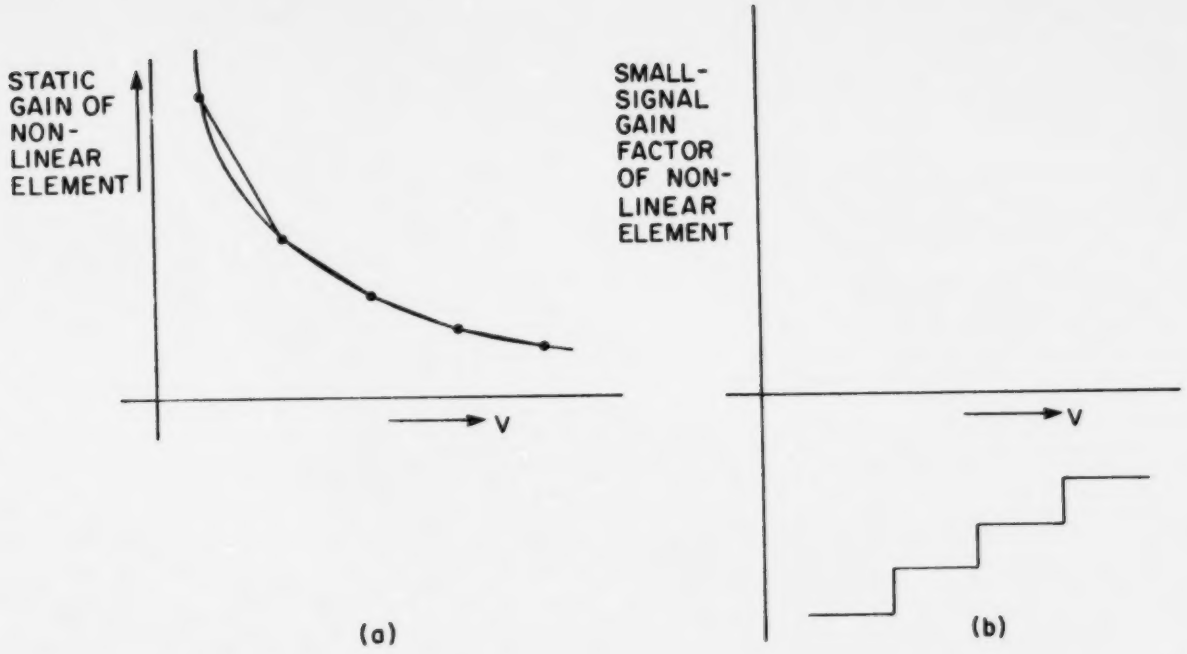

FIG. 40

11.2 General Solution, over Interval Δt, for Arbitrary Input

$$A \frac{d^2y}{dt^2} + B \frac{dy}{dt} + y = x \tag{47}$$

The differential equation is linearized by restricting the solution to a small time interval Δt. The Laplace Transform of the differential equation is then, for arbitrary input conditions:

$$y(p) = \left[\frac{pAy_0 + Ay_1 + By_0}{p^2A + Bp + 1} + \frac{\mathcal{L}x(t)}{p^2A + pB + 1} \right] \tag{48}$$

where y_0 and y_1 are the values of $y(t)$ and $\frac{dy(t)}{dt}$ at $t = 0$, and $\mathcal{L}x(t)$ the Laplace Transform of $x(t)$.

The solution $y(t)$ of the differential equation, for a time interval Δt, is obtained by applying the inverse Laplace Transform to (48). There are three solutions depending on the relative values of A and B:

For $B^2 < 4A$:

$$y(t) = \left[y_0 \cos\left\{\left(\frac{1}{A} - \frac{B^2}{4A^2}\right)^{1/2} t\right\} + \left\{\frac{y_1 + \frac{By_0}{2A}}{\left(\frac{1}{A} - \frac{B^2}{4A^2}\right)^{1/2}}\right\} \sin\left\{\left(\frac{1}{A} - \frac{B^2}{4A^2}\right)^{1/2} t\right\}\right] \times e^{-B/2A\ t}$$

$$+ \mathcal{L}^{-1}\left[\frac{\mathcal{L}x(t)}{\left(p^2 A + pB + 1\right)}\right] \qquad (49)$$

For $B^2 = 4A$:

$$y(t) = \left[y_0 + \left(y_1 + \frac{2}{B} y_0\right)t\right] e^{-2/B\ t} + \mathcal{L}^{-1}\left[\frac{\mathcal{L}x(t)}{\left(p\,\frac{1}{2}\,B + 1\right)^2}\right] \qquad (50)$$

For $B^2 > 4A$:

$$y(t) = \left[y_0 \cosh\left\{\left(\frac{1}{A} - \frac{B^2}{4A^2}\right)^{1/2} t\right\} + \left\{\frac{y_1 + y_0\,\frac{B}{2A}}{\left(\frac{1}{A} - \frac{B^2}{4A^2}\right)^{1/2}}\right\} \sinh\left\{\left(\frac{1}{A} - \frac{B^2}{4A^2}\right)^{1/2} t\right\}\right] \times e^{-B/2A\ t}$$

$$+ \mathcal{L}^{-1}\left[\frac{\mathcal{L}x(t)}{\left(p^2 A + pB + 1\right)}\right] \qquad (51)$$

11.3 Solution, over Interval Δt, for Velocity Ramp Input

The input velocity signal is,

$$x(t) = x_0 + \alpha t$$

where x_0 is the magnitude of the input velocity for $t \leqslant 0$, and $(\alpha \cdot t)$ is the ramp input signal, superimposed on the initial value x_0 of the input speed. The parameter V in A(V) and B(V) is therefore equal to x(t):

$$V = x_0 + \alpha t$$

Using V(t) as given by (43) we can relate A and B to time:

$$A(V) = A\{V(t)\} \qquad (52)$$

$$B(V) = B\{V(t)\} \qquad (53)$$

The Laplace Transform of x(t) is:

$$\mathcal{L}x(t) = \left(\frac{x_0}{p} + \frac{\alpha}{p^2}\right) \tag{54}$$

Hence

$$\frac{\mathcal{L}x(t)}{(p^2A + pB + 1)} = \frac{(px_0 + \alpha)}{p^2(p^2A + pB + 1)} = \left[\frac{\alpha}{p^2} + \frac{(x_0 - \alpha B)}{p} - \frac{pA(x_0 - \alpha B) + \alpha A + (x_0 - \alpha B)B}{(p^2A + pB + 1)}\right] \tag{55}$$

the inverse Laplace Transformation is:

$$\mathcal{L}^{-1}\left[\frac{\mathcal{L}x(t)}{(p^2A + pB + 1)}\right] = x_0 - \alpha B + \alpha t$$

$$- (x_0 - \alpha B)\left[\cos\left\{\left(\frac{1}{A} - \frac{B^2}{4A^2}\right)^{1/2} t\right\} + \left\{\frac{\frac{B}{2A} + \frac{\alpha}{x_0 - \alpha B}}{\left(\frac{1}{A} - \frac{B^2}{4A^2}\right)^{1/2}}\right\} \sin\left\{\left(\frac{1}{A} - \frac{B^2}{4A^2}\right)^{1/2} t\right\}\right] e^{-B/2A\ t} \tag{56}$$

Substitution of (56) into (49) yields for the solution y(t):

$$y(t) = x_0 - \alpha B + \alpha t + \left[(y_0 - x_0 + \alpha B)\cos\left\{\left(\frac{1}{A} - \frac{B^2}{4A^2}\right)^{1/2} t\right\} + \left\{\frac{y_1 - \alpha + (y_0 - x_0 + \alpha B)\frac{B}{2A}}{\left(\frac{1}{A} - \frac{B^2}{4A^2}\right)^{1/2}}\right\} \sin\left\{\left(\frac{1}{A} - \frac{B^2}{4A^2}\right)^{1/2} t\right\}\right] e^{-B/2A\ t} \tag{57}$$

The function y(t), as given by relationship (57), in the solution of the non-linear differential equation over a time interval from t = 0 to t = Δt and for arbitrary initial conditions at t = 0 for x_0, y_0, y_1, A and B.

To be able to find y_1, by iteration, at intervals Δt one needs $\frac{dy}{dt}$, which can readily be derived from (57),

$$\frac{dy}{dt} = \alpha + \left[(y_1 - \alpha)\cos\left\{\left(\frac{1}{A} - \frac{B^2}{4A^2}\right)^{1/2} t\right\} - \left\{\frac{(y_1 + \alpha)\frac{B}{2A} + (y_0 - x_0)\frac{1}{A}}{\left(\frac{1}{A} - \frac{B^2}{4A^2}\right)^{1/2}}\right\} \sin\left\{\left(\frac{1}{A} - \frac{B^2}{4A^2}\right)^{1/2} t\right\}\right] e^{-B/2A\ t} \tag{58}$$

The solution for $\int y dt$, the "distance travelled", follows from (57) by integration,

$$\int y dt = (y_1 - \alpha)A + (y_0 - x_0 + \alpha B)B + (x_0 - \alpha B)t + \frac{1}{2}\alpha t^2 - \left[(y_1 A + y_0 B - x_0 B - \alpha A + \alpha B^2) \right.$$

$$\cos\left\{\left(\frac{1}{A} - \frac{B^2}{4A^2}\right)^{1/2} t\right\} + \left\{\frac{y_1 \frac{B}{2} - (y_0 - x_0)\left(1 - \frac{B^2}{2A}\right) - \frac{\alpha B}{2}\left(3 - \frac{B^2}{A}\right)}{\left(\frac{1}{A} - \frac{B^2}{4A^2}\right)^{1/2}}\right\}$$

$$\left. \sin\left\{\left(\frac{1}{A} - \frac{B^2}{4A^2}\right)^{1/2} t\right\}\right] e^{-B/2A\ t} \qquad (59)$$

Again relationships (58) and (59) are valid from $t = 0$ to $t = \Delta t$ and can be used to determine $\frac{dy}{dt}$ and $\int y dt$ at arbitrary time $t = n\Delta t$ by n iterations.

The formulas above apply from $t = 0$ and assume a constant velocity for $t \leq 0$ and a constant acceleration for $t > 0$. The "distance travelled" is set to zero at $t = 0$.

The solution given above is not complete. It applies to a system having a damping coefficient below critical damping. In the formulas this implies: $\left(\frac{1}{A} - \frac{B^2}{4A^2}\right) > 0$. Above critical damping another solution has to be derived. Using the same approach as above, one can derive for $\left(\frac{1}{A} - \frac{B^2}{4A^2}\right) < 0$:

$$y(t) = x_0 - \alpha B + \alpha t + \frac{1}{2}\left[(y_0 - x_0 + \alpha B) + \left\{\frac{y_1 - \alpha + \frac{B}{2A}(y_0 - x_0) + \frac{\alpha B^2}{2A}}{\left(\frac{B^2}{4A^2} - \frac{1}{A}\right)^{1/2}}\right\}\right] e^{\left\{(B^2/4A^2 - 1/A)^{1/2} - B/2A\right\}t}$$

$$+ \frac{1}{2}\left[(y_0 - x_0 + \alpha B) - \left\{\frac{y_1 - \alpha + \frac{B}{2A}(y_0 - x_0) + \frac{\alpha B^2}{2A}}{\left(\frac{B^2}{4A^2} - \frac{1}{A}\right)^{1/2}}\right\}\right] e^{-\left\{(B^2/4A^2 - 1/A)^{1/2} + B/2A\right\}t} \qquad (60)$$

$$\frac{dy}{dt} = \alpha + \frac{1}{2}\left\{\left(\frac{B^2}{4A^2} - \frac{1}{A}\right)^{1/2} - \frac{B}{2A}\right\} \times \left[(y_0 - x_0 + \alpha B) + \left\{\frac{y_1 - \alpha + \frac{B}{2A}(y_0 - x_0) + \frac{\alpha B^2}{2A}}{\left(\frac{B^2}{4A^2} - \frac{1}{A}\right)^{1/2}}\right\}\right] e^{\left\{(B^2/4A^2 - 1/A)^{1/2} - B/2A\right\}t} - \frac{1}{2}\left\{\left(\frac{B^2}{4A^2} - \frac{1}{A}\right)^{1/2} + \frac{B}{2A}\right\}$$

$$\times \left[(y_0 - x_0 + \alpha B) - \left\{\frac{y_1 - \alpha + \frac{B}{2A}(y_0 - x_0) + \frac{\alpha B^2}{2A}}{\left(\frac{B^2}{4A^2} - \frac{1}{A}\right)^{1/2}}\right\}\right] e^{-\left\{(B^2/4A^2 - 1/A)^{1/2} + B/2A\right\}t} \qquad (61)$$

$$\int \frac{dy}{dt} = (y_1 - \alpha)A + (y_0 - x_0 + \alpha B)B + (x_0 - \alpha B)t + \frac{1}{2}\alpha t^2$$

$$+ \frac{1}{2}\left[(y_0 - x_0 + \alpha B) + \left\{\frac{y_1 - \alpha + \frac{B}{2A}(y_0 - x_0 + \alpha B)}{\left(\frac{B^2}{4A^2} - \frac{1}{A}\right)^{1/2}}\right\}\right] \frac{e^{\left\{(B^2/4A^2 - 1/A)^{1/2} - B/2A\right\}t}}{\left\{(B^2/4A^2 - 1/A)^{1/2} - B/2A\right\}}$$

$$- \frac{1}{2}\left[(y_0 - x_0 + \alpha B) - \left\{\frac{y_1 - \alpha + \frac{B}{2A}(y_0 - x_0 + \alpha B)}{\left(\frac{B^2}{4A^2} - \frac{1}{A}\right)^{1/2}}\right\}\right] \frac{e^{-\left\{(B^2/4A^2 - 1/A)^{1/2} + B/2A\right\}t}}{\left\{(B^2/4A^2 - 1/A)^{1/2} + B/2A\right\}} \qquad (62)$$

The two sets of equations (57-59) and (60-62) are the solution for $t = 0$ to $t = \Delta t$. To obtain solutions for $t > \Delta t$, a series of iterations using the equations above, have to be performed. Each set of solutions for a particular time interval $n(\Delta t)$ to $(n+1)\Delta t$ is used to find the initial conditions over the next time interval $(n+1)\Delta t$ to $(n+2)\Delta t$.

The non-linear system coefficients A and B can be calculated as a function of time, realizing that A and B are functions of V(t) and that $V(t) = x_0 + \alpha t$.

The values to be calculated for each interval are: x_0, A, B, y_0 and y_1.

The procedure is schematically outlined below:

$$x_{0,n} = x_0 + \alpha n\Delta t; \quad V_n = x_{0,n} \tag{63}$$

$$A_n = F\left(\frac{V_{n+1} - V_n}{2}\right) = F^*\left(x_0 + \frac{\alpha n\Delta t}{2}\right) \tag{64}$$

$$B_n = G\left(\frac{V_{n+1} - V_n}{2}\right) = G^*\left(x_0 + \frac{\alpha n\Delta t}{2}\right) \tag{65}$$

The coefficients A and B are taken as the average over an interval to increase the accuracy.

$$y_{0,n+1} = H(x_{0,n}, A_n, B_n, y_{0,n}, y_{1,n}) \tag{66}$$

$$y_{1,n+1} = K(x_{0,n}, A_n, B_n, y_{0,n}, y_{1,n}) \tag{67}$$

where the functions H and K represent relations (60) and (61),

The solutions for y(t) and $\frac{dy(t)}{dt}$, for $t = (n+1)\Delta t$ to $t = (n+2)\Delta t$, can be obtained, substituting the initial conditions calculated at $t = (n+1)\Delta t$.

The "distance travelled" from $t = 0$ to $t = \Delta t$ is:

$$\int_0^{\Delta t} y\,dt = M(x_{0,1}, A_1, B_1, y_0, y_{1,1}) \tag{68}$$

where M is relation (62).

To obtain the "distance travelled" at $t = n\Delta t$ one has to sum up all the previous results of the iterations, therefore:

$$\int_0^{n\Delta t} y\,dt = \sum_{n=1}^{n} M(x_{0,n}, A_n, B_n, y_{0,n}, y_{1,n}) \tag{69}$$

The program developed in BASIC to do these calculations, continuously senses, during the iterations, if the system is above or below critical damping and selects automatically the appropriate set of equations.

11.4 Error in Velocity and "Distance Travelled" for Velocity Ramp Input

The error in the velocity and the "distance travelled" will be calculated using the technique outlined in the previous sections for both the exponential and the inverse non-linear system function. The values taken for the input velocity and acceleration are related to those of trains, Figure 41.

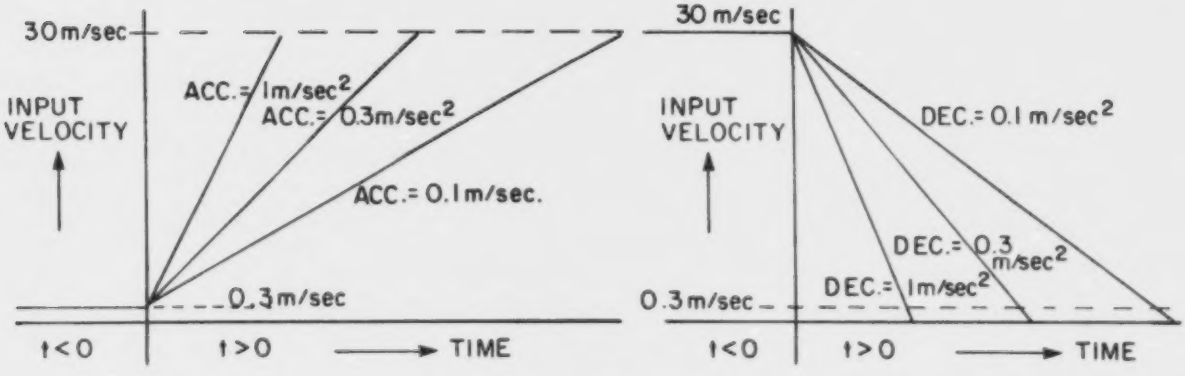

FIG. 41

11.4.1 Exponential Non-Linear System Function

The small signal transfer function $\psi(p)$ has been derived in Section 6.0,

$$\psi(p) = \frac{1}{p^2\left(\frac{n_3\tau L}{2En_1\beta V}\right) + p\left(\frac{n_3\tau}{\beta n_1 E}\right) + 1} \qquad (24)$$

The system coefficients A and B are therefore:

$$A = \left(\frac{n_3\tau L}{2E\beta n_1}\right)\left(\frac{1}{V}\right); \quad B = \left(\frac{n_3\tau}{E\beta n_1}\right) \qquad (70)$$

The system parameters selected are the same as those in Section 6.0 for Figure 25:

$n_1 = 64$; $n_2 = 2$; $K = 10^4$ Hz/V; $\tau = 5$ sec; $L = 510^{-2}$ m; $E = 7$V; $\beta = 0.134$; hence

$$A = \frac{4.17\ 10^{-3}}{V}\ \text{sec}^2 \quad \text{and} \quad B = 0.167\ \text{sec.}$$

These values result in a small signal bandwidth of about 1 Hz, virtually independent of velocity as shown in Figure 25.

For a positive velocity ramp input the system behaviour goes from underdamped to overdamped, and vice versa for a negative velocity ramp. Both sets of equations are therefore required (57-59) and (60-62).

There are three sets of graphs: transient behaviour of velocity, error in velocity versus input velocity and error in "distance travelled" versus input "distance travelled" (Figs. 42-47). Each set gives the response for a positive and a negative going velocity ramp input signal respectively.

In one case,we start from a very low velocity, $\simeq$ 1 km/hr and accelerate steadily to $\approx$ 100 km/hr, in the second case,we start from $\approx$ 100 km/hr and steadily decelerate to $\approx$ 1 km/hr. This is shown for three different values of acceleration and deceleration.

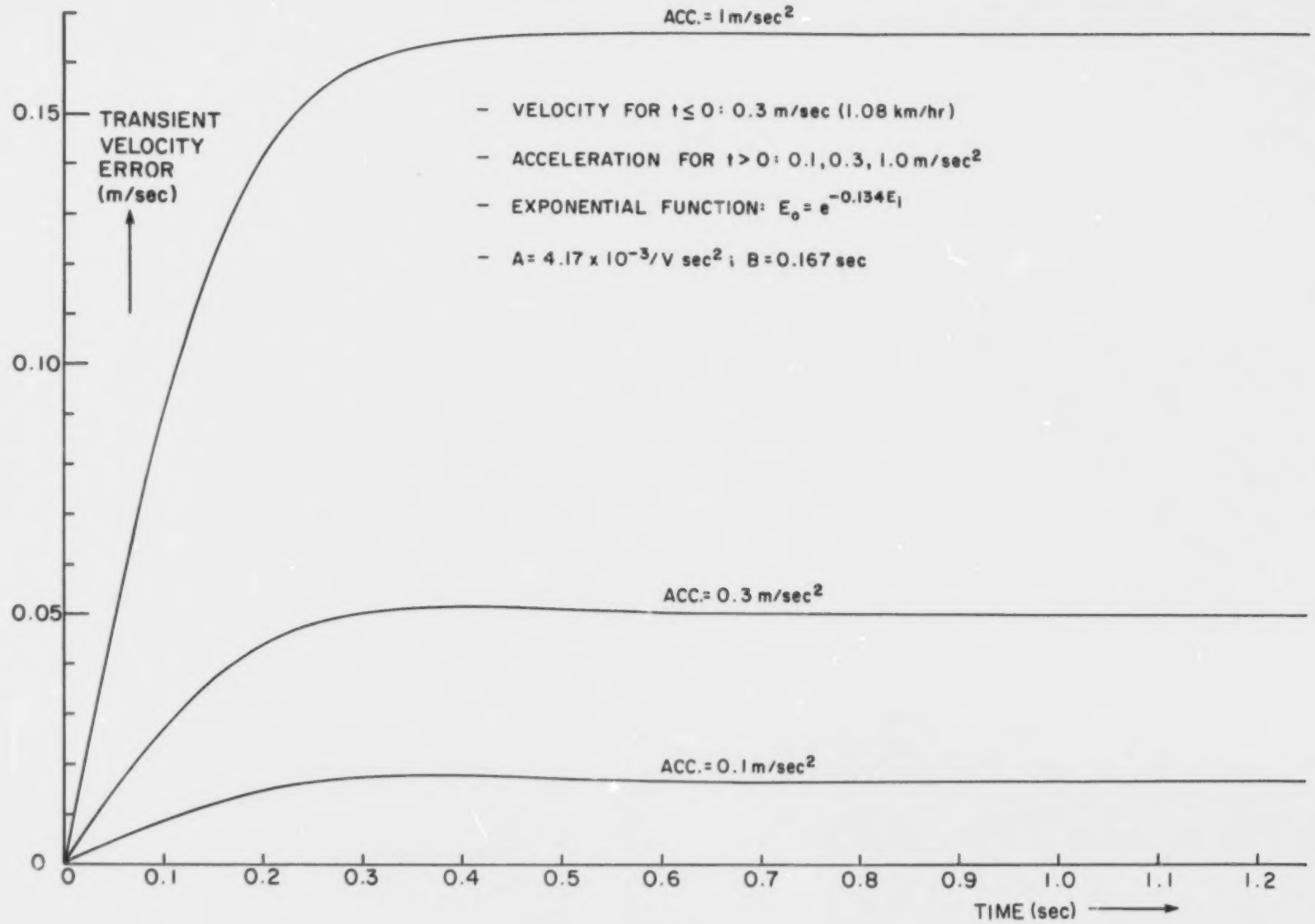
ACC.= 1 m/sec²
0.15
TRANSIENT VELOCITY ERROR (m/sec)
0.10
0.05
0
ACC.= 0.3 m/sec²
ACC.= 0.1 m/sec²
- VELOCITY FOR t ≤ 0: 0.3 m/sec (1.08 km/hr)
- ACCELERATION FOR t > 0: 0.1, 0.3, 1.0 m/sec²
- EXPONENTIAL FUNCTION: $E_o = e^{-0.134E_i}$
- A = 4.17 x 10⁻³/V sec² ; B = 0.167 sec
0 0.1 0.2 0.3 0.4 0.5 0.6 0.7 0.8 0.9 1.0 1.1 1.2
TIME (sec)

FIG. 42

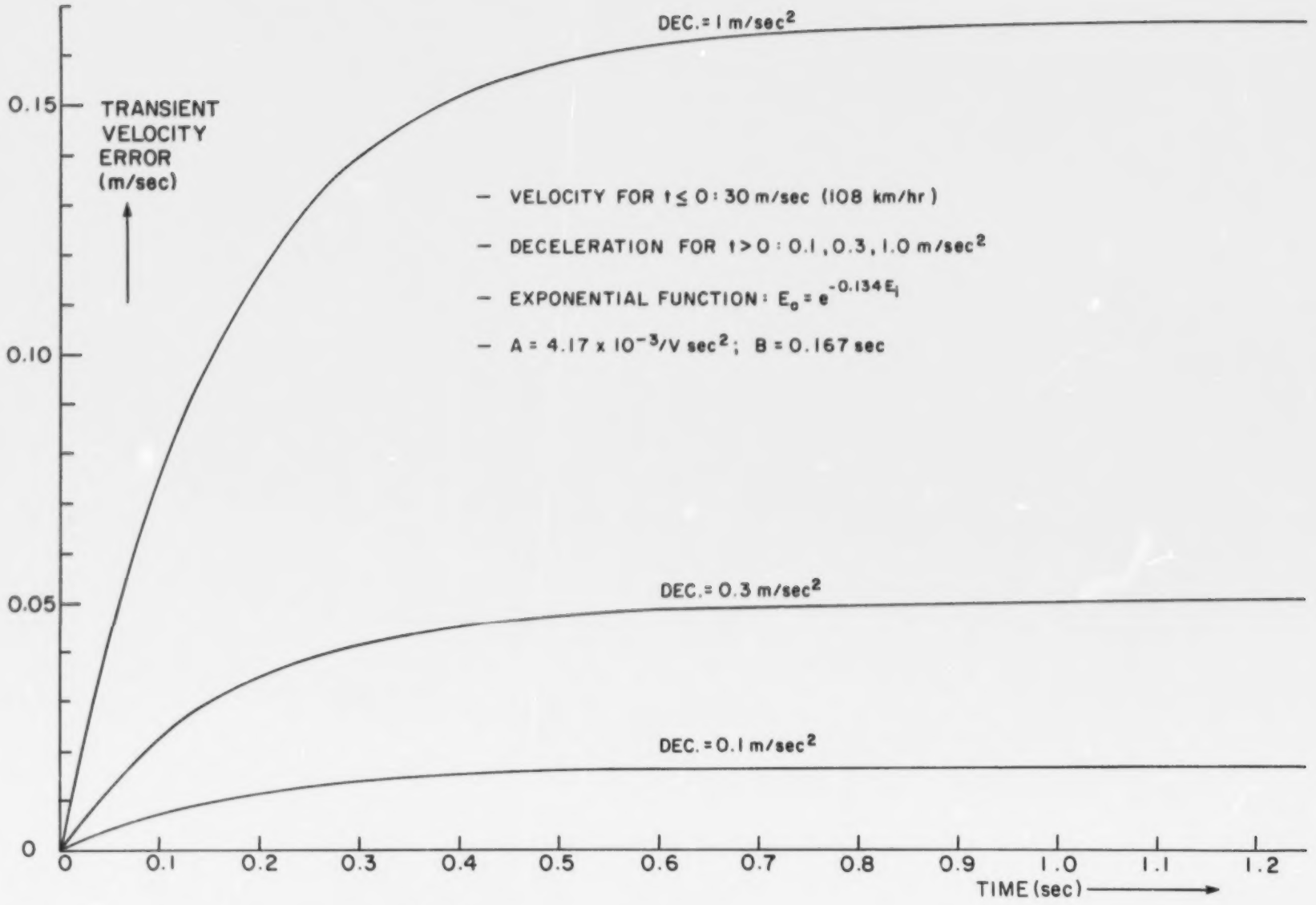
DEC.= 1 m/sec²
0.15
TRANSIENT
VELOCITY
ERROR
(m/sec)
– VELOCITY FOR t ≤ 0 : 30 m/sec (108 km/hr)
– DECELERATION FOR t > 0 : 0.1, 0.3, 1.0 m/sec²
– EXPONENTIAL FUNCTION : $E_o = e^{-0.134 E_i}$
– A = 4.17 x 10⁻³/V sec²; B = 0.167 sec
0.10
DEC.= 0.3 m/sec²
0.05
DEC.= 0.1 m/sec²
0
0
0.1
0.2
0.3
0.4
0.5
0.6
0.7
0.8
0.9
1.0
1.1
1.2
TIME (sec)

FIG. 43

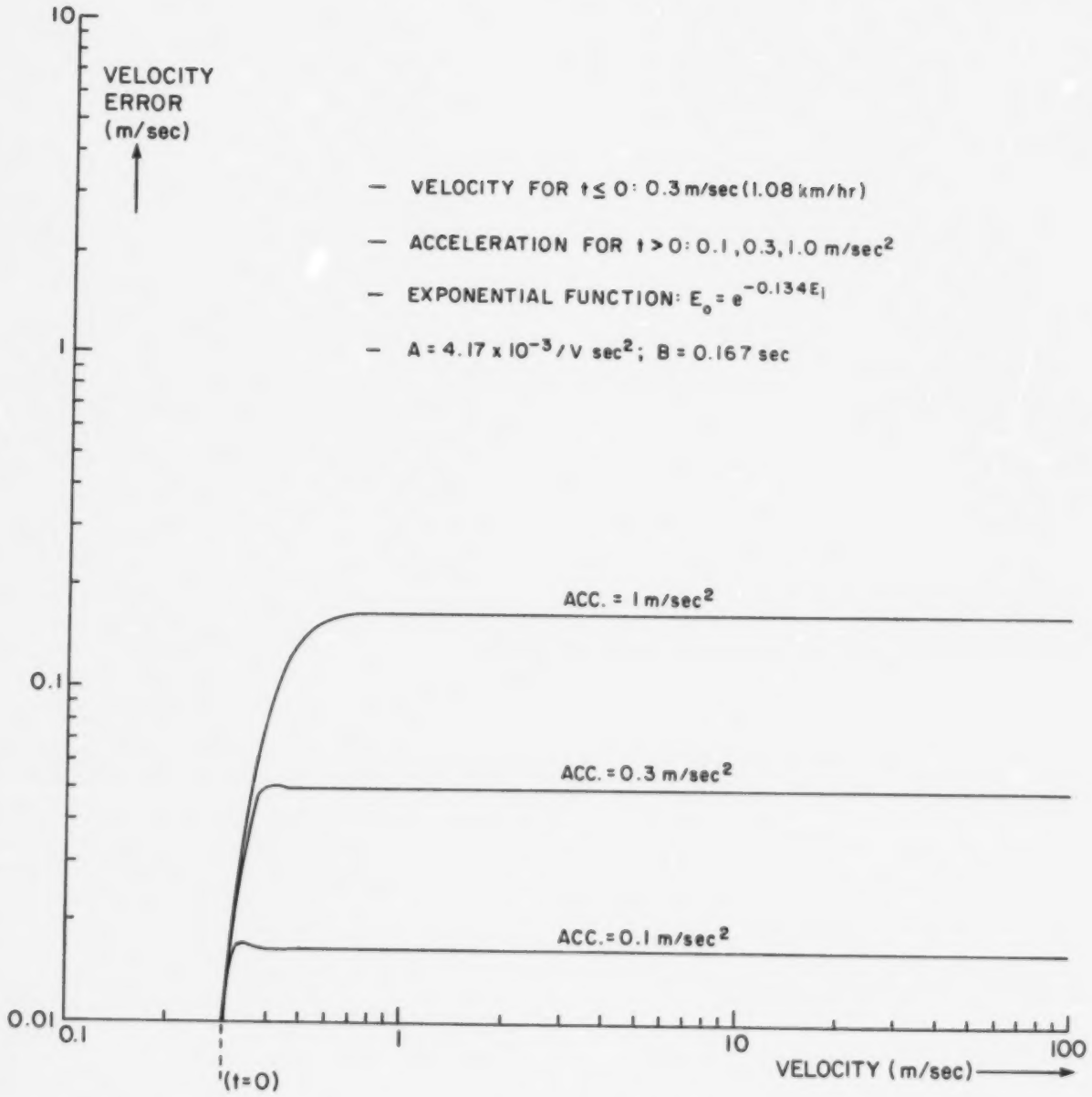
10
VELOCITY
ERROR
(m/sec)
1
0.1
0.01
— VELOCITY FOR t ≤ 0: 0.3 m/sec (1.08 km/hr)
— ACCELERATION FOR t > 0: 0.1, 0.3, 1.0 m/sec²
— EXPONENTIAL FUNCTION: $E_o = e^{-0.134E_i}$
— A = 4.17 x 10⁻³/V sec²; B = 0.167 sec
ACC. = 1 m/sec²
ACC. = 0.3 m/sec²
ACC. = 0.1 m/sec²
0.1
1
10
100
(t=0)
VELOCITY (m/sec)

FIG. 44

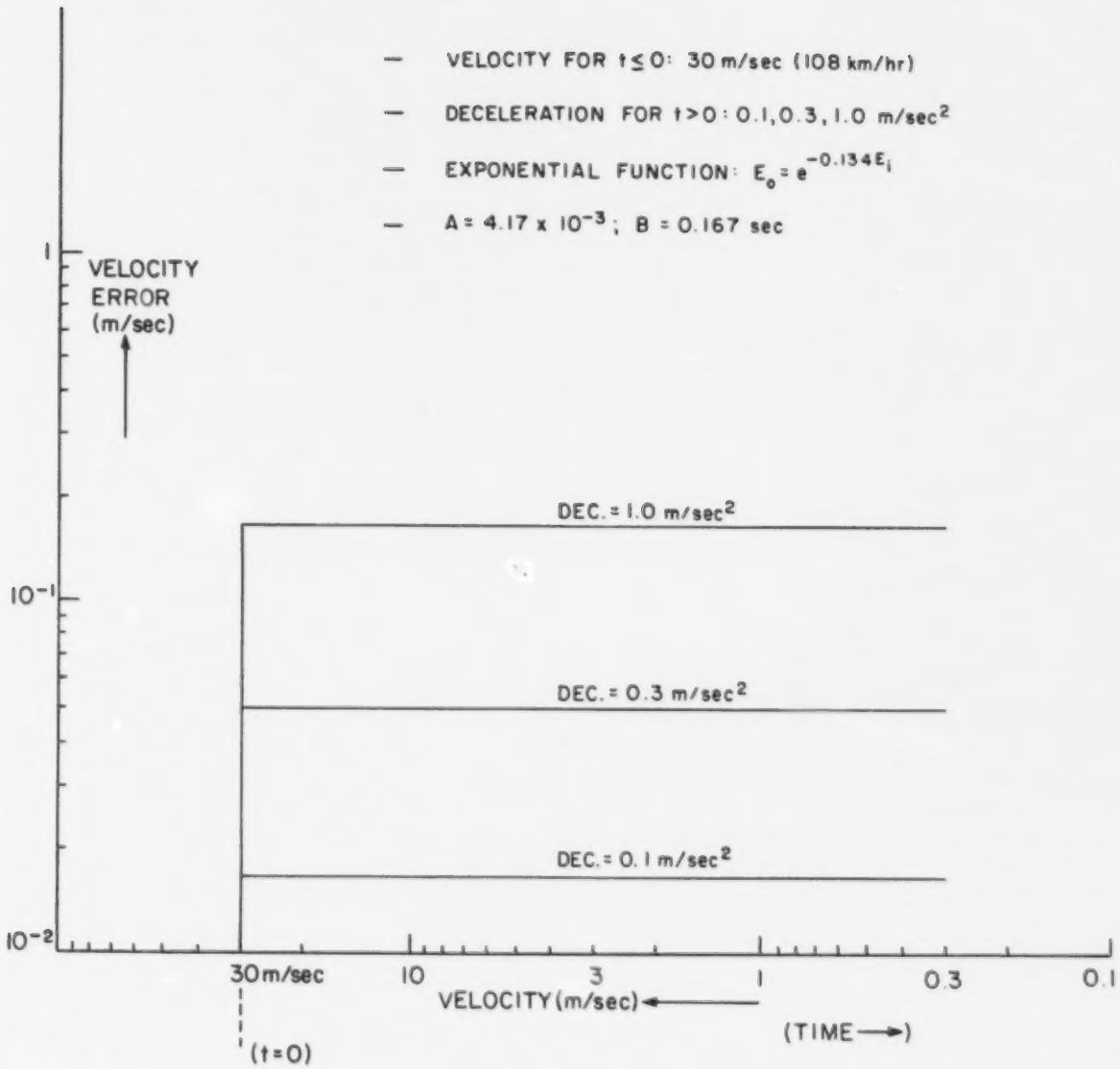
— VELOCITY FOR t ≤ 0: 30 m/sec (108 km/hr)
— DECELERATION FOR t > 0: 0.1, 0.3, 1.0 m/sec²
— EXPONENTIAL FUNCTION: $E_o = e^{-0.134 E_i}$
— A = 4.17 x 10⁻³; B = 0.167 sec
1
VELOCITY ERROR (m/sec)
DEC. = 1.0 m/sec²
10⁻¹
DEC. = 0.3 m/sec²
DEC. = 0.1 m/sec²
10⁻²
30 m/sec
10
3
1
0.3
0.1
VELOCITY (m/sec) ←
(TIME →)
(t = 0)

FIG. 45

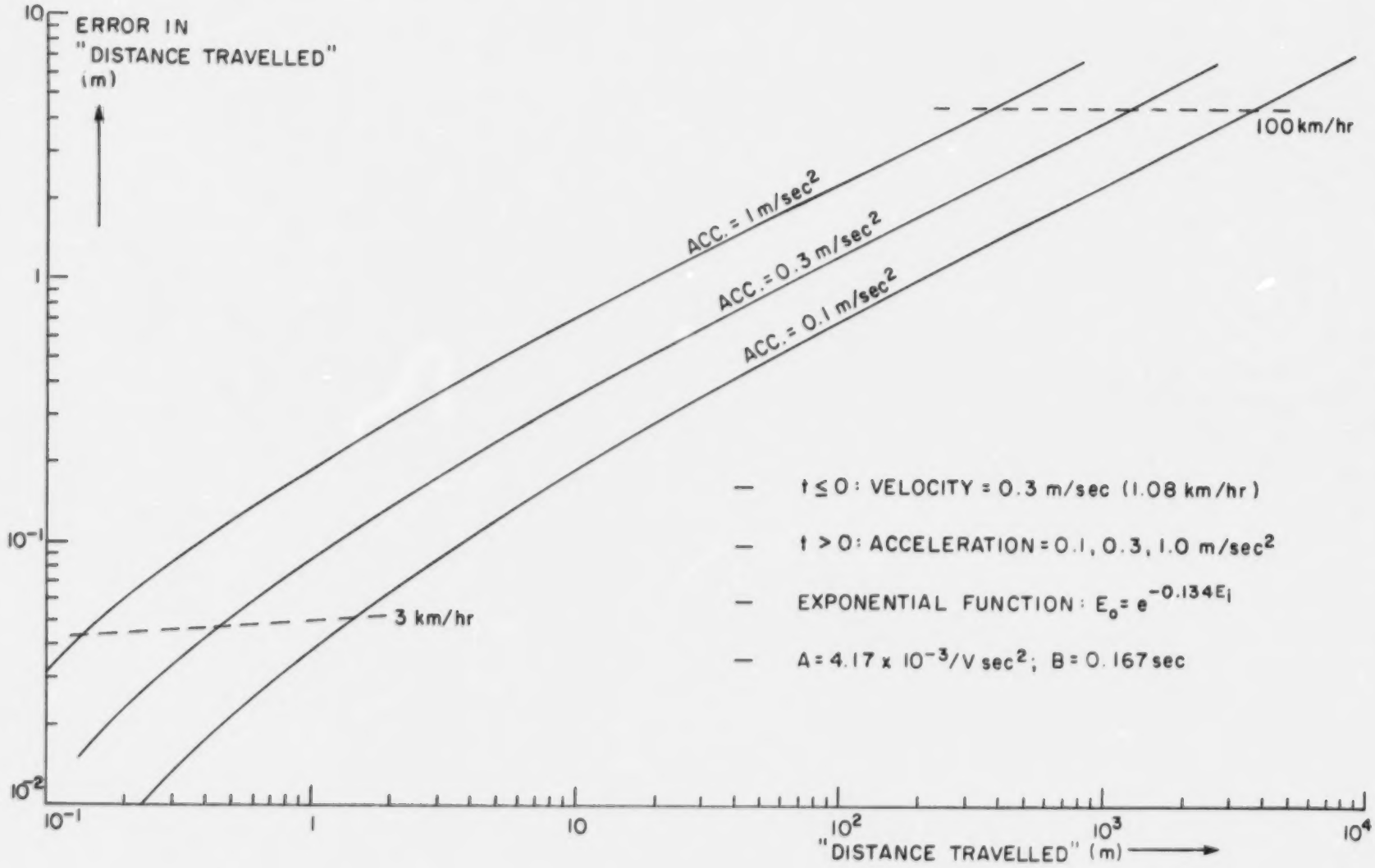
10
ERROR IN
"DISTANCE TRAVELLED"
(m)
1
10^{-1}
10^{-2}
100 km/hr
ACC. = 1 m/sec^2
ACC. = 0.3 m/sec^2
ACC. = 0.1 m/sec^2
3 km/hr
— $t \leq 0$: VELOCITY = 0.3 m/sec (1.08 km/hr)
— $t > 0$: ACCELERATION = 0.1, 0.3, 1.0 m/sec^2
— EXPONENTIAL FUNCTION: $E_o = e^{-0.134E_i}$
— $A = 4.17 \times 10^{-3}/V\,sec^2$; B = 0.167 sec
10^{-1}
1
10
10^2
10^3
10^4
"DISTANCE TRAVELLED" (m)

FIG. 46

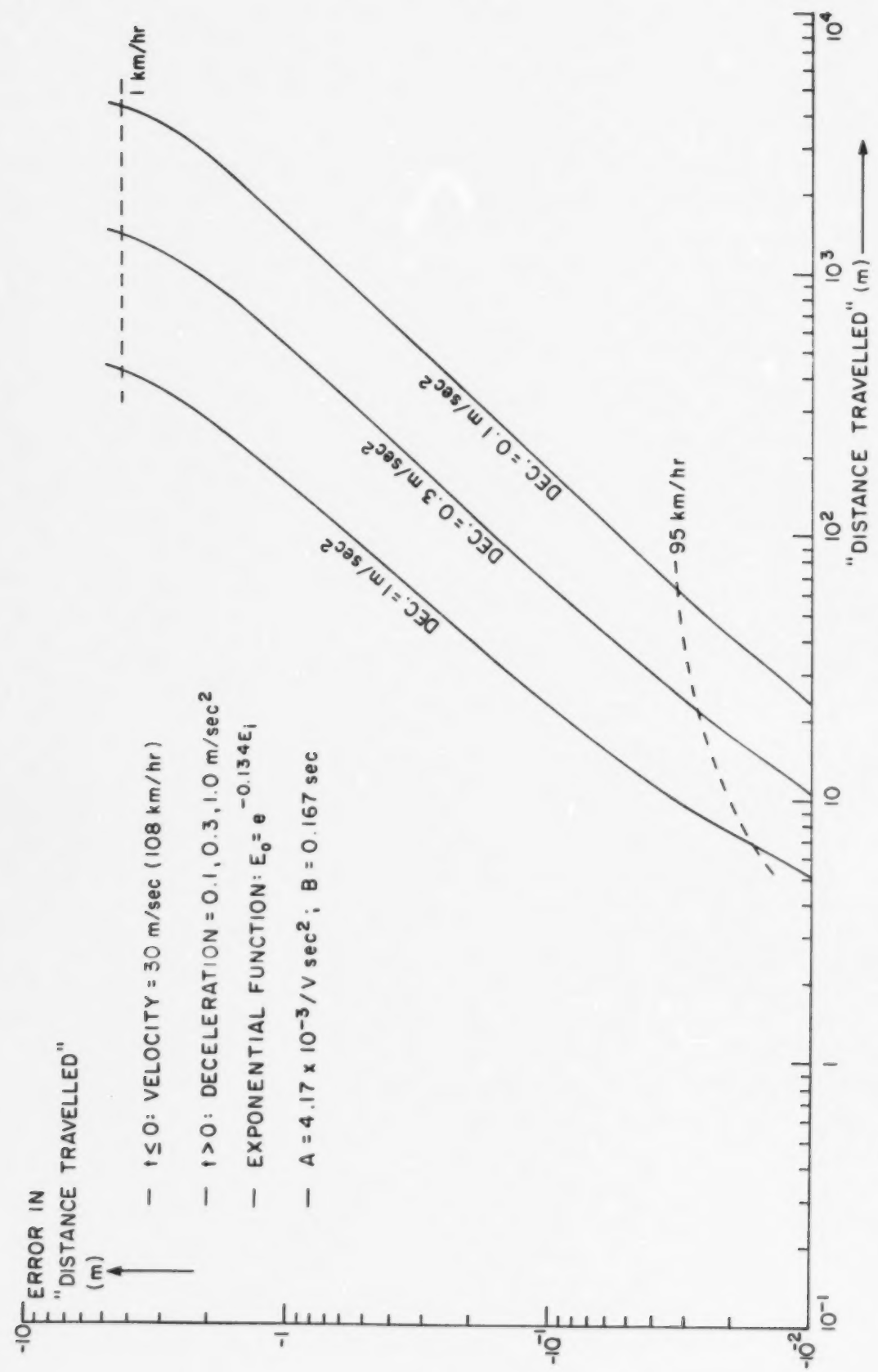
ERROR IN "DISTANCE TRAVELLED" (m)
-10
-1
-10^{-1}
-10^{-2}
10^{-1}
1
10
10^2
10^3
10^4
"DISTANCE TRAVELLED" (m)
— t ≤ 0: VELOCITY = 30 m/sec (108 km/hr)
— t > 0: DECELERATION = 0.1, 0.3, 1.0 m/sec²
— EXPONENTIAL FUNCTION: $E_0 = e^{-0.134E_i}$
— A = 4.17 x 10^{-3}/V sec²; B = 0.167 sec
DEC. = 1 m/sec²
DEC. = 0.3 m/sec²
DEC. = 0.1 m/sec²
95 km/hr
1 km/hr

FIG. 47

11.4.2 Inverse Non-Linear System Function

The small signal analysis in Section 6.1 showed that the inverse function gave a closed loop bandwidth proportional to velocity and a constant damping.

The transfer function $\psi(p)$ was derived in Section 6.0,

$$\psi(p) = \left[\frac{1}{p^2\left(\frac{L^2}{2V^2}\right) + p\left(\frac{L}{V}\right) + 1}\right] \tag{19}$$

Hence, $A = \frac{L^2}{2V^2}$ and $B = \frac{L}{V}$ (71)

The damping coefficient is constant and equal to $\sqrt{2}$.

Furthermore $\left(\frac{1}{A} - \frac{B^2}{4A^2}\right) = \frac{V^2}{L^2} > 0$ for all V, hence relationships (57), (58) and (59) are to be used to calculate distance, velocity and acceleration.

The coefficients A and B, as given by (71), when substituted in (57), (58) and (59) result in simpler expressions:

$$y(t) = \left(x_0 - \alpha\frac{L}{V} + \alpha t\right) + \left[\left(y_0 - x_0 + \alpha\frac{L}{V}\right)\cos\left(\frac{V}{L}t\right) + \left(y_1\frac{V}{L} + y_0 - x_0\right)\sin\left(\frac{V}{L}t\right)\right] e^{-V/L\ t} \tag{72}$$

$$\frac{dy}{dt} = \alpha + \left[(y_1 - \alpha)\cos\left(\frac{V}{L}t\right) - \left\{y_1 + \alpha + (y_0 - x_0)\frac{2V}{L}\right\}\sin\left(\frac{V}{L}t\right)\right] e^{-V/L\ t} \tag{73}$$

$$\int y\,dt = \left(x_0 - \alpha\frac{V}{L}\right)t + \frac{1}{2}\alpha t^2 + \left\{(y_1 + \alpha)\frac{L^2}{2V^2} + (y_0 - x_0)\frac{L}{V}\right\}$$

$$- \left[\left\{(y_1 + \alpha)\frac{L^2}{2V^2} + (y_0 - x_0)\frac{L}{V}\right\}\cos\left(\frac{V}{L}t\right) + \frac{1}{2}(y_1 - \alpha)\sin\left(\frac{V}{L}t\right)\right] e^{-V/L\ t} \tag{74}$$

The system parameters are selected as in Section 6.0 (Fig. 23): E = 7V; K = 10^4 Hz/V; n_1 = 64; n_2 = 2; L = 510^{-2} m; τ = 5 sec; $\beta = \sqrt{2}$; $E_0 = 0.29\,E_i^{-1}$, hence,

$$A = \frac{1.25\ 10^{-3}}{V^2}\ \text{sec}^2 \quad \text{and} \quad B = \frac{520^{-2}}{V}\ \text{sec}$$

The three sets of graphs (Figs. 48-53) were derived with (72), (73), and (74) by iteration and are equivalent to those of Section 11.4.1.

The system bandwidth is "self-adaptive", i.e. it shifts proportionally to the velocity. The system behaviour is therefore quite different at low and high velocities as is clearly demonstrated by the graphs. The error in the "distance travelled" is one to two orders of magnitude better in comparison to a loop using the exponential non-linear function with all system parameters, other than the non-linear function, being equal.

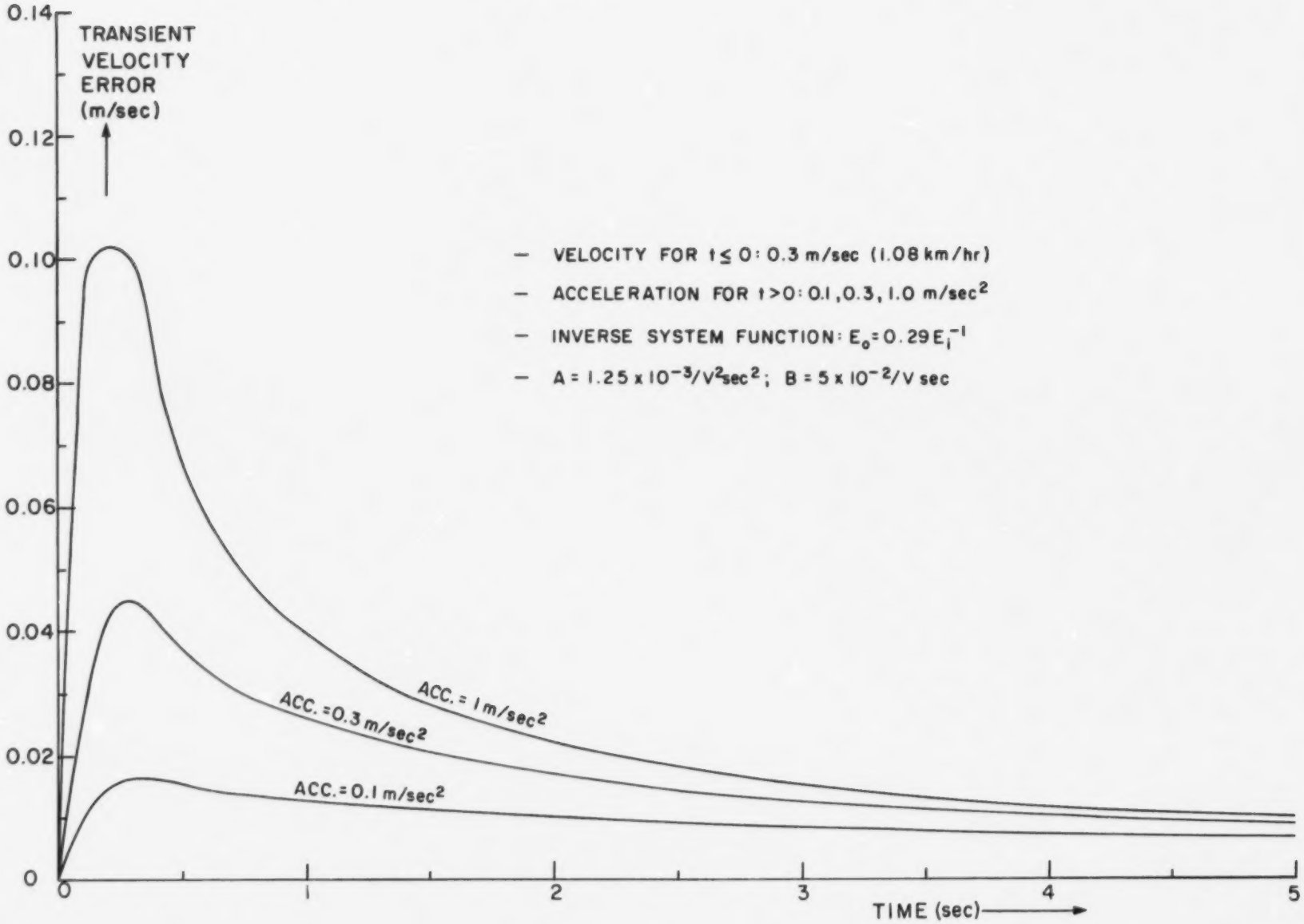
0.14
TRANSIENT VELOCITY ERROR (m/sec)
0.12
0.10
0.08
0.06
0.04
0.02
0
0
1
2
3
4
5
TIME (sec)
— VELOCITY FOR t ≤ 0: 0.3 m/sec (1.08 km/hr)
— ACCELERATION FOR t > 0: 0.1, 0.3, 1.0 m/sec²
— INVERSE SYSTEM FUNCTION: $E_o = 0.29 E_i^{-1}$
— $A = 1.25 \times 10^{-3}/V^2 sec^2$; $B = 5 \times 10^{-2}/V$ sec
ACC. = 1 m/sec²
ACC. = 0.3 m/sec²
ACC. = 0.1 m/sec²

FIG. 48

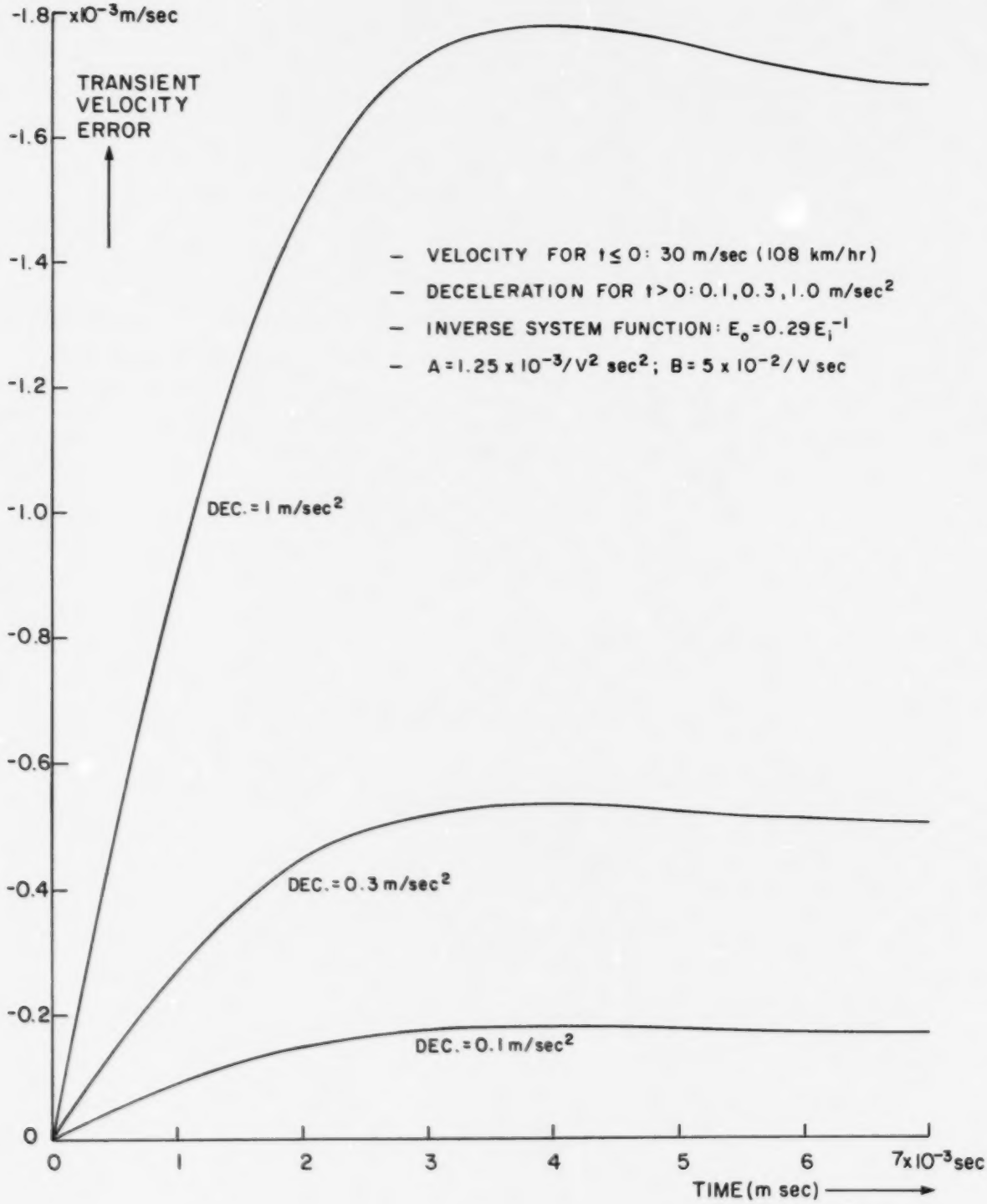
-1.8 x10⁻³m/sec
TRANSIENT VELOCITY ERROR
-1.6
-1.4
-1.2
-1.0
-0.8
-0.6
-0.4
-0.2
0
– VELOCITY FOR t≤ 0: 30 m/sec (108 km/hr)
– DECELERATION FOR t>0: 0.1, 0.3, 1.0 m/sec²
– INVERSE SYSTEM FUNCTION: E₀=0.29 Eᵢ⁻¹
– A=1.25 x 10⁻³/V² sec²; B=5 x 10⁻²/V sec
DEC.=1 m/sec²
DEC.=0.3 m/sec²
DEC.=0.1 m/sec²
0
1
2
3
4
5
6
7x10⁻³sec
TIME (m sec)

FIG. 49

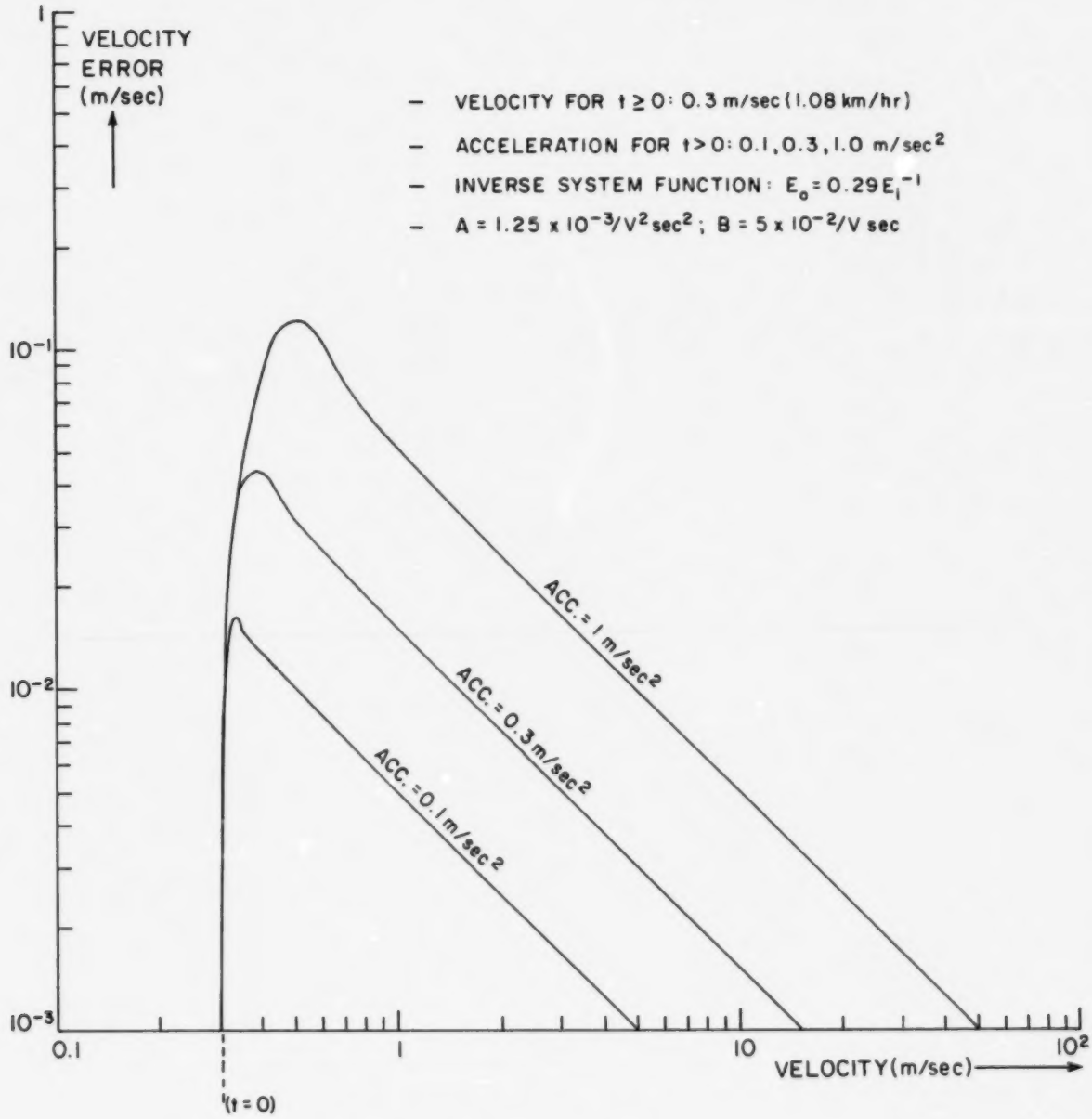
1
VELOCITY
ERROR
(m/sec)
– VELOCITY FOR t ≥ 0: 0.3 m/sec (1.08 km/hr)
– ACCELERATION FOR t > 0: 0.1, 0.3, 1.0 m/sec²
– INVERSE SYSTEM FUNCTION: E₀ = 0.29 E₁⁻¹
– A = 1.25 x 10⁻³/V²sec²; B = 5 x 10⁻²/V sec
10⁻¹
10⁻²
10⁻³
ACC. = 1 m/sec²
ACC. = 0.3 m/sec²
ACC. = 0.1 m/sec²
0.1
1
10
10²
VELOCITY (m/sec)
(t = 0)

FIG. 50

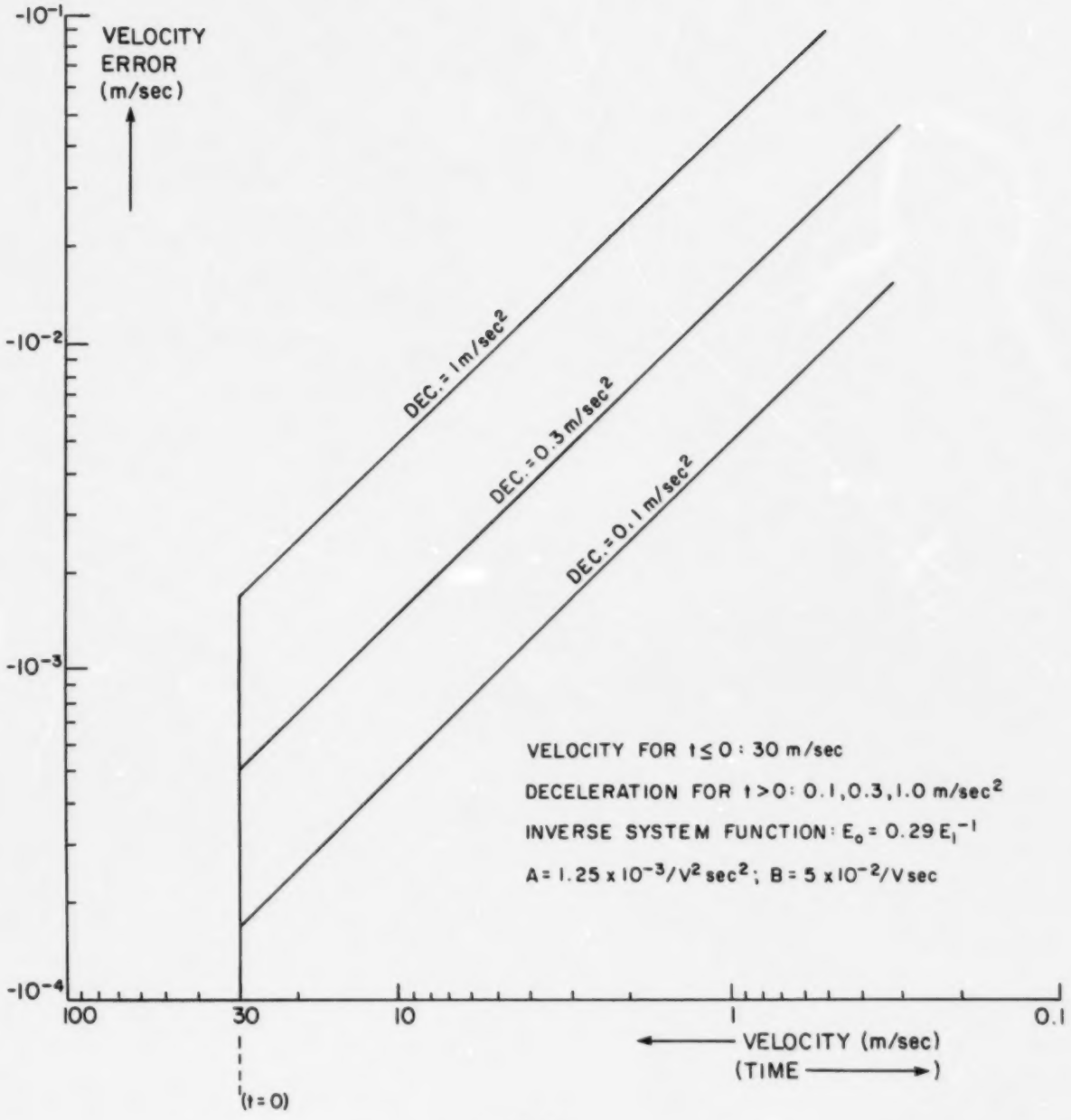
-10⁻¹
VELOCITY
ERROR
(m/sec)
-10⁻²
-10⁻³
-10⁻⁴
DEC. = 1 m/sec²
DEC. = 0.3 m/sec²
DEC. = 0.1 m/sec²
VELOCITY FOR t ≤ 0 : 30 m/sec
DECELERATION FOR t > 0 : 0.1, 0.3, 1.0 m/sec²
INVERSE SYSTEM FUNCTION: E₀ = 0.29 E_I⁻¹
A = 1.25 x 10⁻³/V² sec²; B = 5 x 10⁻²/V sec
100
30
10
1
0.1
VELOCITY (m/sec)
(TIME ⟶)
(t = 0)

FIG. 51

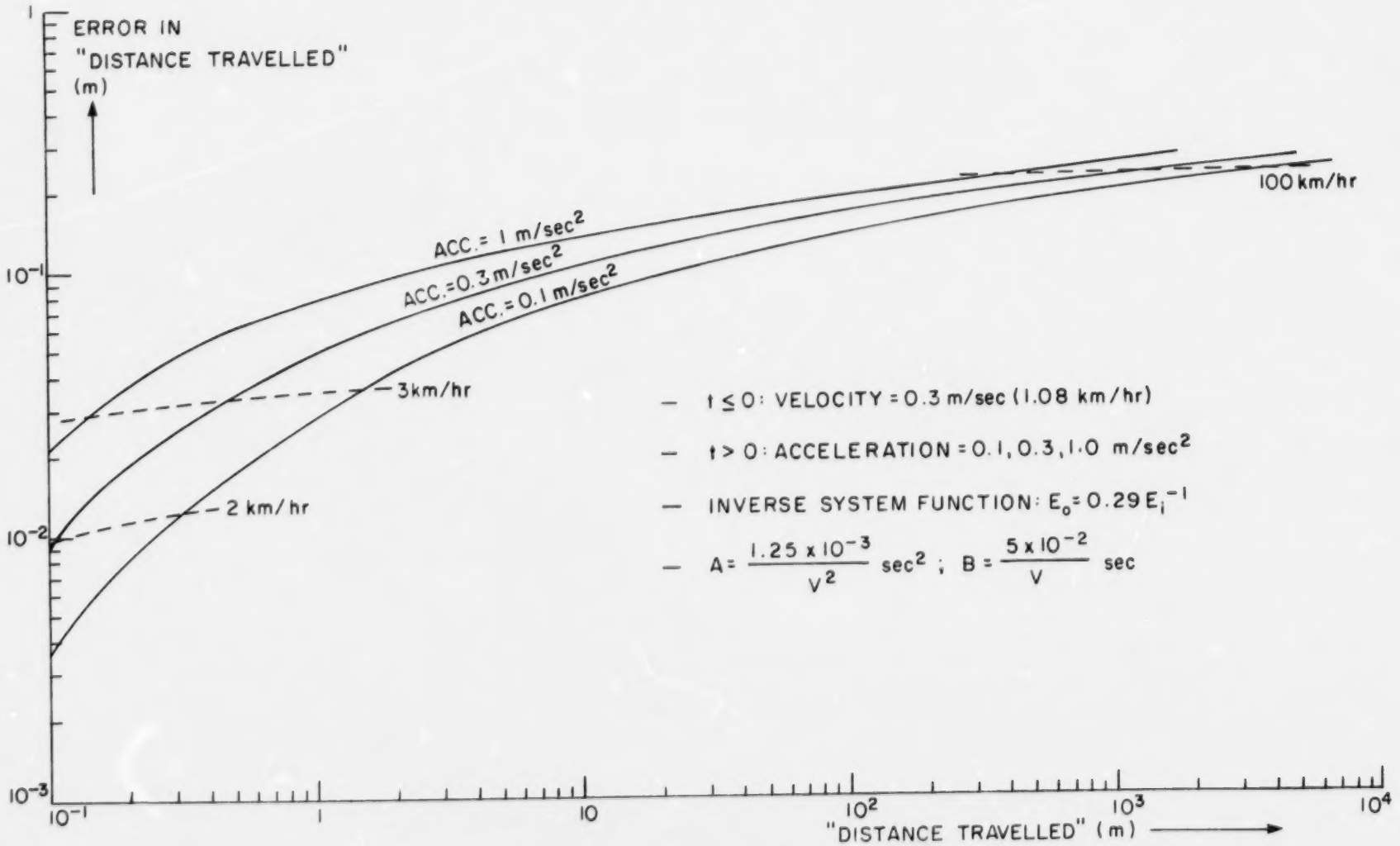
ERROR IN
"DISTANCE TRAVELLED"
(m)
1
10^{-1}
10^{-2}
10^{-3}
ACC. = 1 m/sec²
ACC. = 0.3 m/sec²
ACC. = 0.1 m/sec²
100 km/hr
3km/hr
2 km/hr
— t ≤ 0: VELOCITY = 0.3 m/sec (1.08 km/hr)
— t > 0: ACCELERATION = 0.1, 0.3, 1.0 m/sec²
— INVERSE SYSTEM FUNCTION: $E_o = 0.29 E_i^{-1}$
— $A = \frac{1.25 \times 10^{-3}}{V^2}$ sec² ; $B = \frac{5 \times 10^{-2}}{V}$ sec
10^{-1}
1
10
10^2
10^3
10^4
"DISTANCE TRAVELLED" (m)

FIG. 52

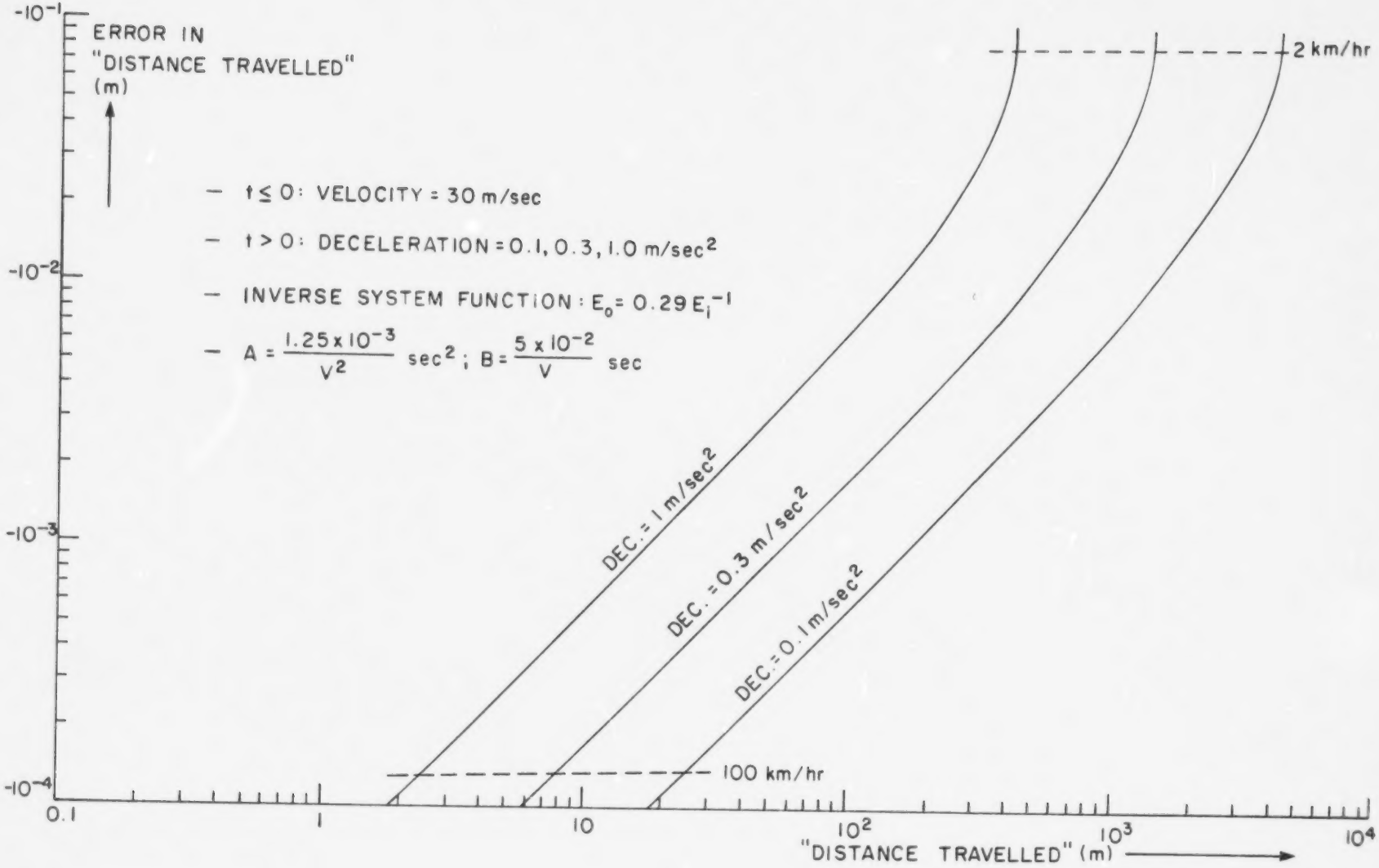
-10⁻¹
-10⁻²
-10⁻³
-10⁻⁴
ERROR IN
"DISTANCE TRAVELLED"
(m)
— t ≤ 0: VELOCITY = 30 m/sec
— t > 0: DECELERATION = 0.1, 0.3, 1.0 m/sec²
— INVERSE SYSTEM FUNCTION: E₀ = 0.29 E_i⁻¹
— A = 1.25 x 10⁻³ / V² sec²; B = 5 x 10⁻² / V sec
2 km/hr
100 km/hr
DEC. = 1 m/sec²
DEC. = 0.3 m/sec²
DEC. = 0.1 m/sec²
0.1
1
10
10²
10³
10⁴
"DISTANCE TRAVELLED" (m)

FIG. 53

12.0 ANALYSIS OF FOURTH-ORDER DELAY-LOCKED LOOP SYSTEM

The fourth order system was developed as a result of efforts to optimize the second order system for velocity ramp inputs. Optimizing for velocity ramp inputs means providing phase compensation such that the steady state value for the velocity error is zero.

Using the Laplace Final Value Theorem one can readily derive, for linear systems, the desired general form for a transfer function to obtain zero steady state error for a ramp input.

Let the transfer function H(p) be:

$$H(p) = \frac{y(p)}{x(p)} = \left\{ \frac{1 + b_1 p + b_2 p^2 + \ldots b_{n-1} p^{n-1}}{1 + a_1 p + a_2 p^2 + \ldots a_n p^n} \right\} \tag{75}$$

The error in the output signal y(p) is then:

$$x(p) - y(p) = \{1 - H(p)\}\, x(p) \tag{76}$$

The input signal x(p) is a ramp hence $x(p) = \frac{A}{p^2}$ thus,

$$x(p) - y(p) = \{1 - H(p)\} \frac{A}{p^2} \tag{77}$$

Applying the Laplace Final Value Theorem,

$\lim_{t \to \infty} z(t) = \lim_{p \to 0} pz(p)$ gives,

$$\lim_{t \to \infty} \{x(t) - y(t)\} = \lim_{p \to 0} p\{1 - H(p)\} \frac{A}{p^2} = \lim_{p \to 0} \frac{A}{p} \{1 - H(p)\} = 0 \tag{78}$$

Substituting H(p) it follows that for zero steady state error for ramp inputs the condition to be satisfied is: $a_1 = b_1$.

The general form of H(p) therefore is:

$$H(p) = \left\{ \frac{1 + a_1 p + b_2 p^2 + \ldots b_{n-1} p^{n-1}}{1 + a_1 p + a_2 p^2 + \ldots a_n p^n} \right\} \tag{79}$$

Whereas this applies to linear systems,the basic idea applies also to the non-linear transfer function of the delay-locked loop.

The simplest way to obtain phase compensation is to introduce an additional first order filter in the loop of the form,

$$h(p) = \left(\frac{1 + p\tau_2}{p\tau_1} \right)$$

The disadvantage however, is that we are unable to control the transfer function as readily with non-linear functions.

Whilst experimenting with various loop configurations, with the aim to obtaining phase compensation, a rather interesting configuration was found. It consists of two second order loops linked together. It has added complexity but phase compensation can be obtained whilst maintaining control over the system behaviour with non-linear system functions. The resulting overall transfer function is therefore that of a fourth order system but its behaviour is readily made to resemble that of a second order system, having additional phase compensation for velocity ramp inputs. The small signal transfer function, the non-linear differential equation and the error in velocity and "distance travelled" will be analyzed in the next four sections.

12.1 Small Signal Transfer Function

The signal flow graph of the two linked second order systems is shown in Figure 54. Systems I and II don't have to be identical but we will examine this particular case. Both delay-locked loops have the two input noise sensors in common. All partial transfer functions are identical.

The coupling link between the two systems is established at the outputs of the difference integrators of Systems I and II respectively.

The transfer system of System I is:

$$\psi(p) = \frac{\Delta\hat{T}(p)}{\Delta T(p)} \tag{80}$$

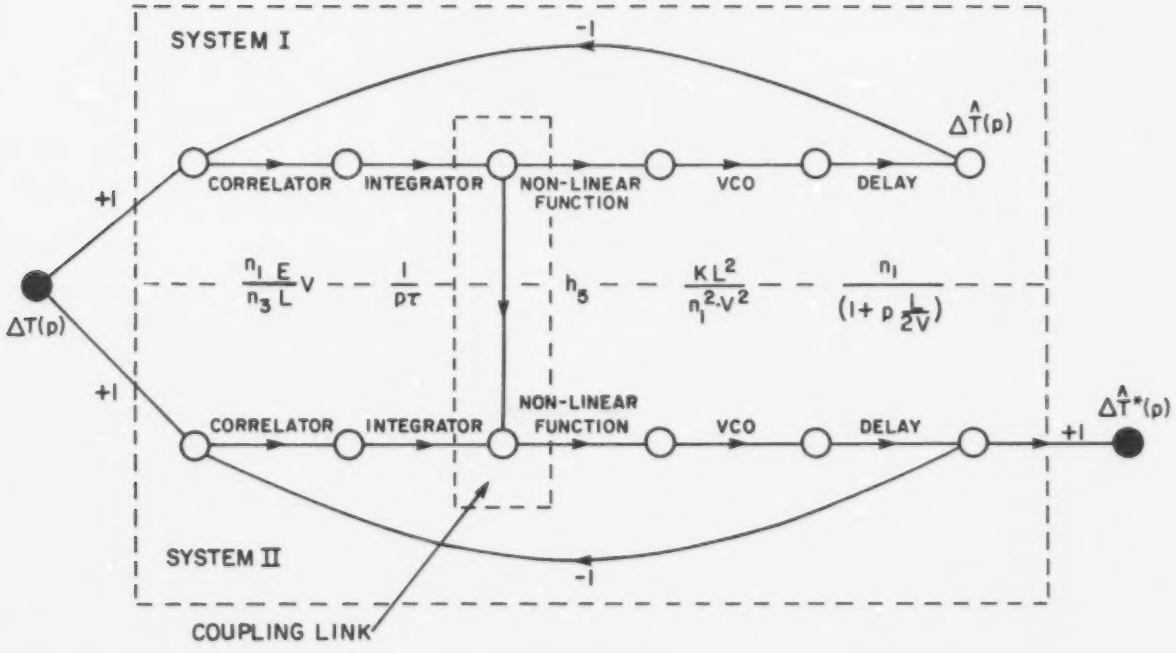

FIG. 54

The relation between input and output of System II is:

$$\Delta\hat{T}^*(p) = \Delta T(p)\,\psi(p) + \left\{\left(\frac{pn_3V\tau_1}{EKLh_3}\right)\left(1 + p\,\frac{L}{2V}\right)\Delta T(p)\,\psi(p)\right\}\psi(p) \tag{81}$$

The transfer function of System II therefore is:

$$\psi^*(p) = \frac{\Delta\hat{T}^*(p)}{\Delta T(p)} = \psi(p)\left[1 + \psi(p)\left(\frac{pn_3V\tau}{EKLh_3}\right)\left(1 + p\,\frac{L}{2V}\right)\right] \tag{82}$$

Substituting,

$$\psi(p) = \left\{\frac{1}{1 + p\left(\frac{n_3V\tau}{EKLh_3}\right) + p^2\left(\frac{n_3\tau}{2EKh_3}\right)}\right\} \tag{2}$$

into (82) yields for $\psi^*(p)$:

$$\psi^*(p) = \frac{\left\{1 + p\left(\frac{2n_3V\tau}{EKLh_3}\right) + p^2\left(\frac{n_3\tau}{EKh_3}\right)\right\}}{\left\{1 + p\left(\frac{n_3V\tau}{EKLh_3}\right) + p^2\left(\frac{n_3\tau}{2EKh_3}\right)\right\}^2} \tag{83}$$

With reference to (79) one can see that the condition for zero steady state error, for ramp inputs, is more than satisfied; not only is $a_1 = b_1$ but also $a_2 = b_2$.

The fourth order system will be analyzed using the inverse non-linear function derived earlier for the second order system in Section 6.1.

$$E_0 = \left(\frac{\beta^2 n_1^2 E}{2n_3\tau K}\right) \cdot \frac{1}{E_i} \tag{18}$$

having a small signal transfer gain h_5

$$h_5 = \left(\frac{2n_3\tau V^2}{\beta^2 EKL^2}\right) \tag{7}$$

Substition of (7), with $\beta = 2$, in (83) yields for $\psi^*(p)$,

$$\psi^*(p) = \frac{\left\{1 + p\left(\frac{4L}{V}\right) + p^2\left(\frac{2L^2}{V^2}\right)\right\}}{\left\{1 + p\left(\frac{L}{V}\right)\right\}^4} \tag{84}$$

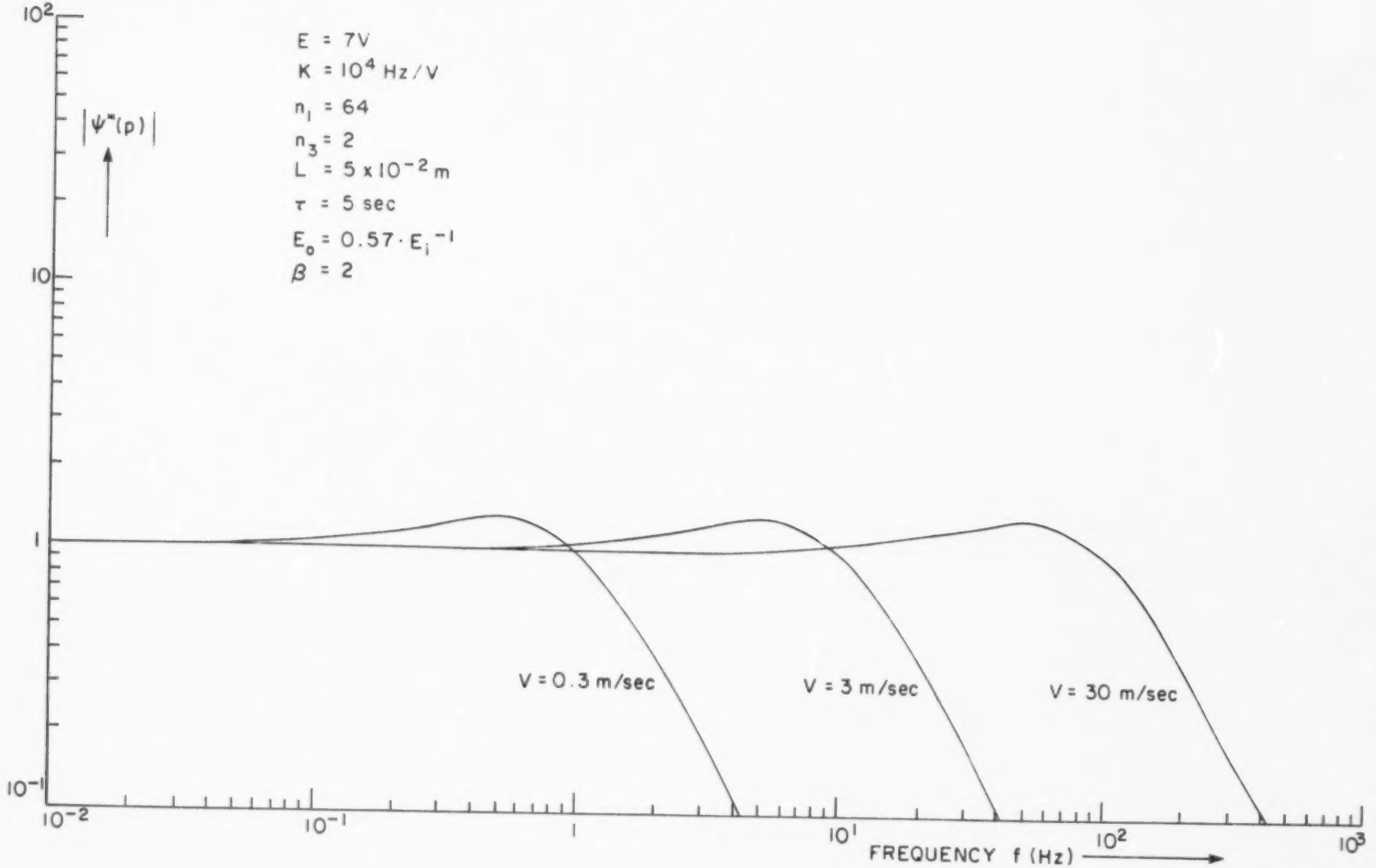

FIG. 55: SMALL SIGNAL TRANSFER GAIN OF FOURTH ORDER SYSTEM

The small signal transfer gain $\left| \psi^*(p) \right|$ is shown in Figure 55. Notice again the self-adaptive behaviour of the loop for the inverse non-linear function; the bandwidth shifts proportional with the input velocity.

The values for the system parameters are taken to be the same as for the second order system, i.e., E = 7V; K = 10^4 Hz/V; n_1 = 64; n_3 = 2; L = 510^{-2} m, τ = 5 sec. The value for the coefficient β is chosen 2 instead of $\sqrt{2}$. This results in a non-linear function $E_0 = \xi(E_i)$: $E_0 = 0.57/E_i$.

As can be seen, comparing Figures 23 and 55, the fourth order system with $\beta = 2$ behaves very similar to the second order system with $\beta = \sqrt{2}$ (there is a small overshoot in the transfer gain for the fourth order system). This was done to allow a valid comparison to be made with respect to errors in velocity and "distance travelled" for a velocity ramp input.

12.2 Derivation of Non-Linear Differential Equation

One can use relationship (84) to derive the non-linear differential equation for arbitrary input conditions. The variables x(t) and y(t) will be used, as before, for the input and output velocity, respectively. Using $\eta = \frac{L}{V}$ to simplify the notation one can rewrite (84) as:

$$y(p)\,(1 + p\eta)^4 = x(p)\,(1 + p^4\eta + p^2 2\eta^2) \tag{85}$$

Relationship (85) corresponds to a differential equation

$$\eta^4 \frac{d^4y}{dt^4} + 4\eta^3 \frac{d^3y}{dt^3} + 6\eta^2 \frac{d^2y}{dt^2} + 4\eta \frac{dy}{dt} + y = 2\eta^2 \frac{d^2x}{dt^2} + 4\eta \frac{dx}{dt} + x \tag{86}$$

The differential equation is non-linear with η being a function of x.

Again, as before, we linearize the differential equation by restricting the solution to a small time interval Δt, allowing us to consider η to be a constant for this time interval.

The solution at $t = n\Delta t$ is found by n successive iterations. At the beginning of each time interval one has to calculate a set of initial conditions, x and y and their derivatives and η.

The following notation will be used to indicate the initial conditions for an arbitrary time interval.

$$y\Big|_{t=n\Delta t} = y_{0,n}; \quad \frac{dy}{dt}\Big|_{t=n\Delta t} = y_{1,n}; \quad \frac{dy^2}{dt^2}\Big|_{t=n\Delta t} = y_{2,n};$$

$$\frac{d^3y}{dt^3}\Big|_{t=n\Delta t} = y_{3,n}; \quad x\Big|_{t=n\Delta t} = x_{0,n}; \quad \frac{dx}{dt}\Big|_{t=n\Delta t} = x_{1,n};$$

$$\eta\Big|_{t=n\Delta t} = \eta_n\,, \tag{87}$$

where η_n is the average value over the time interval $t = n\Delta t$ to $(n + 1)\Delta t$

The solution for y(t), for the time interval $t = n\Delta t$ to $t = (n + 1)\Delta t$, will be indicated by $y_n(t)$.

12.3 Solution, Over Interval Δt, for Velocity Ramp Input

The input signal x(t) is a ramp,

$$x(t) = x_0 + \alpha t \tag{88}$$

where x_0 is the velocity for $t \leq 0$ and αt the ramp input, applied at $t = 0$.

The acceleration α is constant, thus,

$$x_{1,n} = x_1 = \alpha = \text{constant} \tag{89}$$

The input velocity at intervals Δt is:

$$x_{0,n} = x_0 + n\Delta t \tag{90}$$

The coefficient $\eta = \frac{L}{V}$, $V = x(t)$, hence the average value of η_n over the time interval $t = n\Delta t$ to $t = (n + 1)\Delta t$ is:

$$\eta_n = \frac{L}{\left(x_0 + \frac{1}{2}\, n\Delta t\right)} \tag{91}$$

The initial values for acceleration, velocity and system coefficient are given by (89), (90), and (91) for an arbitrary interval Δt.

The initial values $y_{0,n}$, $y_{1,n}$, $y_{2,n}$, and $y_{3,n}$ are obtained from y, i.e., the solution of the differential equation.

This solution is obtained by applying the Laplace Transform to the differential equation (86) for arbitrary initial conditions and for a ramp input.

$$y_{n+1}(p) = \frac{(\eta_n y_{0,n})p^3 + (4\eta_n^3 y_{0,n} + \eta_n^4 y_{1,n})p^2 + (6\eta_n^2 y_{0,n} + 4\eta_n^3 y_{1,n}}{(1 + \eta_n p)^4}$$

$$+ \frac{\eta_n^4 y_{2,n} - 2\eta_n^2 x_{0,n})p + (4\eta_n y_{0,n} + 6\eta_n^2 y_{1,n} + 4\eta_n^3 y_{2,n} + \eta_n^4 y_{3,n} - 2\eta_n^2 x_1 - 4\eta_n x_{0,n})}{(1 + \eta_n p)^4}$$

$$+ \frac{(2\eta_n^2 p^2 + 4\eta_n p + 1)\,(x_{0,n} p + x_1)}{p^2 (1 + \eta_n p)^4} \tag{92}$$

The solution in the time domain is obtained applying the inverse Laplace Transform to relation (92).

$$y_{n+1}(t) = x_{0,n} + x_1 t + (y_{0,n} - x_{0,n}) + \left\{(y_{1,n} - x_1) + \frac{1}{\eta_n}(y_{0,n} - x_{0,n})\right\} t$$

$$+ \left\{y_{2,n} + \frac{2}{\eta_n}(y_{1,n} - x_1) + \frac{1}{\eta_n^2}(y_{0,n} - x_{0,n})\right\} \frac{t^2}{2}$$

$$+ \left\{y_{3,n} + \frac{3}{\eta_n} y_{2,n} + \frac{3}{\eta_n^2}(y_{1,n} - x_1) + \frac{1}{\eta_n^3}(y_{0,n} - x_{0,n})\right\} \frac{t^3}{6} e^{-t/\eta_n} \qquad (93)$$

The solution $y_{n+1}(t)$ gives the velocity output signal for the time interval $t = (n+1)\Delta t$ to $t = (n+2)\Delta t$.

The "distance travelled", $\int y dt$, is obtained by integration of (93) and selecting the integration constant to satisfy the initial condition at $t = 0$, i.e., $\int y dt = 0$ for $t = 0$.

$$\int y_{n+1}(t)dt = \left(x_{0,n} t + \frac{1}{2} x_1 t^2\right)$$

$$+ \left\{\eta_n^4 y_{3,n} + 4\eta_n^3 y_{2,n} + 6\eta_n^2 (y_{1,n} - x_1) + 4\eta_n (y_{0,n} - x_{0,n})\right\} \left(1 - e^{-t/\eta_n}\right)$$

$$- \left\{\eta_n^3 y_{3,n} + 4\eta_n^2 y_{2,n} + 6\eta_n (y_{1,n} - x_1) + 3(y_{0,n} - x_{0,n})\right\} t$$

$$+ \left\{\eta_n^2 y_{3,n} + 4\eta_n y_{2,n} + 5(y_{1,n} - x_1) - \frac{2}{\eta_n}(y_{0,n} - x_{0,n})\right\} \frac{t^2}{2}$$

$$+ \left\{\eta_n y_{3,n} + 3y_{2,n} + \frac{3}{\eta_n}(y_{1,n} - x_1) + \frac{1}{\eta_n^2}(y_{0,n} - x_{0,n})\right\} \frac{t^3}{6} e^{-t/\eta_n} \qquad (94)$$

The initial conditions $y_{0,n+1}$, $y_{1,n+1}$, $y_{2,n+1}$, and $y_{3,n+1}$, are derived from (93),

$$y_{0,n+1} = x_{0,n} + x_1 \Delta t + (y_{0,n} - x_{0,n}) + \left\{(y_{1,n} - x_1) + \frac{1}{\eta}(y_{0,n} - x_{0,n})\right\} \Delta t$$

$$+ \left\{y_{2,n} + \frac{2}{\eta_n}(y_{1,n} - x_1) + \frac{1}{\eta_n^2}(y_{0,n} - x_{0,n})\right\} \frac{(\Delta t)^2}{2}$$

$$+ \left\{y_{3,n} + \frac{3}{\eta_n} y_{2,n} + \frac{3}{\eta_n^2}(y_{1,n} - x_1) + \frac{1}{\eta_n^3}(y_{0,n} - x_{0,n})\right\} \frac{(\Delta t)^3}{6} e^{-\Delta t/\eta_n} \qquad (95)$$

$$y_{1,n+1} = x_1 + (y_{1,n} - x_1) + \left\{ y_{2,n} + \frac{1}{\eta_n} (y_{1,n} - x_1) \right\} \Delta t$$

$$+ \left\{ y_{3,n} + \frac{2}{\eta_n} y_{2,n} + \frac{1}{\eta_n^2} (y_{1,n} - x_1) \right\} \frac{(\Delta t)^2}{2}$$

$$- \left\{ \frac{1}{\eta_n} y_{3,n} + \frac{3}{\eta_n^2} y_{2,n} + \frac{3}{\eta_n^3} (y_{1,n} - x_1) + \frac{1}{\eta_n^4} (y_{0,n} - x_{0,n}) \right\} \frac{(\Delta t)^3}{6} e^{-\Delta t/\eta_n} \qquad (96)$$

$$y_{2,n+1} = y_{2,n} + \left(y_{3,n} + \frac{1}{\eta_n} y_{2,n} \right) \Delta t$$

$$- \left\{ \frac{2}{\eta_n} y_{3,n} + \frac{5}{\eta_n^2} y_{2,n} + \frac{4}{\eta_n^3} (y_{1,n} - x_1) + \frac{1}{\eta_n^4} (y_{0,n} - x_{0,n}) \right\} \frac{(\Delta t)^2}{2}$$

$$+ \left\{ \frac{1}{\eta^2} y_{3,n} + \frac{3}{\eta_n^3} y_{2,n} + \frac{3}{\eta_n^4} (y_{1,n} - x_1) + \frac{1}{\eta_n^5} (y_{0,n} - x_{0,n}) \right\} \frac{(\Delta t)^3}{6} e^{-\Delta t/\eta_n} \qquad (97)$$

$$y_{3,n+1} = y_{3,n} - \left\{ \frac{3}{\eta_n} y_{3,n} + \frac{6}{\eta_n^2} y_{2,n} + \frac{4}{\eta_n^3} (y_{1,n} - x_1) + \frac{1}{\eta_n^4} (y_{0,n} - x_{0,n}) \right\} \Delta t$$

$$+ \left\{ \frac{3}{\eta_n^2} y_{3,n} + \frac{8}{\eta_n^3} y_{2,n} + \frac{7}{\eta_n^4} (y_{1,n} - x_1) + \frac{2}{\eta_n^5} (y_{0,n} - x_{0,n}) \right\} \frac{(\Delta t)^2}{2}$$

$$- \left\{ \frac{1}{\eta_n^3} y_{3,n} + \frac{3}{\eta_n^4} y_{2,n} + \frac{3}{\eta_n^5} (y_{1,n} - x_1) + \frac{1}{\eta_n^6} (y_{0,n} - x_{0,n}) \right\} \frac{(\Delta t)^3}{6} e^{-\Delta t/\eta_n} \qquad (98)$$

The solutions for velocity and "distance travelled" are valid only for a small time interval Δt. A complete solution therefore is obtained by repetitive iteration, which also serves to calculate the set of system boundary conditions, using the expressions above, at the onset of each particular time interval. The time interval Δt should be chosen sufficiently small in relation to the rate of change of input and output signals and system coefficient η.

The solution for the "distance travelled" is obtained by accumulating the previous values calculated during iteration, hence:

$$\int_0^{n\Delta t} y_n(t)dt = \int_0^{\Delta t} y_0(t)dt + \int_0^{\Delta t} y_1(t)dt + \ldots + \int_0^{\Delta t} y_n(t)dt = \sum_{n=0}^{n} \left\{ \int_0^{\Delta t} y_n(t)dt \right\} \qquad (99)$$

Note of caution:

The general solution has been derived for a small time interval, **always** from $t = 0$ to $t = \Delta t$. Hence, whilst the values of the solution are obtained at times $t = n\Delta t$, the time variable t in expressions (95) - (98) remain fixed at $t = \Delta t$. It seems strange at first, that solutions at arbitrary times are obtained keeping the time variable constant. Figure 56 however, should help clarify any confusion.

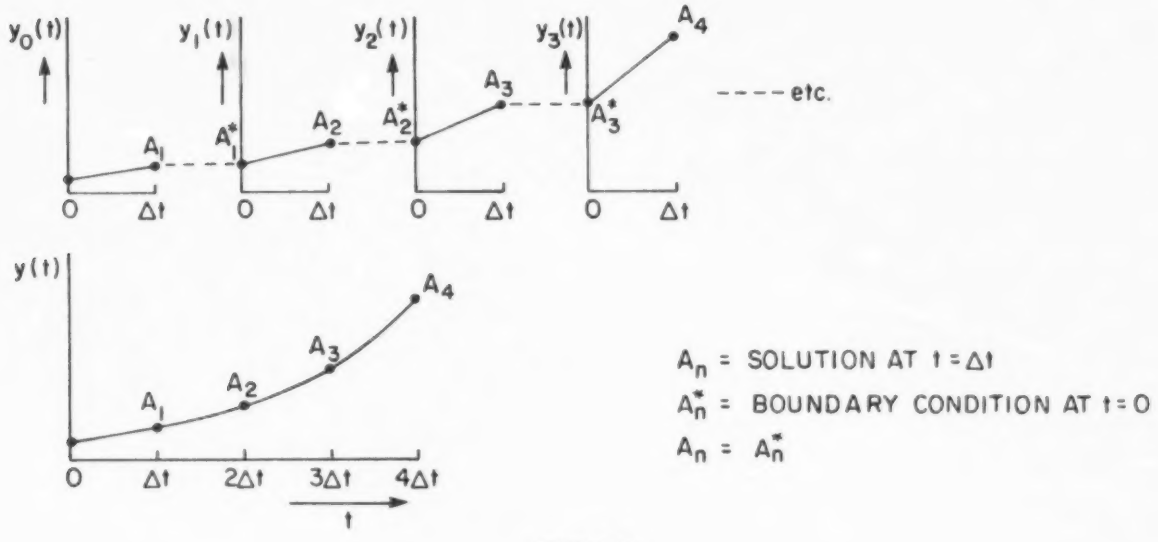

FIG. 56

It is evident from Figure 56 that, even if the partial solutions are restrained for $t = 0$ to $t = \Delta t$, the values for y at $t = \Delta t$ are effectively those for increasing time. The progression of time is actually incorporated in the changing boundary conditions.

12.4 Error in Velocity and "Distance Travelled" for Velocity Ramp Input (Inverse Non-Linear System Function)

Two numerical solutions have been derived for the equations derived in the previous section. One where there is constant acceleration from 0.3 m/sec to 30 m/sec, for three values of acceleration: 0.1, 0.3 and 1 m/sec^2. The other solution is for the case where there is constant deceleration from 30 m/sec to about 0.3 m/sec, for three values of deceleration: 0.1, 0.3 and 1 m/sec^2. Hence, the same conditions as those used for the second order system. The second order and the fourth order system, both using the inverse, non-linear loop function can therefore readily be compared. The results are shown in Figures 57-62. The additional phase-compensation of the fourth order system results in a very rapid decrease of the initial transient error. The resulting error in velocity and "distance travelled" is very small for the case of acceleration; where one starts with a relatively narrow bandwidth and is negligible for the case of deceleration; where one starts with a wide bandwidth.

The values for the system parameters, used in the calculation of the curves in Figures 57-62, are: $E = 7V$, $K = 10^4$ Hz/V, $n_1 = 64$, $n_2 = 2$, $L = 510^{-2}$ m, $\tau = 5$ sec, $\beta = 2$, and $E_0 = 0.57\ E_i^{-1}$.

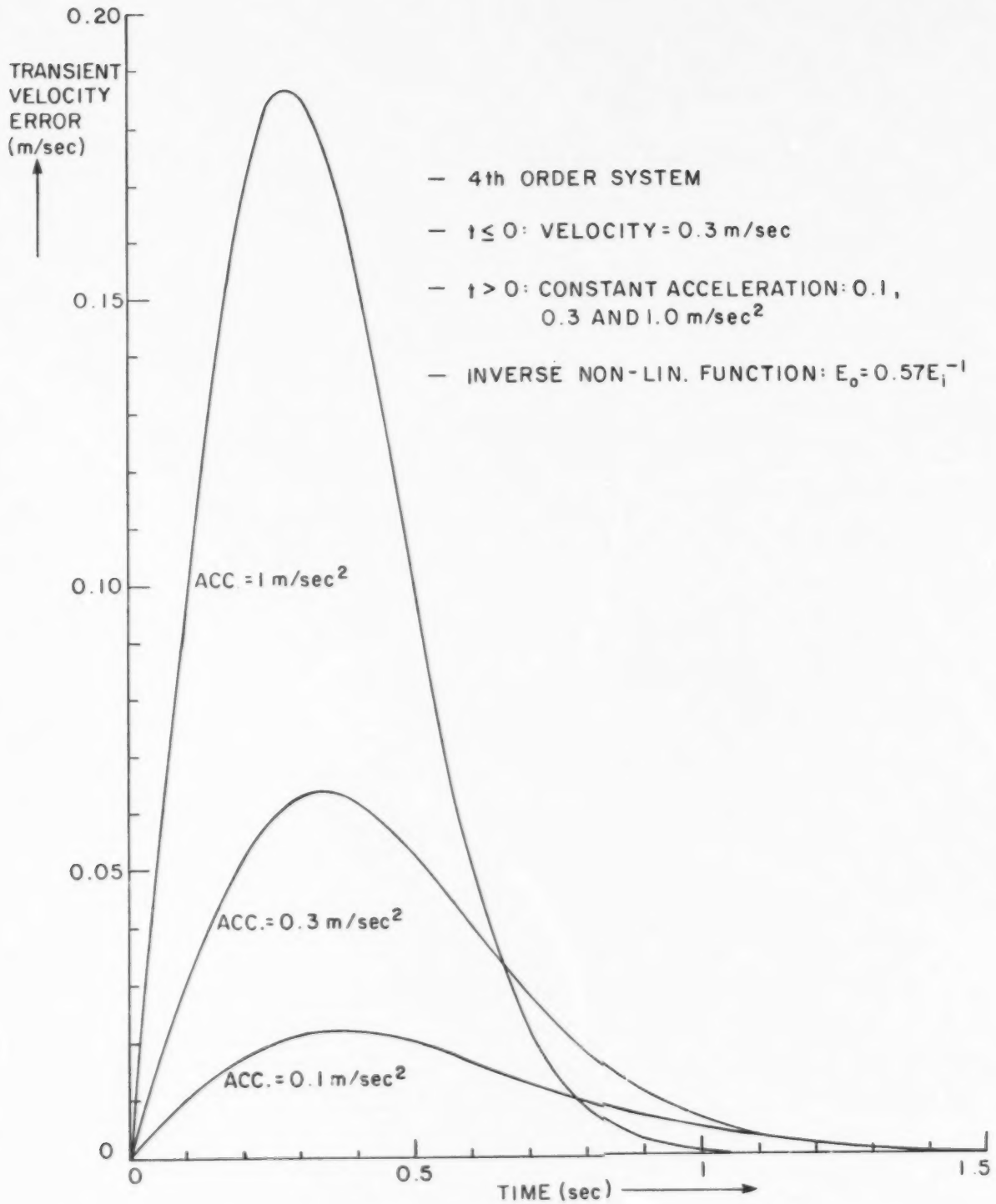
0.20
TRANSIENT VELOCITY ERROR (m/sec)
0.15
0.10
0.05
0
0
0.5
1
1.5
TIME (sec)
— 4th ORDER SYSTEM
— t ≤ 0: VELOCITY = 0.3 m/sec
— t > 0: CONSTANT ACCELERATION: 0.1, 0.3 AND 1.0 m/sec²
— INVERSE NON-LIN. FUNCTION: $E_o = 0.57E_i^{-1}$
ACC = 1 m/sec²
ACC. = 0.3 m/sec²
ACC. = 0.1 m/sec²

FIG. 57

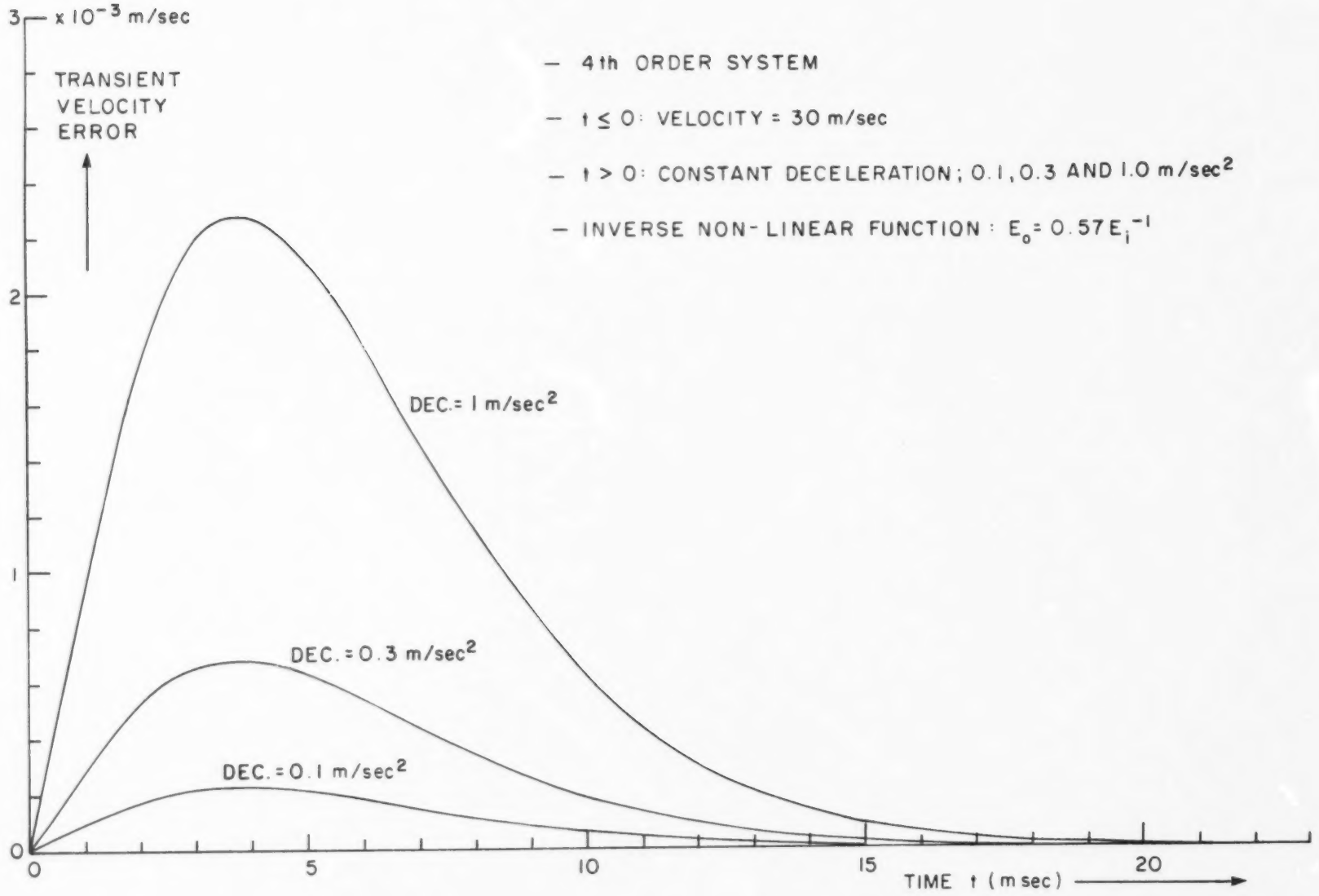
3
x 10⁻³ m/sec
TRANSIENT
VELOCITY
ERROR
2
1
0
— 4th ORDER SYSTEM
— t ≤ 0: VELOCITY = 30 m/sec
— t > 0: CONSTANT DECELERATION; 0.1, 0.3 AND 1.0 m/sec²
— INVERSE NON-LINEAR FUNCTION : E₀ = 0.57 E₁⁻¹
DEC.= 1 m/sec²
DEC.= 0.3 m/sec²
DEC.= 0.1 m/sec²
0
5
10
15
20
TIME t (m sec)

FIG. 58

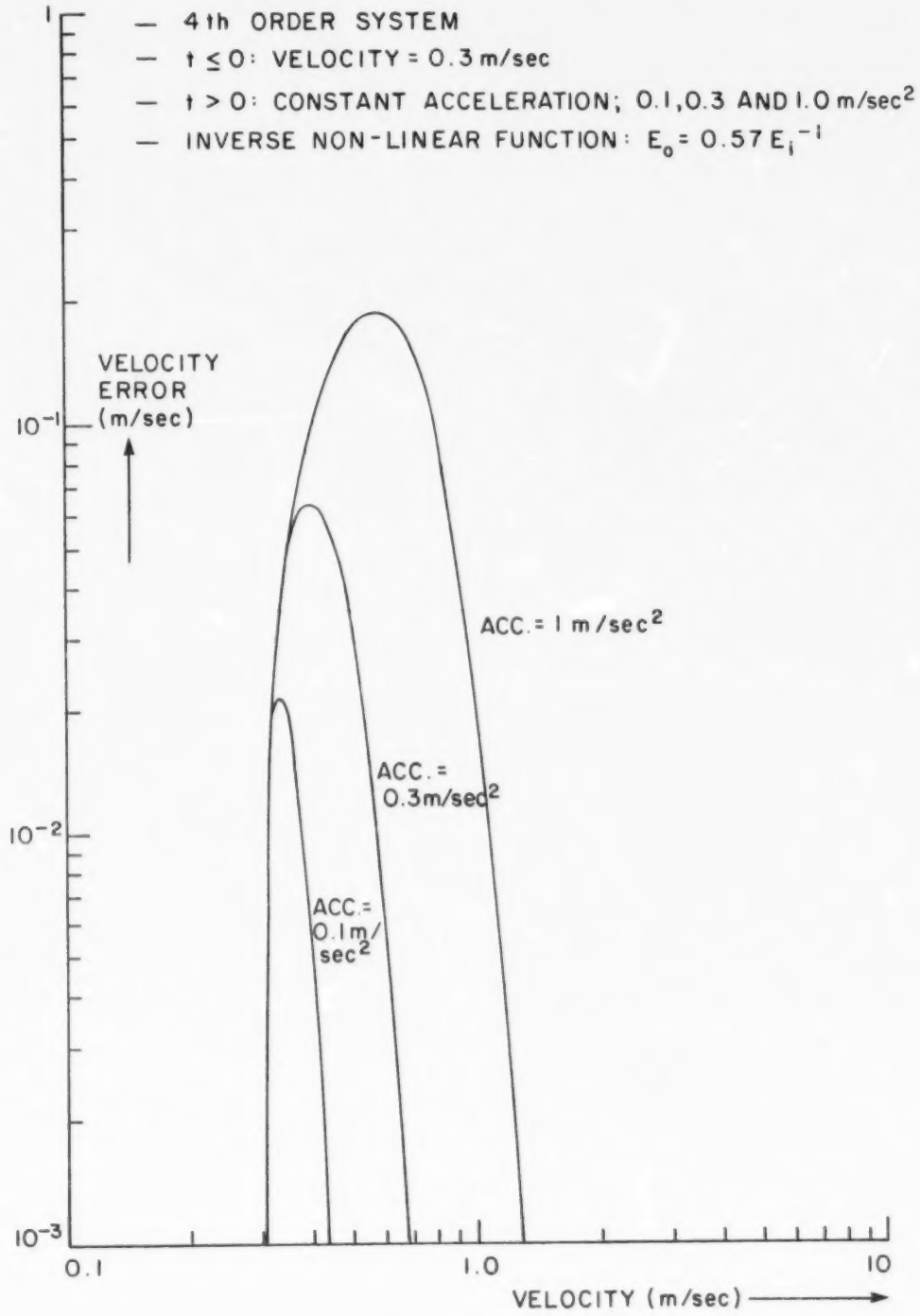
— 4th ORDER SYSTEM
— t ≤ 0: VELOCITY = 0.3 m/sec
— t > 0: CONSTANT ACCELERATION; 0.1, 0.3 AND 1.0 m/sec²
— INVERSE NON-LINEAR FUNCTION: $E_o = 0.57 E_i^{-1}$
VELOCITY ERROR (m/sec)
1
10^{-1}
10^{-2}
10^{-3}
ACC. = 1 m/sec²
ACC. = 0.3m/sec²
ACC. = 0.1m/sec²
0.1
1.0
10
VELOCITY (m/sec)

FIG. 59

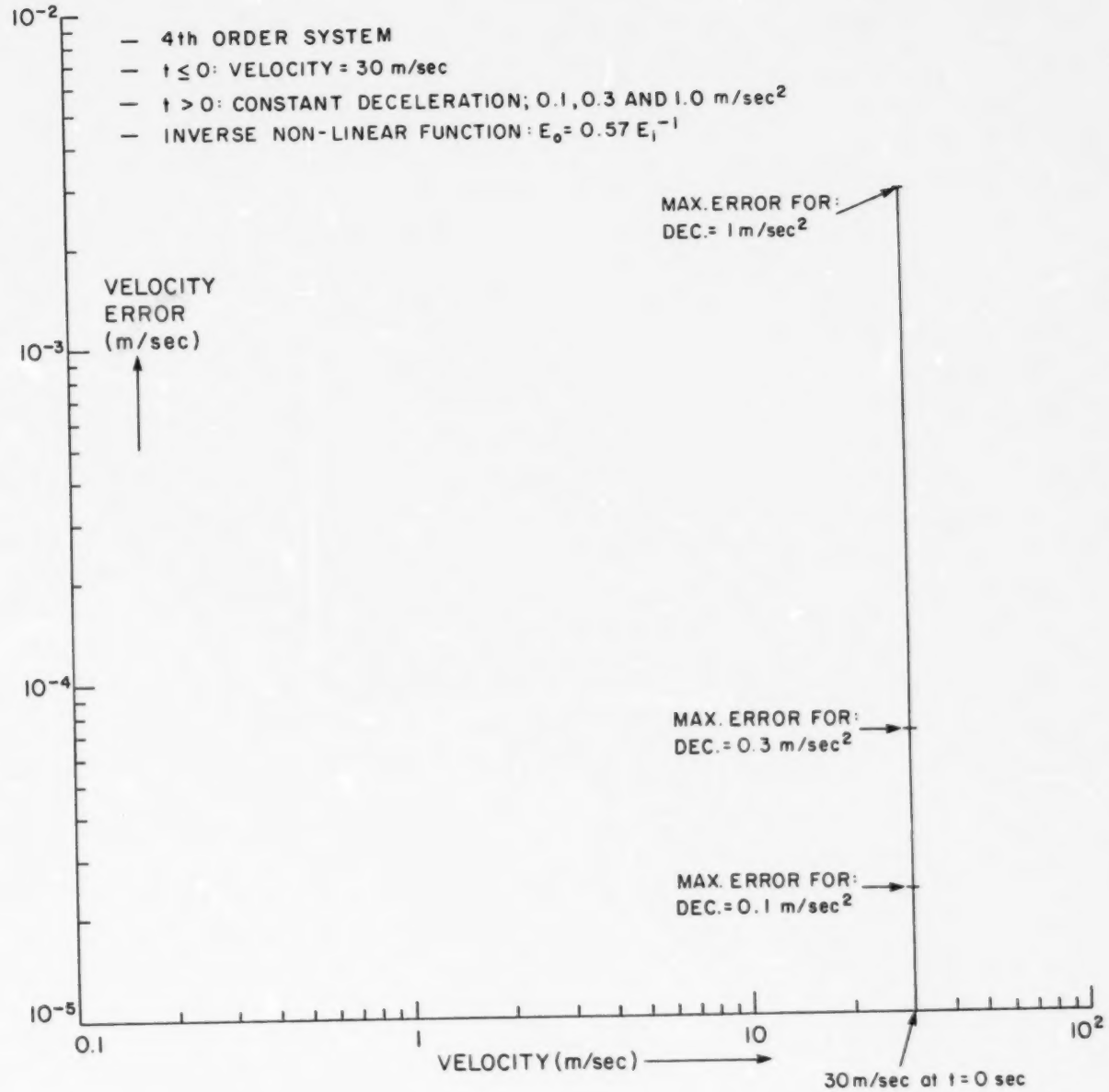
— 4th ORDER SYSTEM
— t ≤ 0: VELOCITY = 30 m/sec
— t > 0: CONSTANT DECELERATION; 0.1, 0.3 AND 1.0 m/sec²
— INVERSE NON-LINEAR FUNCTION: E₀ = 0.57 Eᵢ⁻¹
MAX. ERROR FOR: DEC. = 1 m/sec²
VELOCITY ERROR (m/sec)
MAX. ERROR FOR: DEC. = 0.3 m/sec²
MAX. ERROR FOR: DEC. = 0.1 m/sec²
10⁻²
10⁻³
10⁻⁴
10⁻⁵
0.1
1
10
10²
VELOCITY (m/sec)
30 m/sec at t = 0 sec

FIG. 60

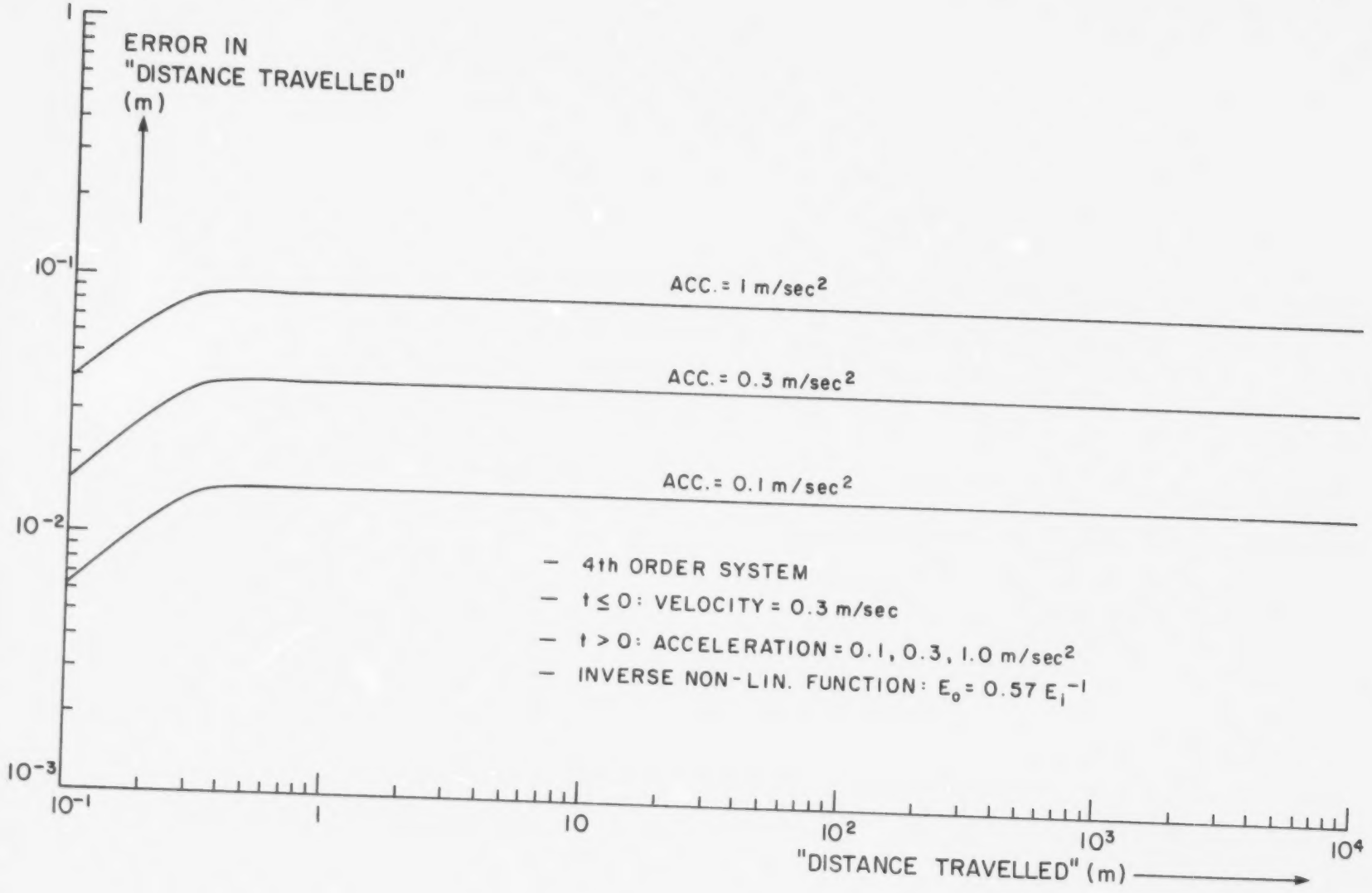
ERROR IN
"DISTANCE TRAVELLED"
(m)
1
10^{-1}
10^{-2}
10^{-3}
ACC. = 1 m/sec^2
ACC. = 0.3 m/sec^2
ACC. = 0.1 m/sec^2
— 4th ORDER SYSTEM
— $t \leq 0$: VELOCITY = 0.3 m/sec
— $t > 0$: ACCELERATION = 0.1, 0.3, 1.0 m/sec^2
— INVERSE NON-LIN. FUNCTION: $E_o = 0.57\ E_i^{-1}$
10^{-1}
1
10
10^2
10^3
10^4
"DISTANCE TRAVELLED" (m)

FIG. 61

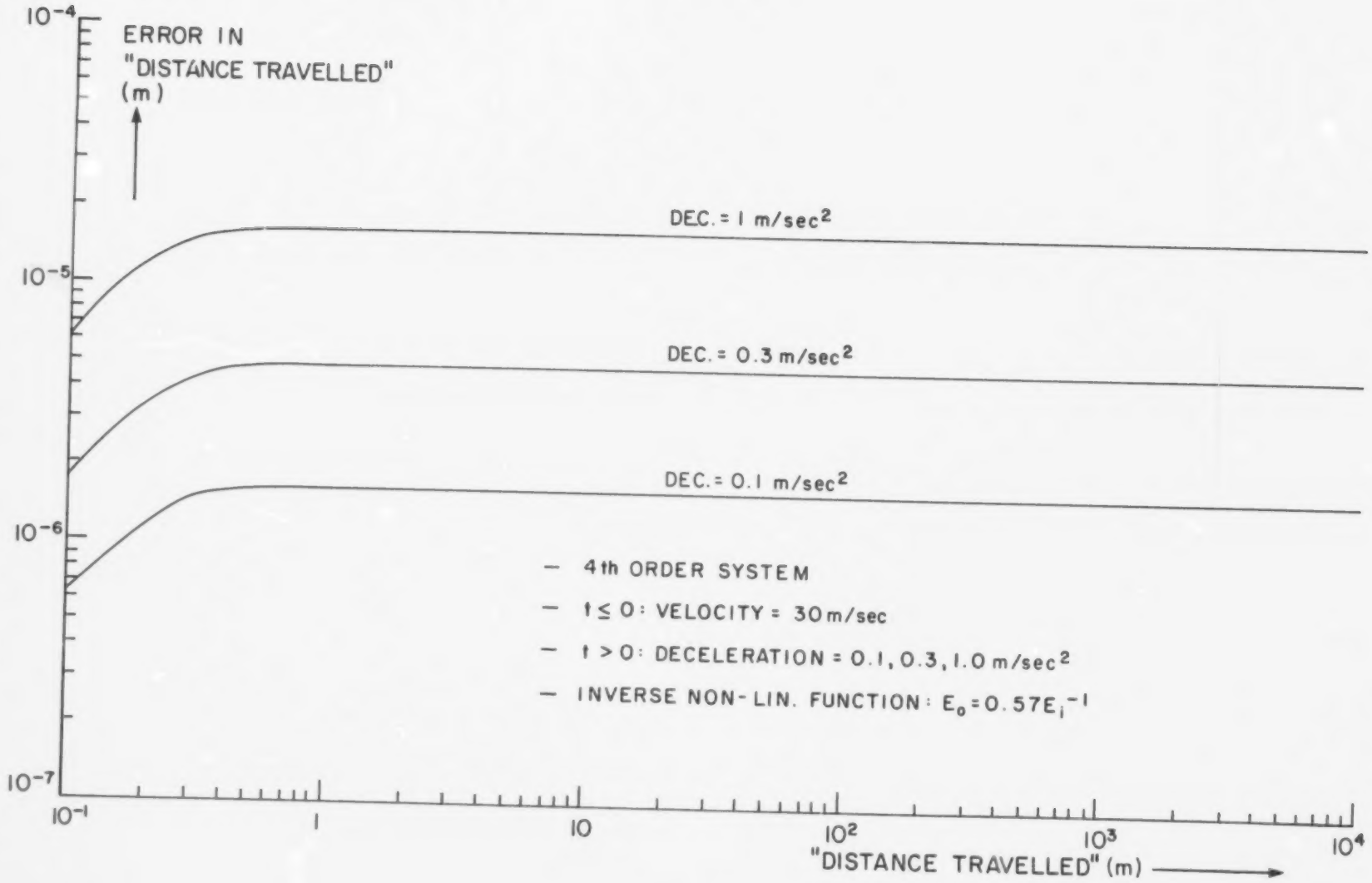
ERROR IN
"DISTANCE TRAVELLED"
(m)
DEC. = 1 m/sec²
DEC. = 0.3 m/sec²
DEC. = 0.1 m/sec²
— 4th ORDER SYSTEM
— t ≤ 0: VELOCITY = 30 m/sec
— t > 0: DECELERATION = 0.1, 0.3, 1.0 m/sec²
— INVERSE NON-LIN. FUNCTION: $E_o = 0.57E_i^{-1}$
10^{-4}
10^{-5}
10^{-6}
10^{-7}
10^{-1}
1
10
10^2
10^3
10^4
"DISTANCE TRAVELLED" (m)

FIG. 62

13.0 ANALYSIS OF LOOP BEHAVIOUR FOR INVARIANT NOISE

The noise power spectrum of the second and fourth order systems analyzed up till now has been variant, i.e., it compressed and expanded as a function of the velocity. The noise input signals were sensed in a moving medium, the noise frequency components therefore shifted proportional to the relative velocity between sensors and medium.

There is another mode of operation for the delay-locked loop where noise isn't sensed in a moving medium but instead generated and transmitted as modulation on some suitable carrier. The delay-locked loop is now tracking the delay of the carrier after it has travelled a certain distance, i.e., round trip to and from target or transponder. If the relative velocity between delay-locked loop and target is much smaller than the propagation speed of the carrier then the demodulated noise power spectrum of the received carrier is invariant, i.e., independent of the relative velocity.

The dynamic loop behaviour is quite different for variant and invariant noise power spectra. The behaviour for invariant noise power spectra will be analyzed in Section 13.

13.1 Measurement of Distance

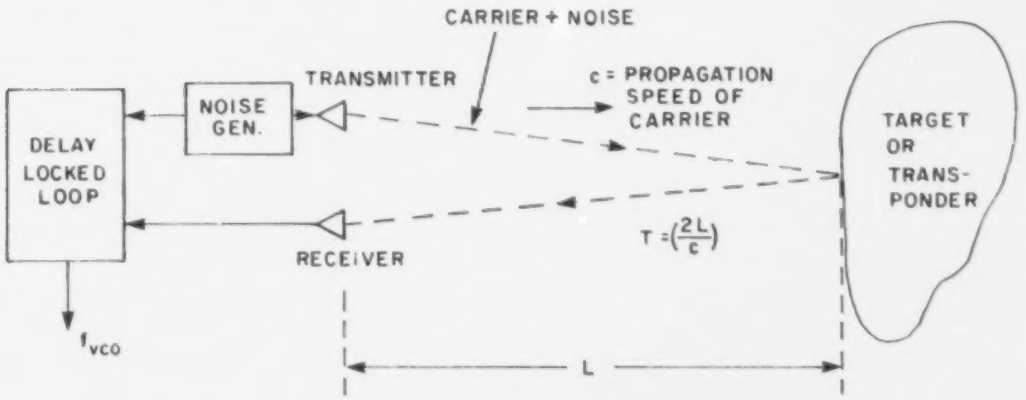

FIG. 63

The delay between the two input noise signals of the delay-locked loop is equal to the turn-around travel time of the carrier,

$$T = \frac{2L}{c} \tag{100}$$

where c is propagation speed of carrier and L the distance to target.

The loop tracks this delay with its internal delay $\hat{T}$, hence

$$\hat{T} = T$$

and since $\hat{T} = \frac{n_1}{f_{VCO}}$,

$$L = \left(\frac{n_1 c}{2}\right) \cdot \frac{1}{f_{VCO}} \tag{101}$$

The output frequency f_{VCO} is inversely proportional to the distance L.

The target can be the ocean floor, earth surface, a passive or active retrodirective antenna system, a transponder with or without frequency translation, etc. Therefore, in general, one is measuring depth, altitude, distance to destination but it could also be the measurement of small movements in a hydro-dam.

There are a variety of set-ups possible such as remote located transmitters, differential measuring schemes, etc. The analysis will be restricted however to the "basic scheme" of Figure 63.

13.2 Small Signal Transfer Function

The measurement of distance will frequently be static or quasi-static. Why then derive the small signal transfer function?

If the system configuration of Figure 63 is used in a dynamic environment, i.e. there are rapid changes in L, then certainly understanding of the loop performance, via the closed loop transfer function, is required.

Even when operating in quasi-static fashion knowledge of the transfer function is very useful. The loop operates on noise signals,and to obtain high accuracy one should strive for minimum noise output level. The output noise amplitude is directly determined by the small signal closed loop transfer function. As will be shown,the behaviour of the bandwidth and damping of the basic loop configuration are far from optimum. In effect the bandwidth increases in proportion to L^2. Also the transfer function becomes rather undamped for large L. This results in increased noise for large L and moreover, amplification of the noise in the region of peaking. Oftern, when measuring large distances, the returned signal will be very weak and therefore careful design of minimum possible bandwidth is required.

The transfer function of the cross-correlator has been derived in Section 4.1. The noise frequency spectrum shifted in proportion to the input velocity which resulted in a transfer gain proportional to velocity. In the present case the noise spectrum is invariant, i.e. independent of velocity. This requires a change in the circuitry as shown in Figure 64. The shift registers, n_3, previously driven by the clock, have to be replaced by constant delays τ.

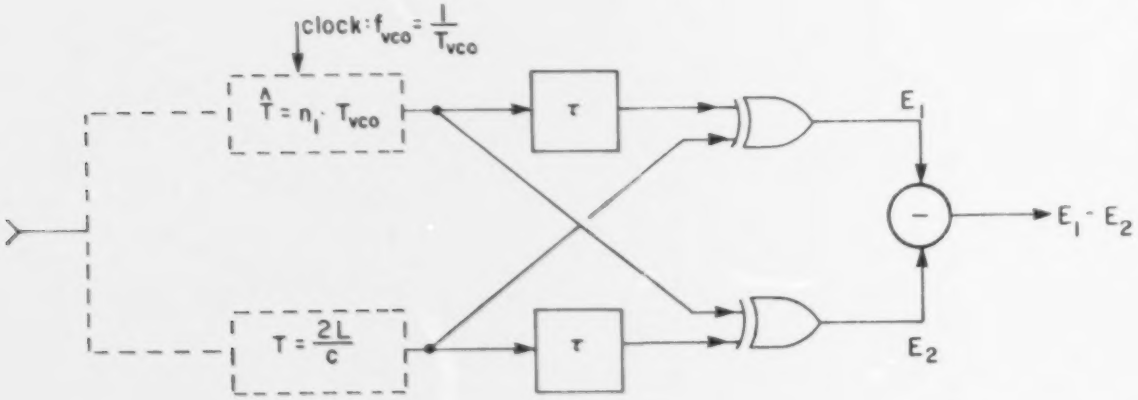

FIG. 64: TWO-POINT CROSS-CORRELATOR

The delays τ are set equal to the half-correlation width, $\tau_{1/2}$, to maximize the linear range of the transfer gain, i.e., $\tau = \tau_{1/2}$.

The output difference voltage is shown in Figure 65. The noise input spectrum being invariant, the slope is constant and the transfer gain simply a constant. The small signal transfer function is therefore:

$$h_1(p) = \text{constant} = \left(\frac{E}{\tau_{1/2}}\right) \qquad (102)$$

The small signal transfer function of the difference integrator is as before:

$$h_2(p) = \left(\frac{1}{p\tau}\right) \qquad (103)$$

where $\tau = RC$.

The relation between input voltage and output clock period of the VCO is shown in Figure 67.

$$T_{VCO} = \frac{1}{KE_{in}} \qquad (104)$$

The small signal transfer gain at the operating point is:

$$h_3(p) = \frac{-1}{KE_{in}^2} \qquad (105)$$

Using the lock-in condition one can express E_{in} as a function of the input variables L and c:

$$T = \hat{T} \Rightarrow \frac{2L}{c} = n_1 T_{VCO} \Rightarrow$$

$$E_{in} = \frac{n_1 c}{2KL}, \text{ hence}$$

$$h_3(p) = -\left(\frac{4KL^2}{n_1^2 c^2}\right) \qquad (106)$$

The transfer function of the delay has been derived in Section 5.1.4.

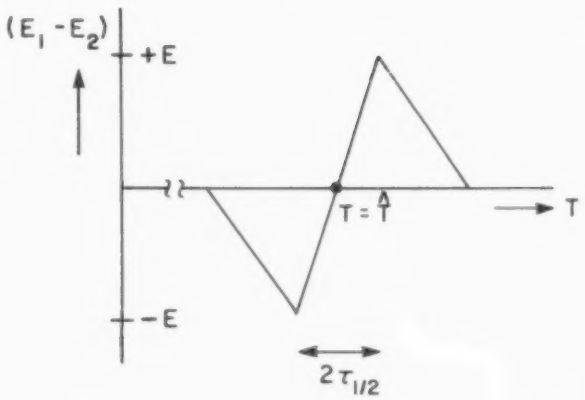

FIG. 65

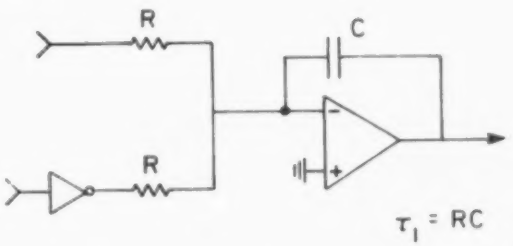

FIG. 66

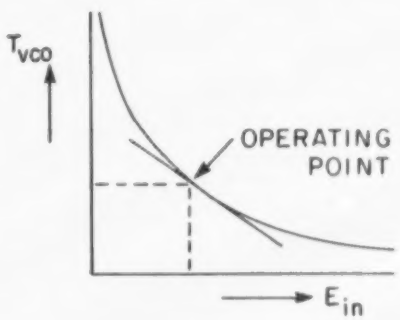

FIG. 67

$$h_4(p) = \frac{n_1}{1 + p\left(\frac{n_1 T_{VCO}}{2}\right)} \qquad (107)$$

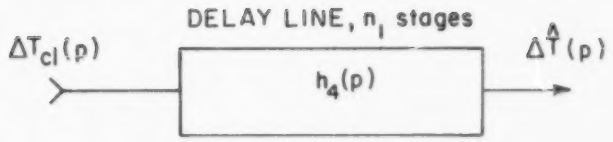

FIG. 68

Using again the lock-in condition $\frac{2L}{c} = n_1 T_{VCO}$ one can write:

$$h_4(p) = \frac{n_1}{1 + p\left(\frac{L}{c}\right)} \qquad (108)$$

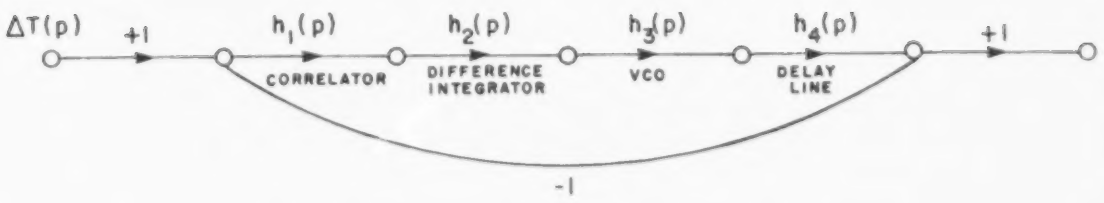

FIG. 69

The transfer function of the loop is:

$$\psi(p) = \frac{\Delta T(p)}{\Delta T(p)} = \frac{h_1(p)h_2(p)h_3(p)h_4(p)}{1 + h_1(p)h_2(p)h_3(p)h_4(p)} \qquad (109)$$

Substitution of the partial transfer function yields:

$$\psi(p) = \frac{1}{1 + p\left(\frac{\tau_{\frac{1}{2}} \tau n_1 c^2}{4EKL^2}\right) + p^2\left(\frac{\tau_{\frac{1}{2}} \tau n_1 c}{4EKL}\right)} \qquad (110)$$

Both the first and the second order term are a function of the input variable L.

The transfer function $\psi(p)$ is a non-linear second order low-pass filter of the general form:

$$\psi(p) = \frac{1}{1 + p\left(\frac{d}{\omega_o}\right) + p^2\left(\frac{1}{\omega_o^2}\right)} \qquad (111)$$

The natural frequency ω_o and the damping coefficient d of (110) are respectively:

$$\omega_u = \left(\frac{4EK}{\tau_{1/2}\,\tau n_1 c}\right)^{1/2} L^{1/2} \tag{112}$$

$$d = \left(\frac{\tau_{1/2}\,\tau n_1 c^3}{4EK}\right)^{1/2} L^{-3/2} \tag{113}$$

Notice that the system becomes very undamped for large values of L. Moreover, the bandwidth is increasing for large L.

For decreasing L the system behaves more and more as a first order system, with the first order term in (110) becoming dominant.

If the propagation speed c is very large then the system behaviour will resemble a first order system even for large values of L.

There are two useful types of carriers, electromagnetic and acoustic. If the carrier is electromagnetic then c is the speed of light; the second order term in (110) is negligible small and the system reduces to a first order system. Using an acoustical carrier one is usually unable to make this simplification and the second order system has to be analyzed.

In Section 13.3 the first order system will be analyzed using an electromagnetic carrier whereas Section 13.4 analyzes the second order loop behaviour for acoustical carriers.

13.3 First Order System

If the propagation speed c is very large, which is the case when using an electromagnetic carrier, i.e. radar or light beam, then the second order term in (110) can be neglected.

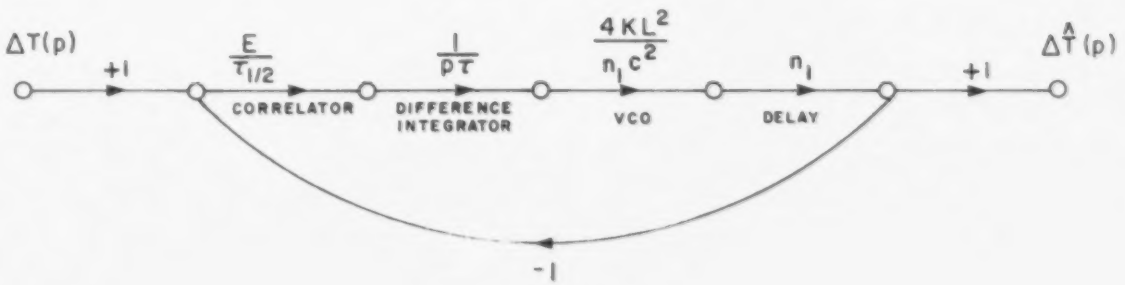

FIG. 70

The closed loop transfer function is:

$$\psi(p) = \frac{\Delta T(p)}{\Delta \hat{T}(p)} = \left[\frac{1}{1 + p\left(\frac{\tau_{1/2}\,\tau n_1 c^2}{4EKL^2}\right)}\right] \tag{114}$$

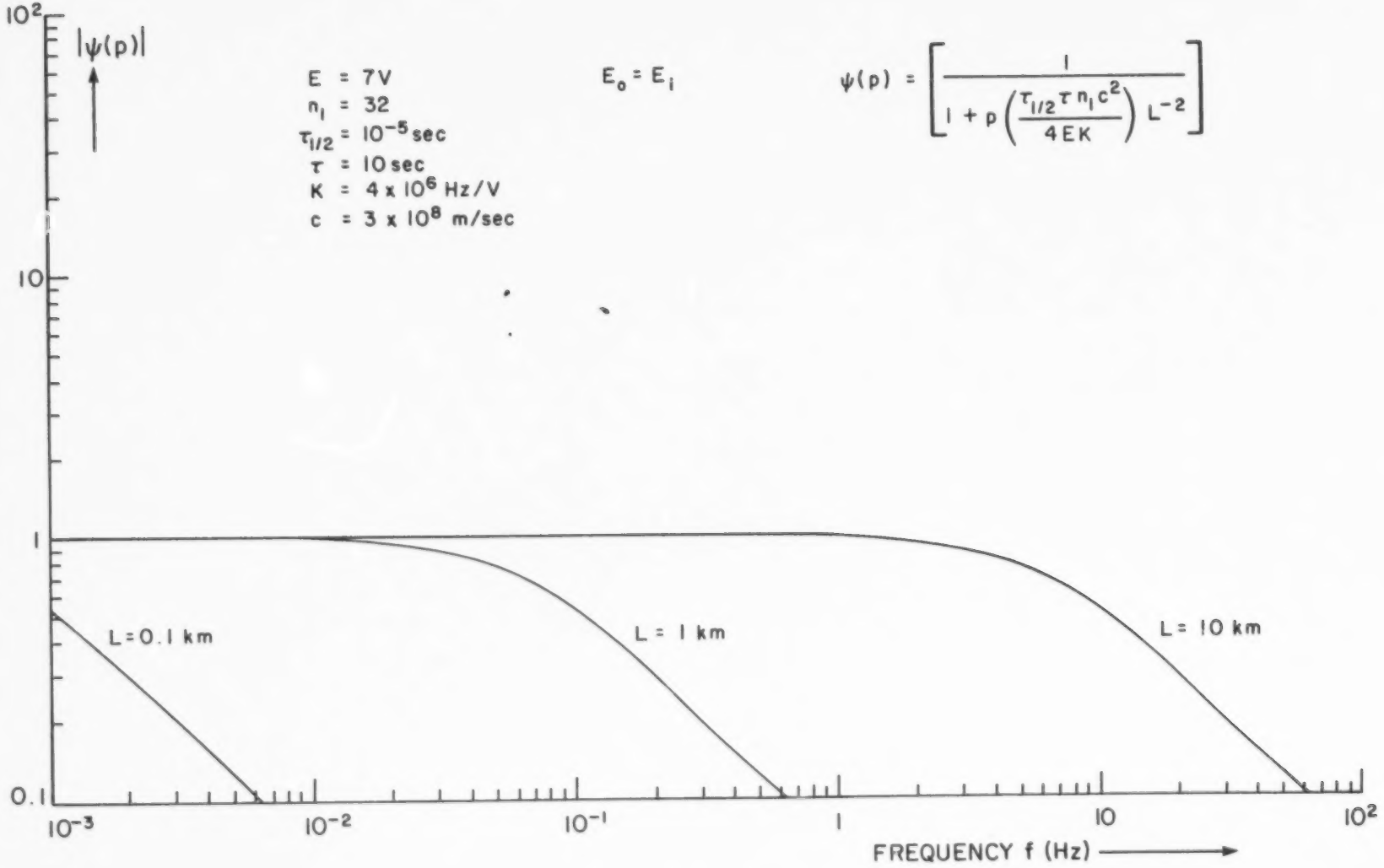
10^2
$|\psi(p)|$
E = 7V
n_1 = 32
$\tau_{1/2} = 10^{-5}$ sec
τ = 10 sec
K = 4×10^6 Hz/V
c = 3×10^8 m/sec
$E_o = E_i$
$\psi(p) = \left[\frac{1}{1 + p\left(\frac{\tau_{1/2}\tau n_1 c^2}{4EK}\right) L^{-2}}\right]$
10
1
0.1
L=0.1 km
L = 1 km
L = 10 km
10^{-3}
10^{-2}
10^{-1}
1
10
10^2
FREQUENCY f (Hz)

FIG. 71

The transfer function is a first order low-pass filter with a time constant, τ_o:

$$\tau_o = \left(\frac{\tau_{1/2}\, \tau\, n_1\, c^2}{4EK}\right) \frac{1}{L^2} \qquad (115)$$

hence, the bandwidth is proportional to L^2.

Example: $E = 7V$; $n_1 = 32$; $\tau_{1/2} = 10\,\mu sec$, $K = 410^6$ Hz/V

$c = 310^8$ m/sec (speed of light); $\tau = 10$ sec

The transfer gain as a function of frequency and distance is shown in Figure 71. The 3dB-bandwidth as a function of distance is shown in Figure 76.

For increasing L there is both an increasing bandwidth and a more heavily attenuated carrier signal, hence a decreasing signal to noise ratio in the loop. If L varies over a limited range then one can readily choose the values for the system parameters to obtain the desired bandwidth. However, if L varies substantially, some control over the bandwidth is required using non-linear functions inserted in the loop. One obvious goal is to strive for constant bandwidth. Alternatively, it might be desirable to have a bandwidth which effectively decreases for increasing L. For instance, when a carrier is attenuated substantially for large L one might want to sacrifice some bandwidth to improve the signal-to-noise ratio. Both cases will be analyzed next, i.e. constant bandwidth and bandwidth decreasing with increasing distance.

13.3.1 Constant Bandwidth

The signal flow diagram is shown in Figure 72.

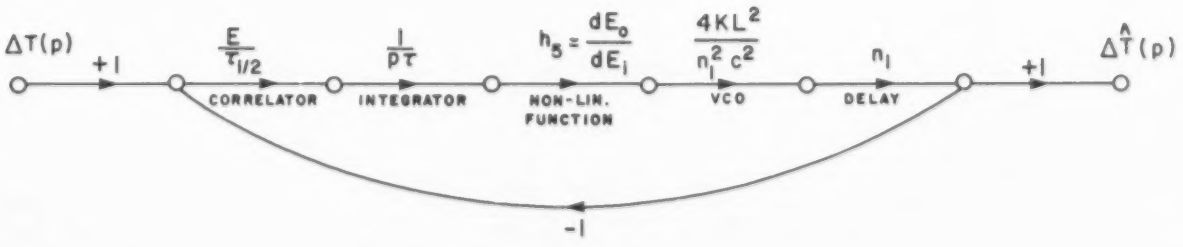

FIG. 72

The closed loop transfer function is:

$$\psi(p) = \frac{\Delta T(p)}{\Delta \hat{T}(p)} = \frac{1}{1 + p\left(\frac{\tau_{1/2}\, \tau\, n_1\, c^2}{4EKh_5 L^2}\right)} \qquad (116)$$

For constant bandwidth:

$$\tau_o = \left(\frac{\tau_{1/2}\, \tau\, n_1\, c^2}{4EKh_5 L^2}\right) = \text{constant} \tag{117}$$

hence,

$$h_5 = \frac{dE_o}{dE_i} = \left(\frac{\tau_{1/2}\, \tau\, n_1\, c^2}{4\tau_o EKL^2}\right) \tag{118}$$

The non-linear function is $E_o = \xi(E_i)$. The output of the non-linear function is the input of the VCO, hence:

$$E_o = \frac{1}{K\, T_{VCO}}$$

The lock-in condition is:

$$n_1\, T_{VCO} = \frac{2L}{c} \text{ therefore,}$$

$$L \quad \frac{n_1 c}{2\, K\, E_o} \tag{119}$$

Substition of (119) in (118) yields:

$$h_5 = \frac{dE_o}{dE_i} = \left(\frac{\tau_{1/2}\, \tau\, K}{\tau_o\, n_1\, E}\right) E_o^2 \tag{120}$$

The non-linear function to obtain constant bandwidth therefore is:

$$E_o = \left(\frac{\tau_o\, n_1\, E}{\tau_{1/2}\, \tau\, K}\right) \cdot \frac{1}{E_i} \tag{121}$$

With the non-linear function, defined by (121), the transfer function is:

$$\psi(p) = \left[\frac{1}{1 + p\,\tau_o}\right] \tag{122}$$

where τ_o is a constant defined by (117).

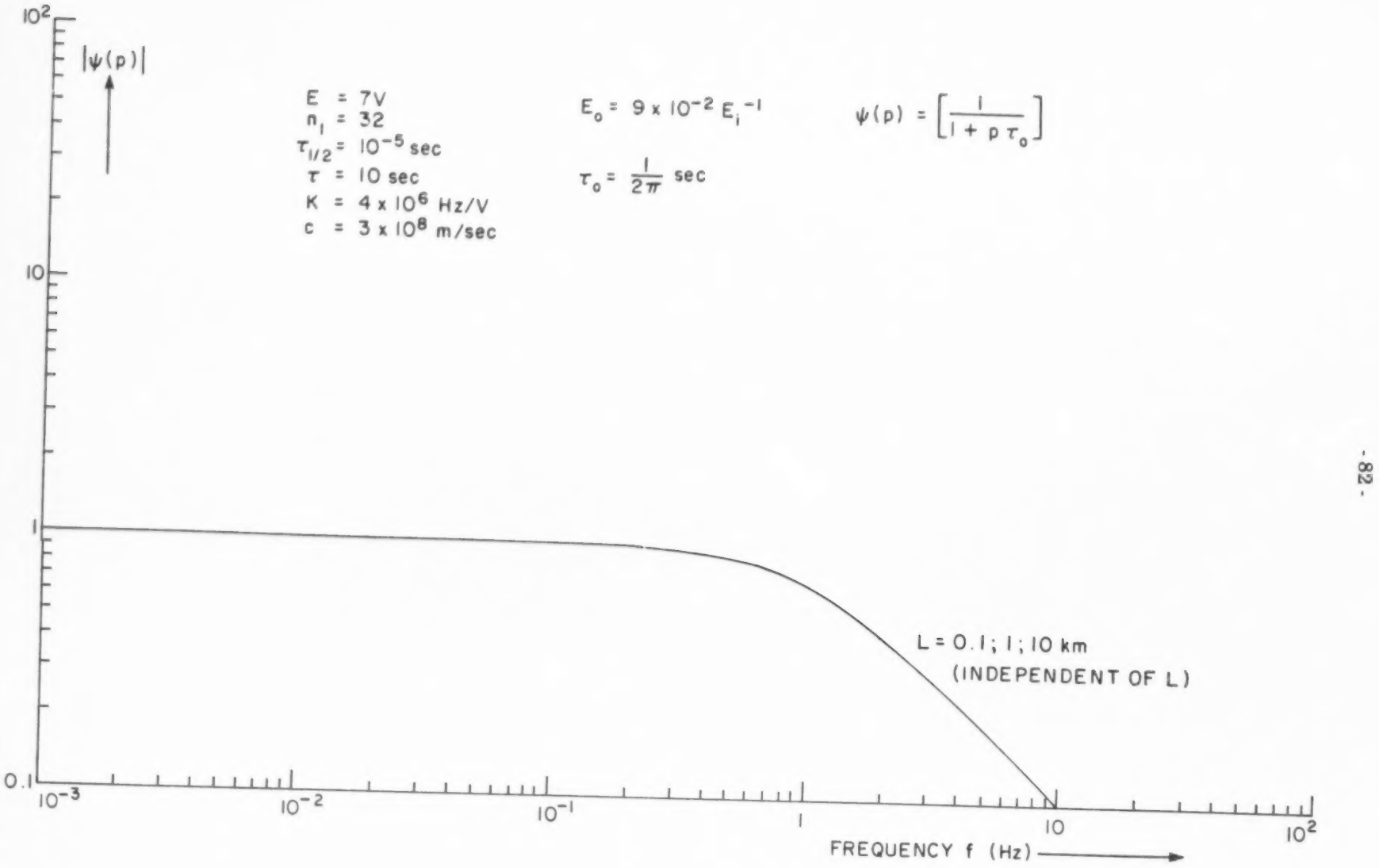
10^2
$|\psi(p)|$
E = 7V
n_1 = 32
$\tau_{1/2} = 10^{-5}$ sec
τ = 10 sec
K = 4×10^6 Hz/V
c = 3×10^8 m/sec
$E_o = 9 \times 10^{-2} E_i^{-1}$
$\tau_o = \frac{1}{2\pi}$ sec
$\psi(p) = \left[\frac{1}{1 + p\tau_o}\right]$
10
1
0.1
L = 0.1; 1; 10 km
(INDEPENDENT OF L)
10^{-3}
10^{-2}
10^{-1}
1
10
10^2
FREQUENCY f (Hz)

FIG. 73

Suppose a constant bandwidth, independent of L, of 1 Hz is required, hence $\tau_o = \frac{1}{2\pi}$ sec.

Let's assume for the system parameters:

$E = 7V$

$n_1 = 32$

$\tau_{1/2} = 10\ \mu sec$

$\tau = 10$ sec

$K = 4 10^6$ Hz/V

$c = 3 10^8$ m/sec (speed of light).

Substitution of these values in (121) yields for the non-linear function required to obtain a constant 1 Hz bandwidth:

$$E_o = \frac{9\ 10^{-2}}{E_i} \tag{123}$$

The transfer gain as a function of frequency and distance is shown in Figure 73. The 3dB-bandwidth, as a function of distance is shown in Figure 76.

13.3.2 Bandwidth Proportional to L^{-1}

In a fashion similar to that used in Section 13.3.1 one can derive the non-linear function $E_o = \xi(E_i)$ to obtain a bandwidth proportional to 1/L.

The condition imposed on the time constant τ_o is now:

$$\tau_o = \left(\frac{\tau_{1/2}\ \tau\ n_1\ c^2}{4EKh_5L^2}\right) = \beta L \tag{124}$$

hence,

$$h_5 = \frac{dE_o}{dE_i} = \left(\frac{\tau_{1/2}\ \tau\ n_1\ c^2}{4\beta EKL^3}\right) \tag{125}$$

The lock-in condition gives:

$$L = \left(\frac{n_1 c}{2KE_o}\right) \tag{126}$$

Substituting (126) in (125) yields:

$$h_5 = \frac{dE_o}{dE_i} = \left(\frac{2\tau_{1/2}\ \tau\ K^2}{\beta E n_1^2\ c}\right) \cdot E_o^3 \tag{127}$$

The non-linear function $E_o = \xi(E_i)$ follows from (127):

$$E_o = \left(\frac{\beta E n_1^2 c}{4 \tau_{1/2} \tau K^2} \right)^{1/2} E_i^{-1/2} \qquad (128)$$

The transfer function $\psi(p)$, with the function (128) in the loop, is:

$$\psi(p) = \left[\frac{1}{1 + p\beta L} \right] \qquad (129)$$

Example:

Bandwidth desired at L = 10 km: 0.1 Hz. From (124) it follows that $\beta = 1.6\ 10^{-4}$.

Let's assume for the system parameters:

E = 7V
n_1 = 32
$\tau_{1/2}$ = 10 μsec
τ = 10 sec
K = $4 10^6$ Hz/V
c = $3 10^8$ m/sec(speed of light).

Substitution of these values in (128) yields for the non-linear function:

$$E_o = 0.23\ E_i^{-1/2} \qquad (130)$$

The transfer gain and the 3dB-bandwidth are shown in Figures 74 and 76 respectively.

13.3.3 Bandwidth Proportional to $L^{-1/2}$

A bandwidth proportional to $L^{-1/2}$ is somewhat in between. It isn't constant but decreases at a slower rate compared with a bandwidth proportional to L^{-1}.

The condition imposed on the time constant τ_o is:

$$\tau_o = \frac{\tau_{1/2} \tau n_1 c^2}{4 E K h_s L^2} = \beta L^{1/2} \qquad (131)$$

Proceeding in a similar fashion as before one can derive,

$$E_o = \frac{n_1}{K} \left(\frac{\beta E \sqrt{2c}}{3 \tau_{1/2} \tau} \right)^{2/3} E_i^{-2/3} \qquad (132)$$

The transfer function $\psi(p)$, with (132) inserted in the loop, is:

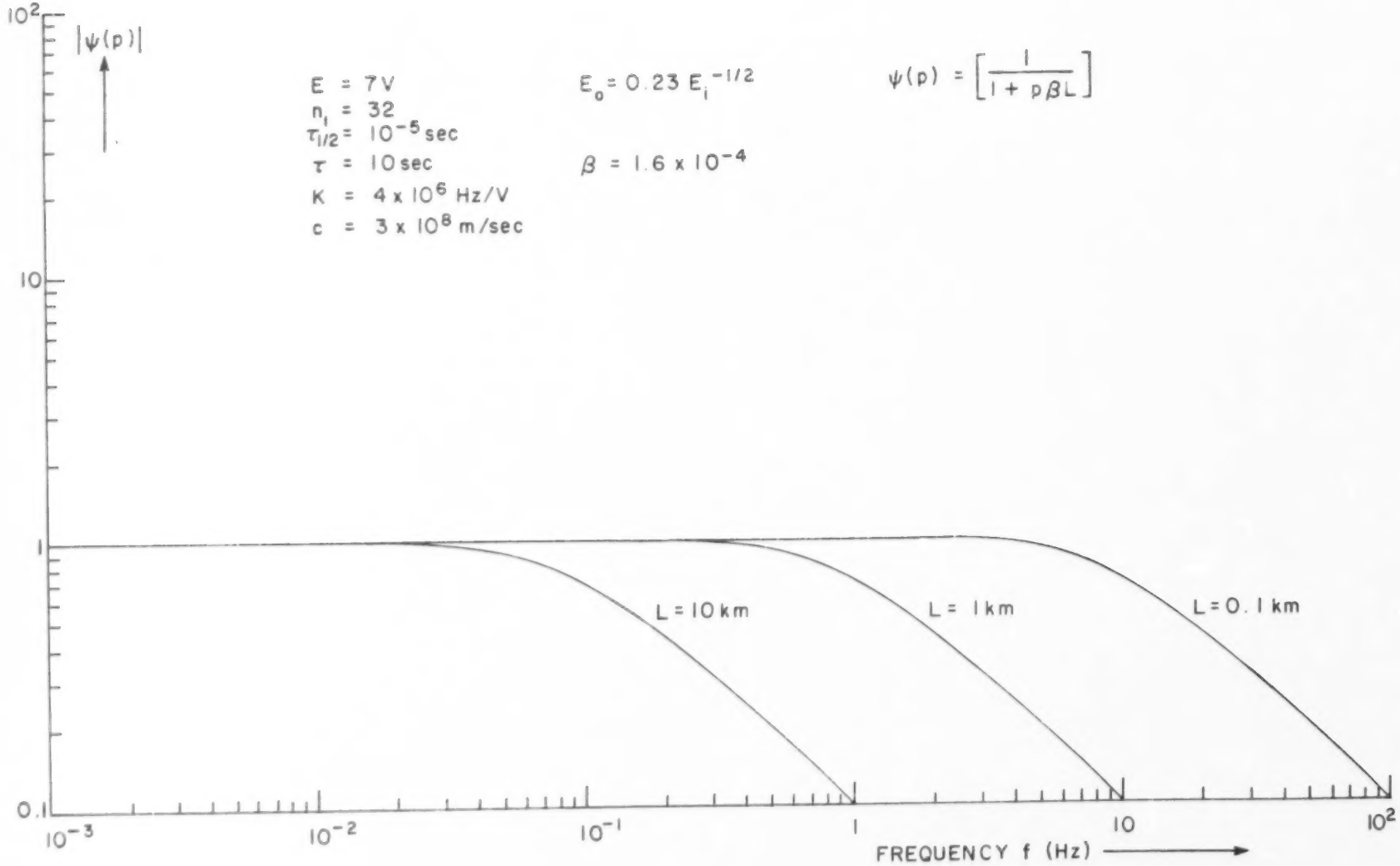
10^2
$|\psi(p)|$
E = 7V
n_i = 32
$\tau_{1/2}$ = 10^{-5} sec
τ = 10 sec
K = 4×10^6 Hz/V
c = 3×10^8 m/sec
$E_o = 0.23\, E_i^{-1/2}$
$\beta = 1.6 \times 10^{-4}$
$\psi(p) = \left[\frac{1}{1 + p\beta L}\right]$
10
1
0.1
L = 10 km
L = 1 km
L = 0.1 km
10^{-3}
10^{-2}
10^{-1}
1
10
10^2
FREQUENCY f (Hz)

FIG. 74

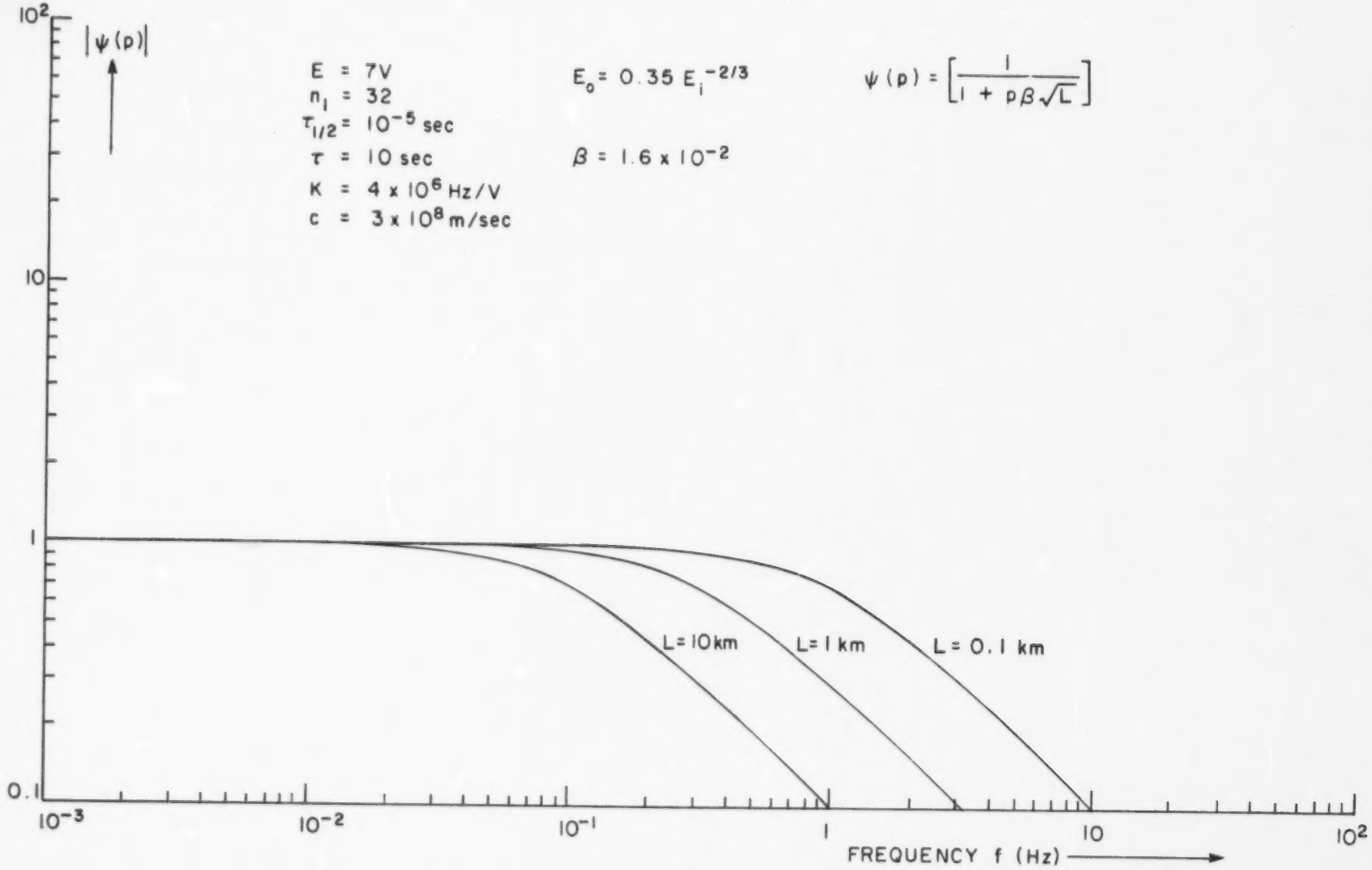
10^2
$|\psi(p)|$
E = 7V
n_1 = 32
$\tau_{1/2} = 10^{-5}$ sec
τ = 10 sec
K = 4×10^6 Hz/V
c = 3×10^8 m/sec
$E_o = 0.35\, E_i^{-2/3}$
$\beta = 1.6 \times 10^{-2}$
$\psi(p) = \left[\frac{1}{1 + p\beta\sqrt{L}}\right]$
10
1
0.1
L=10km
L=1 km
L= 0.1 km
10^{-3}
10^{-2}
10^{-1}
1
10
10^2
FREQUENCY f (Hz)

FIG. 75

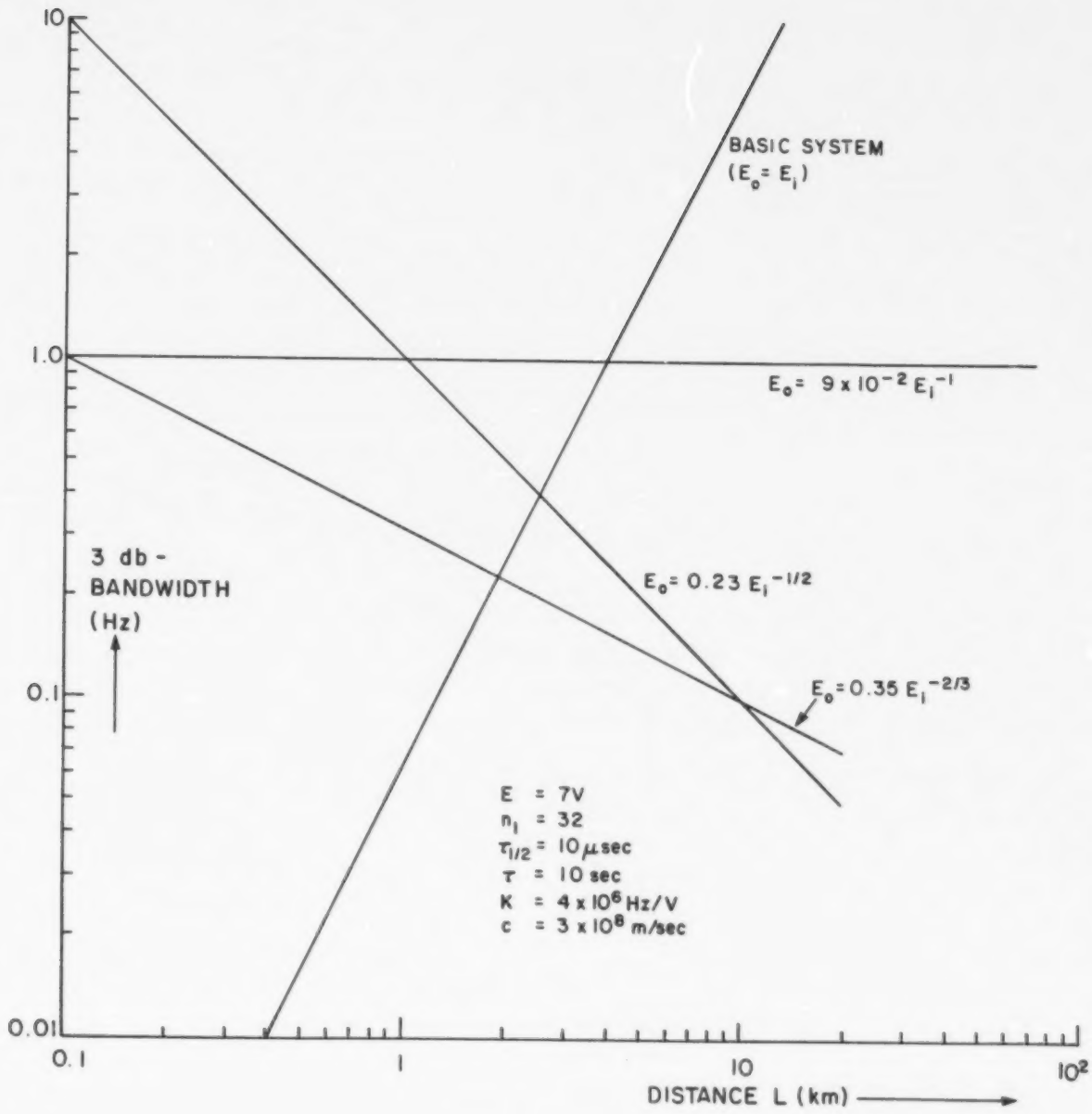
10
1.0
0.1
0.01
0.1
1
10
10^2
BASIC SYSTEM
($E_o = E_i$)
$E_o = 9 \times 10^{-2} E_i^{-1}$
$E_o = 0.23 E_i^{-1/2}$
$E_o = 0.35 E_i^{-2/3}$
3 db -
BANDWIDTH
(Hz)
E = 7V
n_1 = 32
$\tau_{1/2}$ = 10 μsec
τ = 10 sec
K = 4×10^6 Hz/V
c = 3×10^8 m/sec
DISTANCE L (km)

FIG. 76

$$\psi(p) = \left[\frac{1}{1 + p\beta\sqrt{L}}\right] \tag{133}$$

Example:

The same system parameters will be used again to allow a comparison.

Bandwidth = 0.1 Hz at L = 10 km, hence $\beta = 1.6\ 10^{-2}$.

System parameters:

E = 7V
n_1 = 32
$\tau_{½}$ = 10 μsec
τ = 10 sec
K = 410^6 Hz/V
c = 310^8 m/sec (speed of light).

Substitution of these values in (132) yields for the non-linear function:

$$E_o = 0.35\ E_i^{-2/3} \tag{134}$$

The transfer gain as a function of frequency and distance is shown in Figure 75, whereas the 3dB-bandwidth as a function of L is illustrated in Figure 76.

13.4 Second Order System

When using an acoustical carrier one can't, in general, ignore the second order term in the transfer function. The second order transfer function $\psi(p)$ is:

$$\psi(p) = \frac{1}{1 + p\left(\frac{\tau_{½}\,\tau\,n_1\,c^2}{4EKL^2}\right) + p^2\left(\frac{\tau_{½}\,\tau\,n_1\,c}{4EKL}\right)} \tag{135}$$

The natural frequency ω_o and the damping factor d are respectively:

$$\omega_o = \left(\frac{4EK}{\tau_{½}\,\tau\,n_1\,c}\right)^{½} L^{½} \tag{136}$$

$$d = \left(\frac{\tau_{½}\,\tau\,n_1\,c^3}{4EK}\right)^{½} L^{-3/2} \tag{137}$$

The transfer gain $\left|\psi(p)\right|$ is shown for several values of L in Figure 78. It is assumed that:

$\tau_{½} = 10^{-3}$ sec

$\tau = 10$ sec

$n_1 = 64$

$E = 7V$

$K = 410^3$ Hz/V

$c = 1.5\ 10^3$ m/sec (speed of sound in water).

From Figure 78 one notices that the system, for small values of L, behaves like a first order system with a bandwidth proportional to L^2. For large values of L, it behaves like an undamped second order system.

If L varies only over a limited range then one can easily select the values for the system parameters to obtain a particular bandwidth. However, if L varies substantially, it may be required to control the bandwidth with non-linear functions, otherwise, the noise level for large L might become too large for accurate measurements.

In the next three sections the improvement in performance will be analyzed with the same non-linear functions as used in the analysis of the first order system.

The transfer function, with an arbitrary non-linear function $E_o = \xi(E_i)$ inserted in the loop (see Fig. 77). is:

$$\psi(p) = \frac{1}{1 + p\left(\frac{\tau_{½}\,\tau\, n_1\, c^2}{4EKh_5L^2}\right) + p^2\left(\frac{\tau_{½}\,\tau\, n_1\, c}{4EKh_5L}\right)} \qquad (138)$$

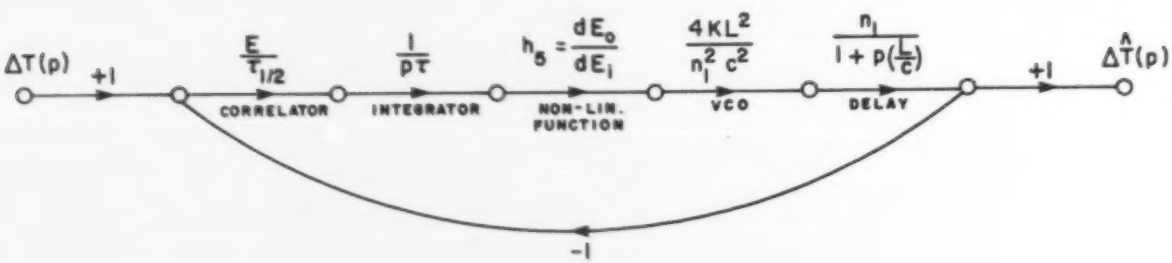

FIG. 77

The transfer function $\psi(p)$ will be analyzed in Sections 13.4.1, 13.4.2, and 13.4.3, for three different non-linear functions. The system parameters will be kept constant to clearly demonstrate the effect of the non-linear functions on the transfer function.

13.4.1 Bandwidth Approximately Constant

Constant bandwidth and damping can't be obtained simultaneously. An approximate solution can be obtained with the non-linear function:

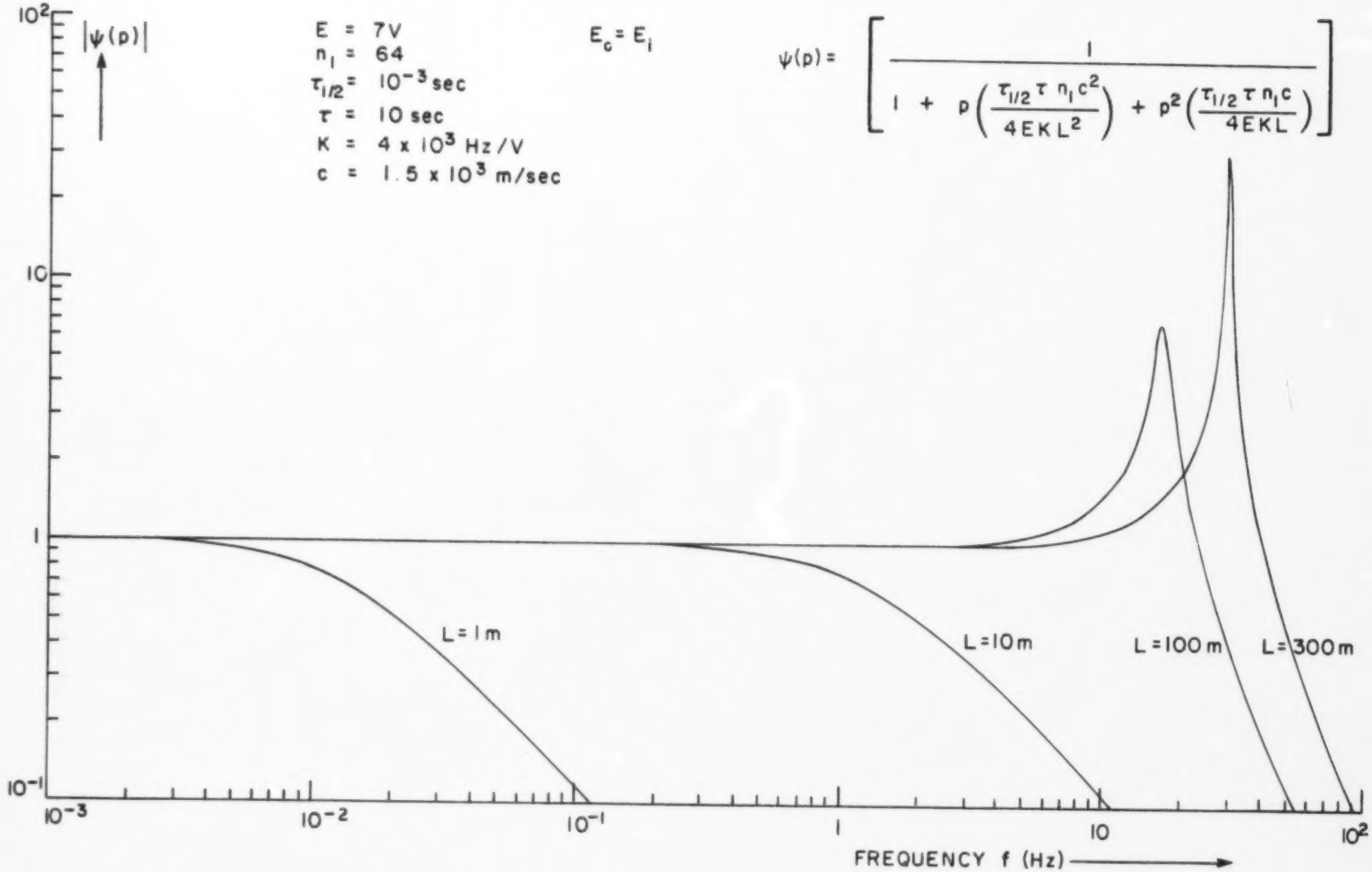
$|\psi(p)|$
E = 7V
n_1 = 64
$\tau_{1/2}$ = 10^{-3} sec
τ = 10 sec
K = 4×10^3 Hz/V
c = 1.5×10^3 m/sec
$E_c = E_i$
$\psi(p) = \left[\frac{1}{1 + p\left(\frac{\tau_{1/2}\tau n_1 c^2}{4EKL^2}\right) + p^2\left(\frac{\tau_{1/2}\tau n_1 c}{4EKL}\right)} \right]$
10^2
10
1
10^{-1}
L = 1m
L = 10m
L = 100m
L = 300m
10^{-3}
10^{-2}
10^{-1}
1
10
10^2
FREQUENCY f (Hz)

FIG. 78

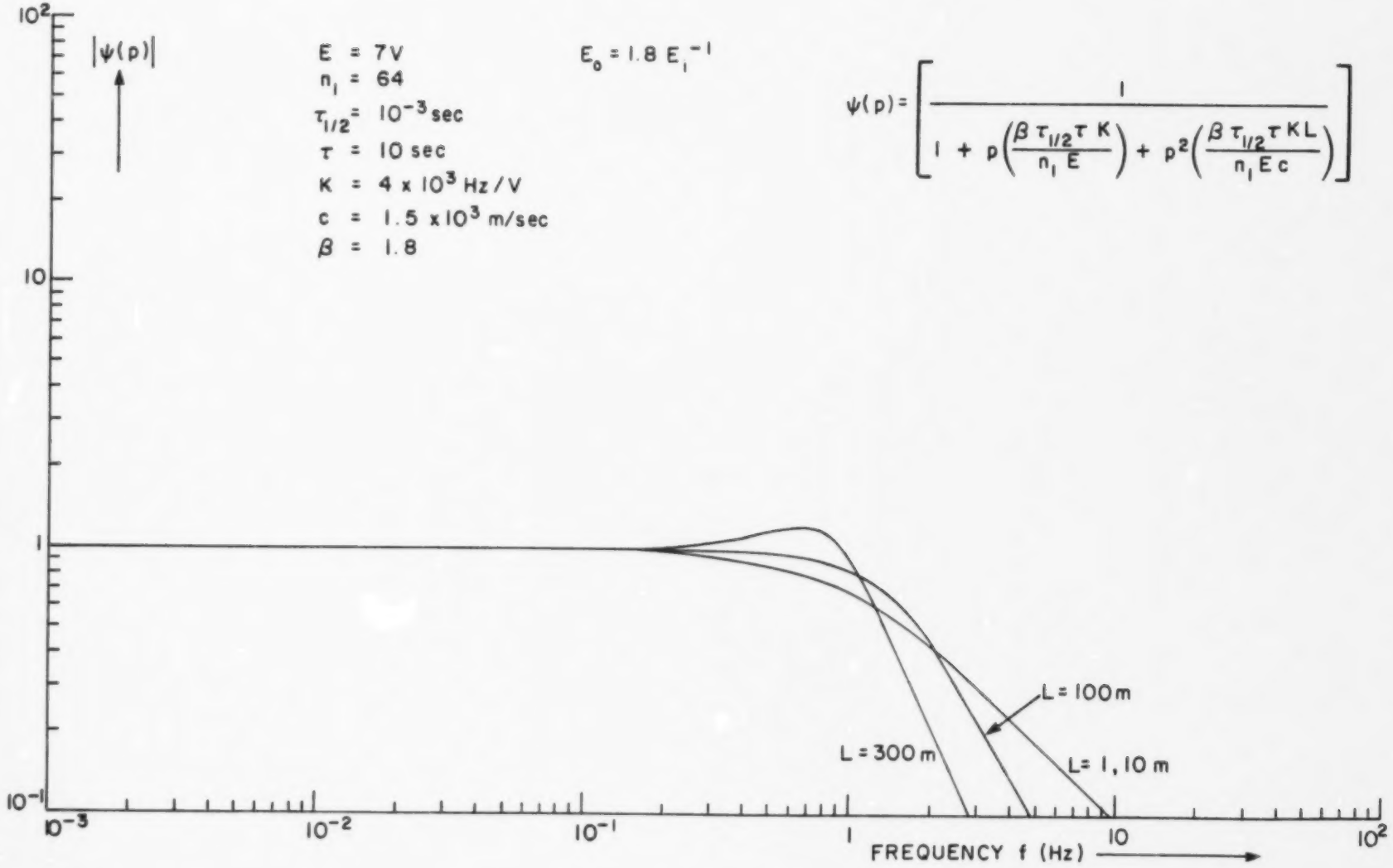
10^2
$|\psi(p)|$
E = 7V
n_1 = 64
$\tau_{1/2}$ = 10^{-3} sec
τ = 10 sec
K = 4×10^3 Hz/V
c = 1.5×10^3 m/sec
β = 1.8
$E_0 = 1.8\, E_1^{-1}$
$\psi(p) = \left[\frac{1}{1 + p\left(\frac{\beta \tau_{1/2} \tau K}{n_1 E}\right) + p^2\left(\frac{\beta \tau_{1/2} \tau K L}{n_1 E c}\right)} \right]$
10
1
10^{-1}
10^{-3}
10^{-2}
10^{-1}
1
10
10^2
L = 100 m
L = 300 m
L = 1, 10 m
FREQUENCY f (Hz)

FIG. 79

$$E_o = \frac{\beta}{E_i} \tag{139}$$

where β = constant.

The lock-in condition yields:

$$E_o = \frac{n_1 c}{2KL} \tag{140}$$

The transfer gain h_S is the derivative of the non-linear function at the operating point:

$$h_S = \frac{dE_o}{dE_i} = -\frac{\beta}{E_i^2} \tag{141}$$

With (139) and (140) one can write for (141):

$$h_S = \left(\frac{n_1^2 \; c^2}{4 \beta K^2 L^2} \right) \tag{142}$$

Substituting (142) in the transfer function yields for $\psi(p)$:

$$\psi(p) = \frac{1}{1 + p \left(\frac{\beta \tau_{½} \tau K}{n_1 E} \right) + p^2 \left(\frac{\beta \tau_{½} \tau K L}{n_1 E c} \right)} \tag{143}$$

The improvement in the transfer function over that of the basic loop configuration is quite evident from Figure 78 and Figure 79. The system parameters are the same in both cases. The constant β was chosen equal to $\beta = 1.8$. The effective bandwidth is nearly constant; at L = 300 m the system becomes slightly undamped. The basic system however shows a large variation in bandwidth and is severely undamped for large values of L.

13.4.2 Bandwidth Proportional to L^{-1}

A bandwidth proportional to L^{-1} as well as constant damping can be obtained with the non-linear function:

$$E_o = \beta E_i^{-½} \tag{144}$$

where β = constant.

Proceeding as in Section 13.4.1 one can derive for h_S:

$$h_S = -\left(\frac{n_1^3 \; c^3}{16 \beta^2 \; K^3 \; L^3} \right) \tag{145}$$

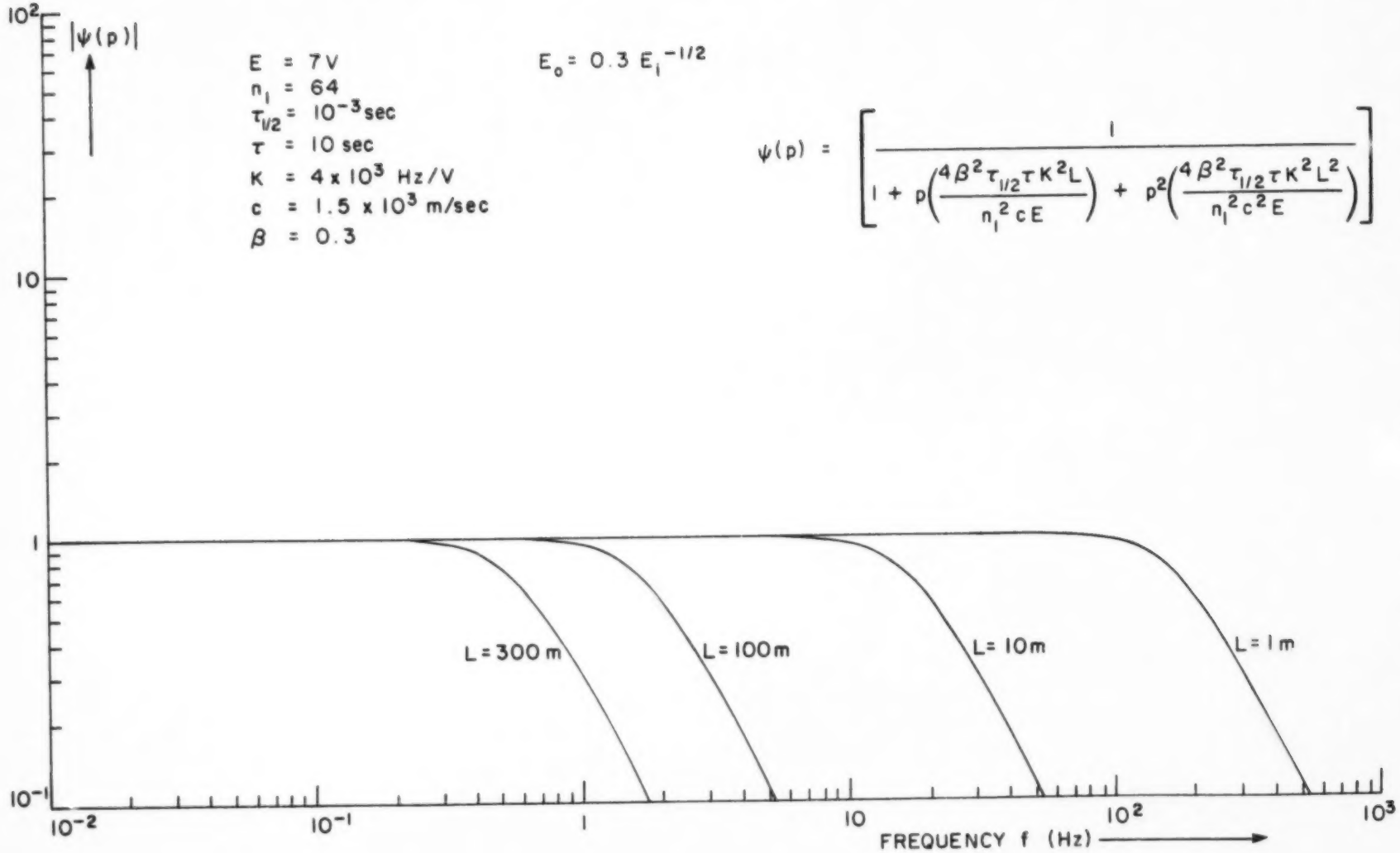
10^2
$|\psi(p)|$
E = 7V
n_1 = 64
$\tau_{1/2}$ = 10^{-3}sec
τ = 10 sec
K = 4×10^3 Hz/V
c = 1.5×10^3 m/sec
β = 0.3
$E_o = 0.3\, E_1^{-1/2}$
$\psi(p) = \left[\frac{1}{1 + p\left(\frac{4\beta^2\tau_{1/2}\tau K^2 L}{n_1^2 c E}\right) + p^2\left(\frac{4\beta^2\tau_{1/2}\tau K^2 L^2}{n_1^2 c^2 E}\right)}\right]$
10
1
10^{-1}
L = 300 m
L = 100m
L = 10m
L = 1 m
10^{-2}
10^{-1}
1
10
10^2
10^3
FREQUENCY f (Hz)

FIG. 80

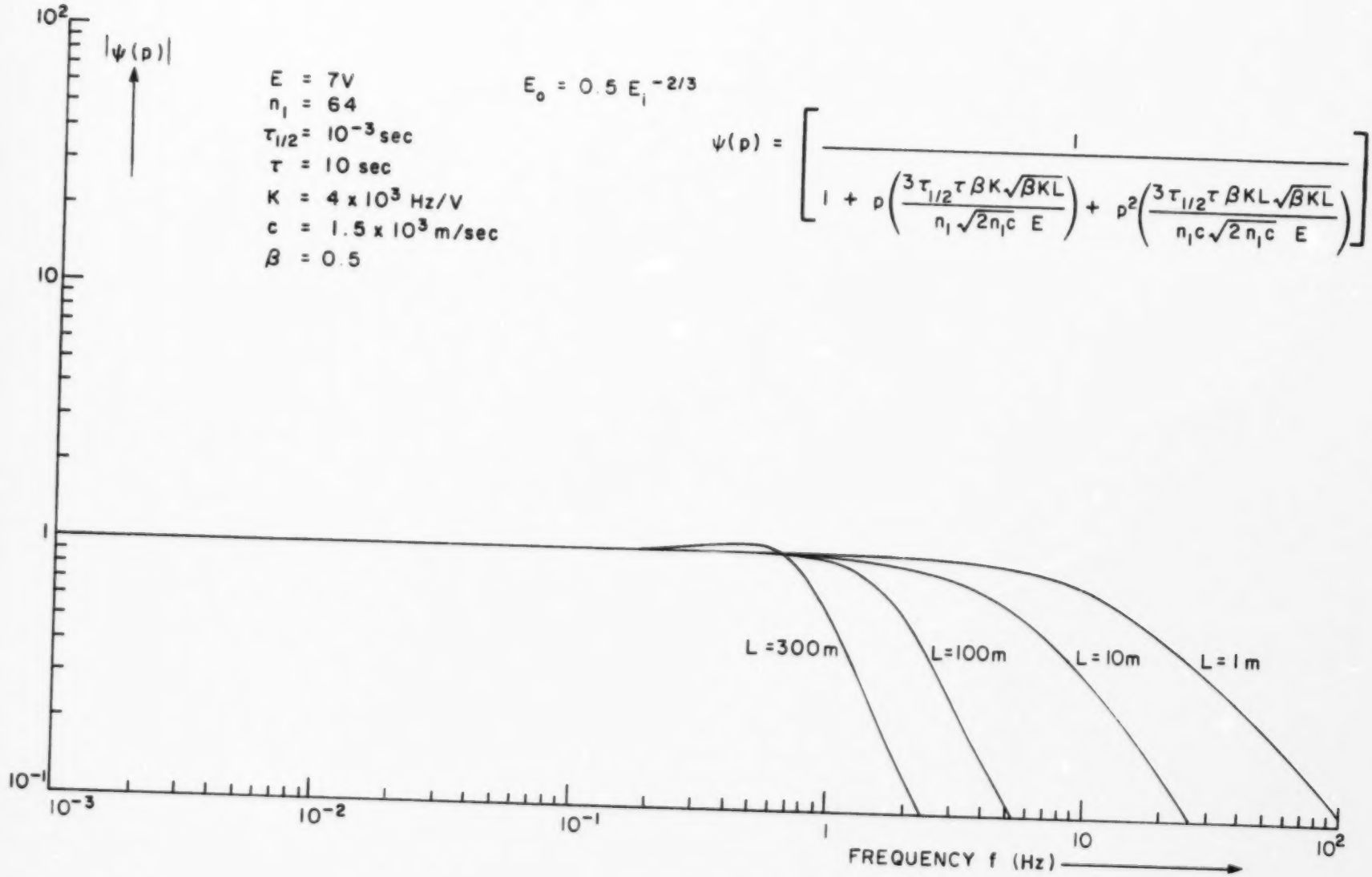
10^2
$|\psi(p)|$
E = 7V
n_1 = 64
$\tau_{1/2}$ = 10^{-3} sec
τ = 10 sec
K = 4×10^3 Hz/V
c = 1.5×10^3 m/sec
β = 0.5
$E_o = 0.5\, E_i^{-2/3}$
$\psi(p) = \left[\frac{1}{1 + p\left(\frac{3\tau_{1/2}\tau\beta K\sqrt{\beta KL}}{n_1\sqrt{2n_1c}\ E}\right) + p^2\left(\frac{3\tau_{1/2}\tau\beta KL\sqrt{\beta KL}}{n_1 c\sqrt{2n_1c}\ E}\right)} \right]$
10
1
10^{-1}
L = 300m
L = 100m
L = 10m
L = 1m
10^{-3}
10^{-2}
10^{-1}
1
10
10^2
FREQUENCY f (Hz)

FIG. 81

and for $\psi(p)$:

$$\psi(p) = \frac{1}{1 + p\left(\frac{4\beta^2 \tau_{1/2} \tau K^2 L}{n_1^2 c E}\right) + p^2\left(\frac{4\beta^2 \tau_{1/2} \tau K^2 L^2}{n_1^2 c^2 E}\right)} \qquad (146)$$

The transfer gain $|\psi(p)|$ is shown in Figure 80. The bandwidth is decreasing inversely proportional to L, with constant damping. Notice by comparing Figures 78 and 80, that the non-linear function completely reverses the relation between bandwidth and distance L.

13.4.3 Bandwidth Approximately Proportional to $L^{-1/2}$

The non-linear function:

$$E_o = \beta E_i^{2/3} \qquad (147)$$

results in a bandwidth decreasing at a somewhat slower rate.

Proceeding as in Section 13.4.1 one can derive h_5:

$$h_5 = \frac{2}{3} \beta^{3/2} \left(\frac{n_1 c}{2KL}\right)^{5/2} \qquad (148)$$

and $\psi(p)$:

$$\psi(p) = \left[\frac{1}{1 + p\left(\frac{3\tau_{1/2} \tau \beta \sqrt{\beta KL}}{n_1 E \sqrt{2n_1 c}}\right) + p^2\left(\frac{3\tau_{1/2} \tau \beta KL \sqrt{\beta KL}}{n_1 Ec \sqrt{2n_1 c}}\right)}\right] \qquad (149)$$

The transfer gain is shown for $E_o = 0.5 E_i^{2/3}$ in Figure 81. The bandwidth is approximately inversely proportional to $\sqrt{L}$.

13.5 Converting Variant to Invariant Noise

If a pseudo random digital noise generator is used to modulate the carrier and if it is driven by the clock of the delay-locked loop then the half correlation width $\tau_{1/2}$ of the noise is a linear function of the clock period $T_{VCO} = \frac{1}{f_{VCO}}$ of the delay-locked loop:

$$\tau_{1/2} = NT_{VCO} \qquad (150)$$

where N = constant.

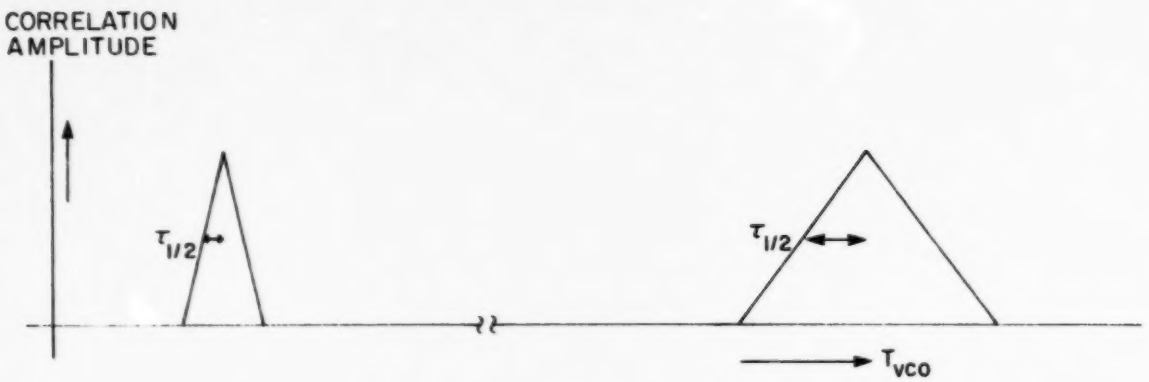

FIG. 82

To maintain a matched condition between half-correlation time constant $\tau_{1/2}$ and correlator one has to make the two points "calculated" by the cross-correlator also a function of the clock as shown in Figure 83.

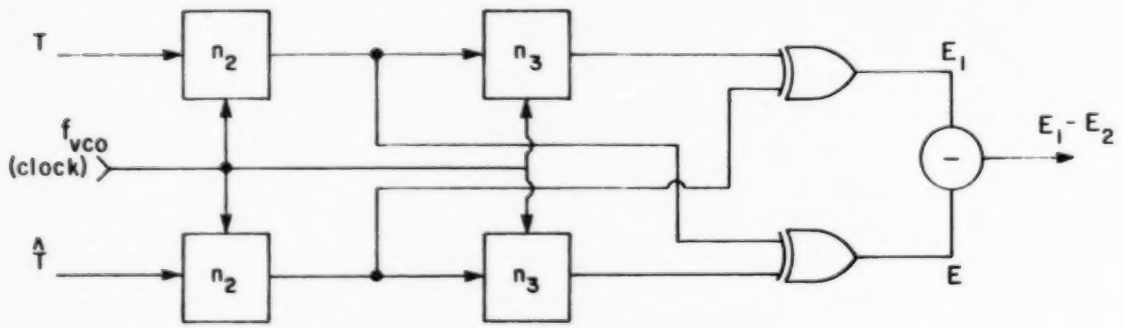

FIG. 83

Optimum linear range transfer gain is obtained for $\tau_{1/2} = n_3 T_{VCO}$. Since $\tau_{1/2} = NT_{VCO}$ one has to select, $N = n_3$.

The transfer function of the correlator is therefore:

$$h_1 = \left(\frac{E}{n_3 T_{VCO}}\right) \qquad (151)$$

Using the lock-in condition one can write for (143):

$$h_1 = \left(\frac{E n_1 c}{2n_3}\right) \frac{1}{L} \qquad (152)$$

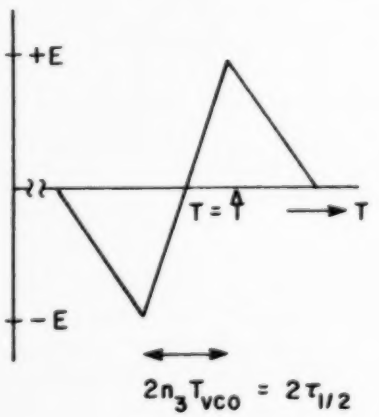

FIG. 84

The gain of the correlator when using invariant noise is inversely proportional to L instead of being a constant. This modifies the non-linear functions required to obtain the transfer functions analyzed in the previous sections. This will be demonstrated only for a second order system where constant bandwidth is required.

In Section 13.4.1 it was shown that the function $E_o = \frac{\beta}{E_i}$ gave a nearly constant effective bandwidth.

To obtain a similar result, an exponential non-linear function is required:

$$E_o = \gamma e^{-\beta E_i} \tag{153}$$

Its transfer gain is:

$$h_5 = \frac{dE_o}{dE_i} = -\beta E_o \tag{154}$$

Substituting $E_o = \frac{n_1 c}{2KL}$ in (154) yields:

$$h_5 = \left(\frac{\beta n_1 c}{2K}\right) \frac{1}{L} \tag{155}$$

Using h_1 and h_5 and the other known partial transfer functions one obtains for the closed loop transfer function $\psi(p)$:

$$\psi(p) = \left[\frac{1}{1 + p\left(\frac{n_3 \tau}{\beta n_1 E}\right) + p^2 \left(\frac{n_3 \tau L}{\beta n_1 E c}\right)}\right] \tag{156}$$

This transfer function is similar to (143), i.e. the first order term is independent of L and the second order term is linearly dependent on L.

Having the option to select from two different approaches can be an advantage, i.e. one can choose the method most easily implemented with regard to practical circuit restraints.

14.0 SELF-ADAPTIVE BEHAVIOUR OF DELAY-LOCKED LOOP

The input noise signal consists of coherent noise and some non-coherent noise. What happens if the level of the non-coherent noise increases?

Naturally the average noise level in the loop will increase and eventually a threshold will be reached beyond which the loop can't maintain lock.

The non-coherent noise will also effect the transfer function. This interaction occurs at the correlator. It will be shown that this results in a self-adaptive behaviour for the delay-locked loop.

Let's define:

$$R = \left(\frac{s}{s+n}\right) \tag{157}$$

where s = coherent noise
and n = non-coherent noise.

The correlation amplitude is shown as a function of R in Figure 85.

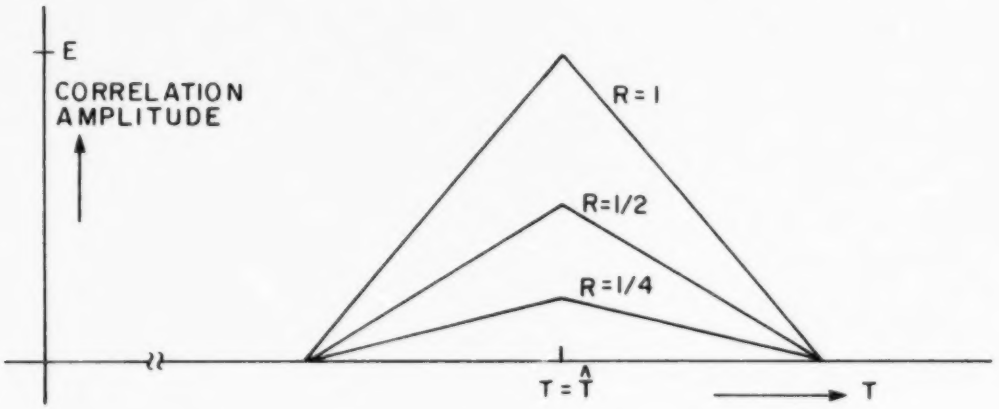

FIG. 85

The maximum correlation amplitude is a linear function of R. The resulting correlator transfer curve is shown in Figure 86.

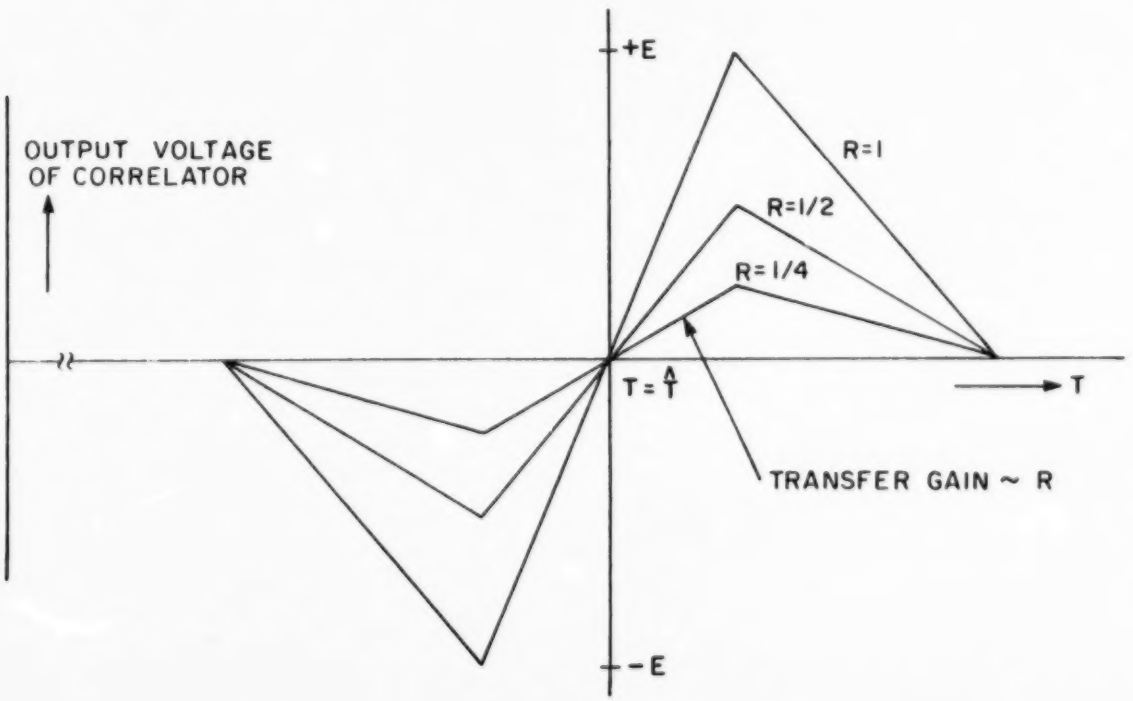

FIG. 86

It is evident from Figure 86 that the transfer gain of the correlator reduces for increasing non-coherent noise level. The effect, on all the transfer functions considered, is to decrease the effective bandwidth of the delay-locked loop. Reducing the bandwidth reduces the noise level in the loop. The delay-locked loop is therefore self-adaptive, when the non-coherent noise increases it automatically "sacrifices" some bandwidth to restrict the increase in noise level in the loop.

This will be analyzed more specifically for the transfer function derived in Section 13.3.1. It is a first order transfer function having a constant bandwidth and therefore the easiest to demonstrate the self-adaptive behaviour for non-coherent noise.

The signal flow diagram of Section 13.3.1, modified to include the noise dependent transfer function of the correlator, is shown in Figure 87.

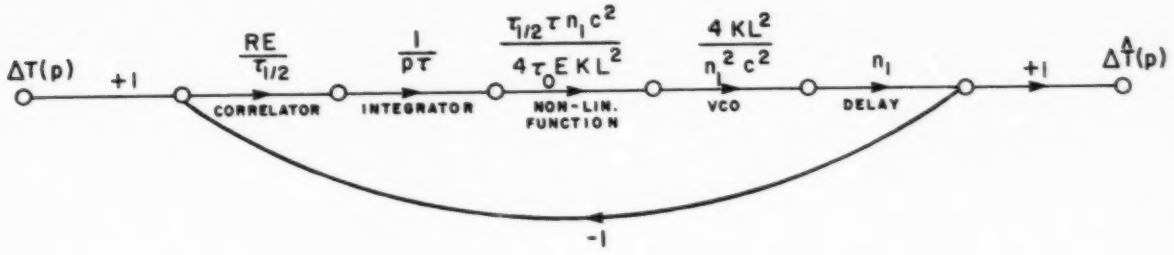

FIG. 87

The transfer function $\psi(p)$ is:

$$\psi(p) = \left[\frac{1}{1 + p \frac{\tau_o}{R}} \right] \tag{158}$$

where τ_o = constant.

The 3dB-bandwidth, BW, is:

$$BW = \frac{R}{2\pi \tau_o} \text{ Hz} \tag{159}$$

The self-adaptive behaviour of the loop for non-coherent noise is clear from (159). If the level of the non-coherent noise increases, R decreases, resulting in a smaller bandwidth.

15.0 IMPLEMENTATION OF NON-LINEAR FUNCTIONS

The non-linear functions can be readily implemented with log-antilog modules. The block diagram of the National Semiconductor LH0094 Multifunction Converter is shown in Figure 88.

The module can generate functions characterized by:

$$E_o = V_y \cdot \left(\frac{V_z}{V_x} \right)^m \quad \text{where } 0.1 \leq m \leq 10$$

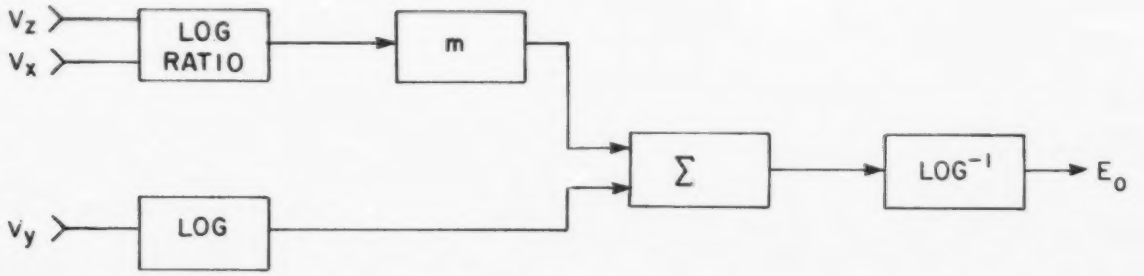

FIG. 88

It can also be used to generate exponential, logarithmic and trigonometric functions.

16.0 LOOP MONITOR AND AUTOMATIC LOCK-IN CIRCUIT

The delay-locked loop does not lock-in at start-up or re-acquires lock when for some reason it jumps out-of-lock. In effect additional electronic means have to be incorporated to perform two functions.

1. **Loop Monitor**

   The loop monitor continuously checks the delay-locked loop for in-lock position. When it detects an out-of-lock condition it passes control to the automatic lock-in circuit.

2. **Automatic Lock-In Circuit**

   When activated by the loop monitor the automatic lock-in circuit takes command of the delay-locked loop and forces it to scan through its whole delay range. The lock-in circuit disengages itself when the loop re-acquires lock-in, passing control back to the delay-locked loop.

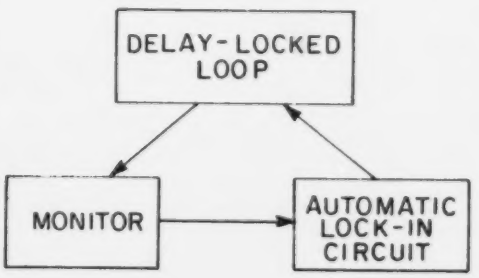

FIG. 89

17.0 OPTIMIZING LOOP PERFORMANCE WITH PSEUDO-RANDOM NOISE GENERATOR

The delay-locked loop does not have to be verified in situ. Instead one can conveniently use a pseudo-random noise generator to simulate the input noise signals. (Pseudo random noise generators are easy to implement with simple digital circuits.)

One can readily vary the correlation width of the noise generator, apply dynamic variations in the delay to analyze the transfer function or simulate large amplitude signals such as ramp inputs. The block diagram of the simulator is shown in Figure 90.

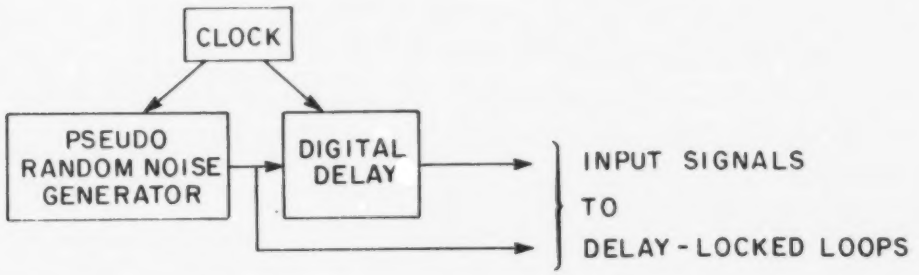

FIG. 90

18.0 CONCLUSIONS

The delay-locked loop is a very useful and versatile type of transducer concept to measure accurately, velocity, "distance travelled", distance or length.

From measuring speed of solids or liquids to depth of oceans, length of sheets of textile, to position of trains are only but a few of the possible applications.

It certainly has much more potential than the present usage of delay-locked loops would seem to indicate.

The flexibility and often the economy are essentially due to the use of random fluctuations as input signals, which are present in many ways in each type of measuring environment. Especially it has the advantage of non-contact type of measurement.

The non-linear delay-locked loop has been analyzed previously with theories [1-4], which take a stochastic point of view, where the loop is considered to be a first order system. The theory presented in this report is entirely analog in nature, using a more exact second order model for the delay-locked loop. This approach avoids the somewhat confusing intricacies of a stochastic treatment.

The two approaches are complementary. A stochastic analysis is required to study the acquisition behaviour, the probability that lock-in is maintained, the threshold signal level for lock-in to occur, the noise level in the loop, etc. The analog analysis presented, assumed sufficient signal amplitude for lock-in to occur and to be maintained. It was used to analyze the dynamic behaviour of the loop both for small and large amplitude input signals. One of the essential elements of the analog theory presented is the use of non-linear system functions to optimize the loop performance. The analog theory is general; the two modes of operation for the delay-locked loop have been analyzed in a unified approach.

19.0 REFERENCES

1. Spilker, J.J.
Magill, D.T.
The Delay-Lock Discriminator — An Optimum Tracking Device.
Proc. IRE, Vol 49, Sept. 1961, pp. 1403-1406.

2. Spilker, J.J.
Delay-Lock Tracking of Binary Signals.
IEEE Trans. Space Electron. Telem., Vol. SET-9, Mar. 1963, pp. 1-8.

3. Bershad, N.J.
Merryman, P.
Sklansky, J.
Adaptive Trackers Based on Continuous Learning Theory.
IEEE Trans. Aerosp. Electron. Syst., Vol. AES-10, Mar. 1974, pp. 245-254.

4. Meyr, H.
Delay-Lock Tracking of Stochastic Signals.
IEEE Trans. Com., Vol. COM-24-3, Mar. 1976.

REPORT DOCUMENTATION PAGE/PAGE DE DOCUMENTATION DE RAPPORT

REPORT/RAPPORT TR-RW-003 1a	REPORT/RAPPORT NRC No. 24506 1b
REPORT SECURITY CLASSIFICATION CLASSIFICATION DE SÉCURITÉ DE RAPPORT UNCLASSIFIED 2	DISTRIBUTION/DIFFUSION UNLIMITED 3

TITLE/SUBTITLE/TITRE/SOUS TITRE (CLASSIFICATION)

AN ANALOG ANALYSIS OF DELAY-LOCK TRACKING OF STOCHASTIC SIGNALS

4

AUTHOR(S)/AUTEUR(S)

C.M.G. Zwarts

5

SERIES/SÉRIE

Technical Report

6

CORPORATE AUTHOR/PERFORMING AGENCY/AUTEUR D'ENTREPRISE/AGENCE D'EXÉCUTION

National Research Council Canada — Railway Laboratory
Division of Mechanical Engineering

7

SPONSORING AGENCY/AGENCE DE SUBVENTION

National Research Council Canada — Railway Laboratory
Division of Mechanical Engineering

8

DATE	FILE/DOSSIER	LAB. ORDER COMMANDE DU LAB.	PAGES	DIAGS	REFS
1985/05 9	10	19757 11	110 12a	90 12b	4 12c

NOTES

13

DESCRIPTORS(KEY WORDS)/MOTS CLÉS

delay-locked loop — transducer — velocity — distance — analog analysis
noise signals — nonlinear functions

14

SUMMARY/SOMMAIRE

The report analyzes the non-contacting measurement of velocity, length and distance with a delay-locked loop, using a novel theoretical approach.

15

ADDRESS/ADRESSE

Mr. C.A.M. Smith, Head
Railway Laboratory
Division of Mechanical Engineering
Ottawa, Ontario K1A 0R6 (613) 998-9638

16